HHS Public Access
Author manuscript
Coord Chem Rev. Author manuscript; available in PMC 2023 December 13.

Published in final edited form as:
Coord Chem Rev. 2020 May 01; 409: . doi:10.1016/j.ccr.2020.213211.

Dithione, the antipodal redox partner of ene-1,2-dithiol ligands and their metal complexes

Partha Basu[a,*], **Kyle J. Colston**[a], **Benjamin Mogesa**[b]

[a]Department of Chemistry and Chemical Biology, IUPUI, Indianapolis, IN 46202, United States

[b]Department of Chemistry and Biochemistry, Duquesne University, Pittsburgh, PA 15282, United States

Abstract

Defining the oxidation state of the central atom in a coordination compound is fundamental in understanding the electronic structure and provides a starting point for elucidating molecular properties. The presence of non-innocent ligand(s) can obscure the oxidation state of the central atom as the ligand contribution to the electronic structure is difficult to ascertain. Redox-active ligands, such as dithiolene ligands, are well known non-innocent ligands that can exist in both a fully reduced (Dt^{2-}) and fully oxidized (Dt^{0}) states. Complexes containing the fully oxidized dithione state of the ligand are uncommon and only a few have been completely characterized. Dithione ligands are of interest due to their electron-deficient nature and ability to act as an electron acceptor for more electron-rich moieties, such as other dithiolene ligands or metal centers. This article focuses the syntheses, structures, and metal coordination, particularly coordination compounds, of dithione ligands. Various examples of mono, bis, and tris dithione complexes are discussed.

Keywords

Dithiolene; Dithione; Donor-acceptor system; Electron-deficient ligand; Diels-Alder reaction; Coordination compound

1. Coordination compounds with Non-innocent ligands

In coordination compounds, defining the oxidation state of the central atom provides a fundamental framework for understanding the properties of the complex. In classical Werner complexes, such as octahedral $[Co(NH_3)_6]Cl_3$, the oxidation state of the central metal ion is derived from simple rules. Accordingly, the oxidation state of cobalt is defined as 3+, which allows one to determine the electron configuration to be d^6. The electronic configuration in a strong octahedral field explains for its substitutional inertness. The description not only guides reactivity but also magnetic properties. In coordination chemistry, defining the

*Corresponding author. basup@iupui.edu (P. Basu).

Declaration of Competing Interest
The authors declare that they have no known competing financial interests or personal relationships that could have appeared to influence the work reported in this paper.

oxidation states of the central metal ion is of paramount importance and ligands like NH_3 and H_2O allow one to easily define the oxidation state of the metal ions [1–3].

A particularly interesting scenario emerges when the ligands do not allow for a definitive determination of the central atom oxidation state. According to Jorgensen's classification [4], these ligands are called non-innocent ligands e.g., a porphyrin ligand, while those similar to NH_3 and H_2O are classified as innocent ligands. Some non-innocent ligands are also redox-active, and transition metal complexes with such ligands allow for both the metal and the ligand to participate in redox processes. The term redox-active has been devised to describe such ligands. In the literature, at times, these two descriptions i.e., redox-active and non-innocent ligands have been used interchangeably. However, they should be used carefully since there is a connotation about the oxidation state of the metal and properties of the complex. In a recent forum article, Chirik argued [5] that in classical organometallic complexes such as $(\eta^5\text{-}C_5Me_5)_2Ti(\eta^2\text{-}CH_2 = CH_2)$, the oxidation state of metal can be either titanium(II) or titanium(IV) due to the presence of a π-acid ligand that provides covalent bonding. Thus, according to Jorgensen's definition, such ligands are non-innocent.

Redox-active ligands are capable of π-bonding pose a challenge in discerning the contributions of each individual ligand to the complete electronic structure. [4,6–10] Such a ligand is 1,2-ene dithiolate(2−), which is part of the dithiolene ligands. The term dithiolene was introduced [11] to describe bidentate sulfur donor ligands connected by an unsaturated carbon–carbon bond. The basic dithiolene unit can be completely aliphatic or a part of heterocyclic and homocyclic rings. These ligands of general formula $R_2C_2S_2$ can be described as an alkene-1,2-dithiolate dianion, a 1,2-dithione, or an intermediate semi-1,2-dithione (Fig. 1). The different redox states of dithiolene ligands have different of π-electrons. In the fully reduced ene-1,2-dithiolate(2−) state, the ligand has six π electrons. The fully oxidized dithione state has four π electrons, while the intermediate semi-1,2-dithione state has five π electrons. In the two extreme oxidation states, the ligand moieties are closed shell, whereas the intermediate state the ligand is in an open shell. The latter case is especially interesting in transition metal complexes where unpaired spin on the ligand framework can differentially interact with the d-electrons in the metal center.

Transition metal chemistry of reduced ene-1,2-dithiolate(2−) ligands has a rich history that continues to garner attention. Dithiolene moieties are also found in biology, namely in the active center of Mo and W enzymes [12–19]. In general, the dithiolene moieties in biological systems are considered to be in their fully reduced sate. Determining the redox state of dithiolene in a macromolecule is difficult and efforts have been made to reproduce the salient features of the dithiolene containing cofactor [17,20–24]. The rich metallodithiolene chemistry has been summarized in excellent review articles and will not be the focus of this article [25–29]. Instead, this article will focus on the chemistry of the oxidized dithione state of the ligand.

2. Synthesis and characterization

2.1. Synthetic approaches to dithione ligands

Dithione ligands have been synthesized as neutral molecules or generated in coordination with metal centers. The different types of dithione ligands are listed in Chart 1. Generally, dithione ligands can be categorized as cyclic or acyclic, and the majority of dithione ligands are a substituted derivative of *N,N′*-dithiooxamide (abbreviated as R_2dto) [30,31]. Substituted acyclic variations of R_2dto were first synthesized and characterized nearly 70 years ago for their potential application in drug development [32–34]. In general, the syntheses of substituted R_2dto molecules were achieved by the following three methods: a) by a condensation reaction of a primary aliphatic amine with dithiooxamide; b) by sulfurizing dioxamides; and c) by esterification of a *N,N′*-bis(carboxymethyl) dithiooxamide.

The general dithiooxamide motif has also been incorporated in the synthesis of heterocyclic dithione ligands, such as the piperazine ring (R_2Dt^0, R = Me, ^{i}Pr, Et, cyclodecyl, CH_2Ph). [33,35–40 41] Heterocyclic derivatives are the most prominent class of dithione ligand, and other examples of heterocyclic dithione ligands include R_2dazDt^0[4], R_2timDt^0, $ddDt^0$ [42], and $tamDt^0$ [43]. The synthesis of heterocyclic dithione ligands can follow the general procedure shown in Fig. 2, A and B. The heterocyclic dithione ligands can be synthesized from a condensation reaction of *N,N′*-substituted 1,2-diamines with diethyl oxalate to form a dione. The dione is then converted to a dithione, through sulfurization using Lawesson's reagent. With a slight modification as in Fig. 3 (A), optically active dithione ligands have been synthesized [44].

The α-dithiones, on the other hand, differ from dithiooxamide in that they do not incorporate an amide group in their RC(=S)C (=S)R common basic subunit. Examples of such derivatives are R_2dt [6,32,33] and the cyclic ligand $ddDt^0$[41,42]. Such molecules have been synthesized utilizing the photochemical activation of dithiocarbonate, such as compound **1**. (Fig. 3) [45]. In solution, the α-dithione molecule, **2**, is in equilibrium with its valence tautomeric dithiete form, **4**.

2.2. Synthesis of Semi-1,2-dithione

The radical anionic oxidation state of the dithiolene ligand is the least studied form of the dithiolene ligands. Semi-1,2-dithiones are transient and very reactive, limiting their study to EPR and computational analysis [46–49]. The first stable anionic radical dithiolene ligand **5** (R = 2,6-diisopropylphenyl) has been synthesized utilizing the first anionic N-heterocyclic dicarbene (NHDC), shown Scheme 1 [50,51]. The distinguishing property of **5** is the ability to readily undergo oxidation or reduction in a chemical reaction [52]. Treatment of **5** with $[Ph_3C][BF_4]$ or trace amounts of O_2 results in oxidation to produce the dimer (**6**) of the corresponding dithione ligand. Conversely, reacting **5** with the reducing agent cobaltocene (CpCo) results in the reduction of the ligand to afford the dimeric dithiolate **7**. Incorporation of the anionic radical dithiolene ligands into coordination compounds can provide precious insight into the chemistry of these ephemeral dithiolene species.

2.3. Spectroscopic properties of dithione ligands

UV–Vis, infrared, and NMR spectroscopies have played an important role in the characterization of free dithione ligands. Dithione ligands exhibit characteristic spectroscopic signatures due to the dithione unit (RC(=S)C(=S)R). Various substituents, however, alters the spectroscopic features of the ligand. In the case of the α-dithione molecule, **2** (Fig. 4), the UV–Vis spectrum can change drastically depending on the solvent polarity in which it was recorded. This is marked by a large change in band intensity of the transition near 470 nm (Fig. 4). [45] The high-intensity band is favored in more polar solvents and intensity increases with a bathochromic shift of the 470 nm band. Band intensity and position are dependent on solvent polarity, which controls the equilibrium between dithione and dithiete tautomeric forms. More polar solvents favor the dithione form which results in the high-intensity band at 470 nm. Decreasing solvent polarity shifts the equilibrium of the dithione form **2** and **3** to the closed dithiete form **4**, which implies that electrons are sufficiently delocalized to stabilize the formation of both tautomeric forms. However, using solvent polarity to control the equilibrium between dithione and dithiete has not been explored in detail for other dithione ligands.

Generally, dithione ligands exhibit a band at ~300–317 nm and overlapping shoulder bands at ~430–460 and 460–516 nm. The high-energy band is due to **π-π** * transition, while the low energy bands originate from n-**π** * transitions. For example, *N,N′*-dimethylpiperazine dithione (Me_2Dt^0) ligand exhibit bands (ε, $M^{-1}cm^{-1}$) of 418 nm (7 2 5); 312 nm (12,370), and 275 nm (22,770, sh). Metal complexes of such ligands often exhibit metal-to-ligand (MLCT) charge transfer transitions which is described in detail in later sections [53].

^{13}C NMR spectroscopy can provide useful electronic information about thiol-containing organic molecules [54]. To date, only a handful of dithione ligands have been characterized by ^{13}C NMR spectroscopy, where the δ(C=S), serves as one of the key signatures of dithione ligands. The heterocyclic dithione ligands (Fig. 5) exhibit δ (C=S) resonances that range from 180 to 190 ppm depending on the ring substituents [44].

Asymmetric substituents on the ring alters the symmetry of dithione ligands, resulting in inequivalent C=S units with different chemical shifts. [44] Dithione ligand δ (C=S) resonances are shifted ~65 ppm upfield from the δ (C=S) resonance of the simplest thioketone, thioacetone. The δ (C=S) resonances observed for dithione ligands are much closer to the reported value for tetramethylthiourea. The inclusion of tertiary amines that are α to the thiocarbonyl allow for electron delocalization between heteroatoms. Electron delocalization provides more shielding to the thiocarbonyl and produces an upfield shift in the δ (C=S) resonance. Thiocarbonyl resonances can be further tuned by adding electron-withdrawing and donating groups to induce further downfield or upfield shifts respectively. Additionally, coordination of the ligand to a metal center can also induce slight upfield shifts in thiocarbonyl resonance.

2.4. Geometric structure

The molecular structures of several dithione ligands have been characterized by single crystal X-ray crystallography. The key bond lengths of the dithiooxamide unit. i.e., C=S, C–C, and C-N are found to be similar (Table 1).

The average C=S bond length is ~1.65 Å, and the C–C bond distance between the two thioamide groups is in the range of 1.45–1.54 Å. This distance falls within the range of C(sp^2)-C(sp^2) bond lengths found in other molecules characterized by X-ray crystallography, indicating that there is no net electronic delocalization in the ground state between the thioamide moieties. [61]. Similar bond lengths in dithione ligands are indicative of the minimal electron delocalization between the two (N-C=S) moieties [42]. The atomic geometry of the nitrogen of the thioamide offers insight into the delocalization of electrons for these ligands. Molecular structures of free dithione ligands show the nitrogen to be in a trigonal planar geometry, the expected geometry of sp^2 hybridized nitrogen, suggesting a delocalization of electrons between nitrogen and sulfur. From the bond distances, thus it appears that molecules exist in the thioamide enolate form (Fig. 6). However, bond length alone cannot exclusively be used in understanding the electron delocalization, as condensed phase effects can also influence bond length. Bond length in corroboration with other spectroscopic signatures, such as vibration spectroscopy, can reveal the true nature of bonding in dithione molecules.

3. Electronic structures

3.1. Ene-1,2-dithiolate(2−) and dithione

The exact nature of the electronic structure of the dithiolene ligands depends on the type of the ligand i.e., substituents on the dithiolene moiety and should be corroborated by experimental data. Thus, the frontier orbitals description discussed here should only be used as a guide; especially in discussing the coordination chemistry of metal dithiolene compounds.

Several models have been developed to elucidate the electronic structure of dithiolene ligands and to better understand their bonding to metals [62–65]. One model describes metal coordination with respect to the symmetry of the participating orbitals. Sulfur p-orbitals can be described based on their symmetry and orientation in relation to the metal. Based on their orientation, sulfur orbitals can either be in-plane (S_{ip}) or out-of-plane (S_{op}) with respect to metal orbitals. Valence orbitals were calculated using density functional theory (DFT) and *ab initio* methods for the basic $[S_2C_2H_2]^{2-}$ unit (Fig. 7) [62–65]. Calculations and experimental data agree that the electron distribution is predominantly localized on the sulfur atom. Theoretical calculations performed on metal(dithiolene) complexes a support that metal-sulfur coordination bond is mostly sulfur in character, with little participation from the ethylene unit [66]. From the description discussed here, sulfur molecular orbitals can be categorized as in-plane ($\phi_{ip}^{a'}$) and ($\phi_{ip}^{a''}$), or out of plane ($\phi_{op}^{a'}$) and ($\phi_{op}^{a''}$). Symmetry labels, a’ and a”, are added with respect to the symmetry of the wave function to the mirror plane that bisects the C=C bond.

DFT calculation at B3LYP/6-311G+(d,p) level of theory on the dithione ligand $^{i}Pr_2Dt^0$ shows frontier orbitals that are rich in sulfur character (Fig. 8). Hoffman's butadienoid model describes the molecular orbitals, χ_1 and χ_2, as C=S π-orbitals that are responsible for metal coordination [67]. The corresponding π * orbitals, χ_5 and χ_6, are energetically well separated from occupied orbitals. The highest occupied molecular orbital HOMO-1 (χ_3) and HOMO (χ_4) are nonbonding S p-orbitals, which are perpendicular to the C=S π-orbitals. The redox-active molecular orbital is the lowest unoccupied orbital (LUMO), χ_5 , which participates as an electron acceptor when the ligand is reduced.

3.2. Effects of oxidation state on geometric and electronic structures

Geometry optimization calculations were performed on the corresponding semi-1,2-dithione and ene-1,2-dithiolate(2−) forms of the $^{i}Pr_2Dt^0$ ligand to probe the effects of reduction. Resulting molecular orbital diagram and select bond lengths are shown in Fig. 9. A good indicator of the ligand oxidation state is the length of the C2-C3 bond. Reduction of the dithione ligand results in a 0.143 Å decrease in C2-C3 bond length, which corresponds to an increased bond order. There are also 0.118 Å and 0.108 Å increases in C-S and C-N bonds respectively as they become more single bond in character. The shortening of the C2-C3 bond imposes slight changes in the geometry of the piperazine ring and its substituents. The S1-C2-C3-S4 dihedral angle flattens from 45.77° in the fully oxidized state to 3.91° in the fully reduced state. The atomic geometry of nitrogen also changes from trigonal planar to trigonal pyramidal as the ligand is reduced to the ene-1,2-dithiolate(2−) form. Change in the atomic geometry of nitrogen was observed in the S1-C2-N5-C6 dihedral angle, which increases from 9.40° to 46.24°.

Molecular orbital diagrams of the redox-active orbitals for each oxidation state of the ligand are shown in Fig. 10. Electron distribution for the HOMO of the dithione ligand is concentrated on sulfur p-orbitals, and after reduction, the electron distribution delocalizes equally across both thioamide moieties. As a result, the HOMOs of the reduced states are almost identical to the LUMOs of the fully oxidized dithione. Mulliken population analysis, used to produce a spin density plot of the unpaired electron of the semi-1,2-dithione form (Fig. 10), places half of the spin density on the sulfur atoms and roughly a third of the spin density on the C2-C3 bond. The increased spin density on the C2-C3 bond reflects the increase bond order and subsequent shortening of the bond. Shortening the C2-C3 bond length changes the geometry of the piperazine ring i.e., the ring is less distorted and more planar. As electrons are added to this system the relative energies of the redox-active orbitals increase, resulting in the flattening of the S1-C2-C3-S4 plane. Such conformational change is unfavored due to the saturated nature of the methylene backbone of the ring, which makes the addition of the second electron to the semi-1,2-dithione more difficult. This is observed in the orbital energy diagram, as the energy difference between donating and accepting orbitals is 0.32 eV less for $^{i}Pr_2Dt^0$ than $^{i}Pr_2Dt^{1-}$.

4. Dithione and butadiene

Direct comparisons can be drawn between dithione ligands and the prominent organic molecule, butadiene. Both molecules contain 4 π-electron systems and coordinate to metals.

The method of coordination for both ligands is different, which directs how orbital binding occurs. In the case of dithione, the lone pairs on the sulfur atoms allow the ligand to chelate to the metal. Butadiene must coordinate through π electron interactions with the metal, which requires the molecule to coordinate at an angle to produce effective orbital overlap with symmetry allowed metal orbitals. Chelation allows the dithione and metal to adopt a planar geometry, which is not a possible conformation for coordinated butadiene. Although, butadiene coordination does allow for π back bonding interactions.

Butadiene is simply two ethylene molecules that are connected serially, and the molecular orbitals of butadiene can be expressed as a combination of π-molecular orbitals from two ethylene molecules. In comparison to the energy of two ethylene molecular orbitals, bonding between the two ethylene units lowers the overall energy of butadiene molecular orbitals. The resulting butadiene HOMO is higher in energy than the HOMO of ethylene, while the LUMO of butadiene is lower than the LUMO of ethylene.

Dithione and butadiene also share similarities in their reactivity with organic molecules containing 2 π-electron systems, such as diene or ene-1,2-dithiolate(2−). Both demonstrate the ability to carry out [4 + 2] Diels-Alder type of cycloaddition reactions. The description of butadiene and ethylene as 4 π and 2 π-electron systems is illustrated in Fig. 11, respectively [68]. The 4 π-electron system dithione can react with ene-1,2-dithiolate(2−) as the dienophile, resulting in a [4 + 2] cycloaddition (Eq. (1)).

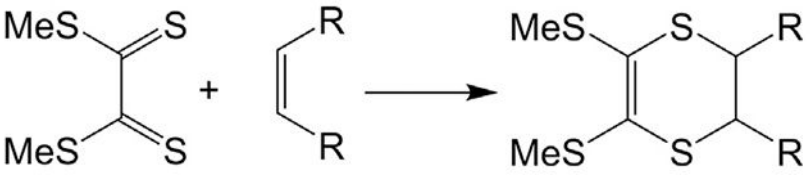

(1)

Typically, the strongest interaction occurs between the HOMO of the diene and the LUMO of the dienophile, as the diene donates electrons to the LUMO of the dienophile to make the bond. The reaction between dithione and ene-1,2-dithiolate is the opposite, and the dithione accepts electrons. The energy of the π * LUMO of dithione is lower in energy than the HOMO of ene-1,2-dithiolate(2−), which results in a reverse of electron demand when compared to a classical Diels-Alder system [69]. The dienophile therefore acts as the electron donator and the electron-deficient dithione the acceptor. Concerted reactions between dithione and a multitude of dienophiles have been performed to better understand the such reactions [70].

5. Metal coordination

5.1. General properties

The first metal dithiolene complexes were first reported as analytical reagents almost 80 years ago [71]. The electron-rich nature of dithiolene complexes makes them well suited for applications in the areas of magnetism, conduction, nonlinear optics, sensors, dyes, and

catalysis [1,72–75]. Interest in such complexes has also expanded to biological applications, as all pterin containing Mo and W enzymes possess a dithiolene unit [12,13,15,17]. Dithiolene mimics with transition metals have been synthesized and characterized to model relevant metal centers that are present in metalloenzymes, such as molybdoenzymes [14].

Despite the interest and the non-innocent nature of the dithiolene ligands, well-characterized metal complexes of fully oxidized dithione ligands are rare, and a majority of the research with fully oxidized ligands is focused on lower valent metal complexes. A Cambridge Crystallographic database search conducted on November, 3rd, 2019 produced only 66 hits where at least one of the ligands is in two-electron oxidized dithione form, compared to ~2000 hits for the metal-ene-1,2-dithiolate(2−) complexes searched at the same time [76]. Therefore, the structure, spectroscopic features, and reactivity of metal-dithione complexes are less explored. Importantly, the metal complexes of the oxidized ligand afford interesting fundamental chemistry that may be important in niche applications and certainly generating new knowledge.

Due to their non-innocent nature, the description of the electronic structures of metallodithiolene complexes is complicated. In order to elucidate the electronic structure of metal dithiolene complexes, many spectroscopic techniques must be corroborated to provide an adequate description. Such spectroscopic techniques include, but are not limited to, UV–Vis, electron paramagnetic resonance (EPR), X-ray absorption (XAS) at the sulfur K edge, resonance Raman (rR), and magnetic circular dichroism (MCD). Such studies have been complemented by electronic structure theoretical studies e.g., DFT and ab initio methods, and together have produced a detailed picture of the metal center. Dithiolene coordination to a metal center requires the interaction of the relatively low lying metal orbitals with higher energy dithiolene molecular orbitals. Sulfur p-orbitals of the right symmetry can interact metal orbitals to produce mixed metal–ligand molecular orbitals [77]. Electron delocalization is therefore extended to the metal ion and electrons are distributed across the five member chelate. [65] Dithiolene complexes of mixed ligand oxidation states result in uneven electron delocalization. In such cases the more electron-rich ligand dominates the HOMO while the relatively electron-poor ligand dominates the LUMO.

The molecular orbitals of $[M(Dt^{2-})(Dt^{1-})]^z$ complexes, where Dt^{2-} = ene-1,2-dithiolate(2−) ligand, Dt^{1-} = semi-1,2-dithione, M = Ni, Pd, Pt, Co, and Cu and z = 1−, and where M = Au, z = 0, are simplified in Fig. 12 [78]. The a_u and b_{1u} orbitals are purely ligand in character, while the $2b_{2g}$, $2b_{3g}$, and 1_{b1g} orbitals are delocalized over both metal and ligand orbitals The redox active $2b_{2g}$ orbital, the antibonding combination of the ligand b_{2b} and metal d_{xy} orbitals, determines whether oxidation is ligand- or metal-centered. This is determined by the extent to which electrons are delocalized across the $2b_{2g}$ orbital. The effects dithiolene substituents on the electronic structure have also been determined [66,79]. The C_2S_2 π-donor substituents generally raises the energy of the HOMO and the LUMO, and interaction between ligand and metal orbitals further decreases the HOMO-LUMO gap.

5.2. Metal coordination by dithione ligands

In acyclic dithiooxamides, the dithione (RC(=S)C(=S)R) unit can exist in either the trans- or cis-conformation (Fig. 13).

Dithiooxamide ligands preferably bond to metal atoms in their cis form through S, S atoms. Coordination in the trans conformation through N, S atoms is not as common. Examples of such coordination has been reported in the synthesis of nitrogen heterocycles, dicopper complexes, and coordination polymers [80–82]. Coordination in the trans conformation is favored in the presence of stabilizing intermolecular N–H···N hydrogen bonding and week N–H···S = C interactions [83,84]. Dithiooxamide ligands coordinate through their sulfurs (Fig. 14), **8** as opposed to S, N coordination, **9** resulting in square planar complexes of D_{2h} symmetry, where the ligand halide forms hydrogen bonds [37,53]. The cis conformation is imposed on dithiooxamide derivatives that are incorporated into a ring, such as the Me_2Dt^0 ligand [44,85]. The molecular structure of both cyclic and acyclic dithione ligands exhibit similar bond lengths. Depending on their substituents, the S-C–C-S torsion angle of *cis*-dithione ligands decrease upon coordination to the metal. The acyclic form of dithione ligands experience a greater reduction in S-C–C-S torsion angle when compared to heterocyclic dithione ligands, where the dithione moiety is appended to a ring. The rigidity of the ring of heterocycles reduces the conformational mobility and the initial S-C–C-S torsion angle of the free ligand to −35°, whereas acyclic *cis*-dithione ligands are observed to have a torsion angle of −90°. Consequently, acyclic dithione ligands also have larger torsion angles after coordination to the metal.

Electronic study of Ni, Pd and Pt complexes, of D_{2h} symmetry, showed low energy transitions between 400 and 600 nm that were like those of $M(mnt)^{2-}{}_2$ (mnt = maleonitriledithiolate). Low energy transitions have been designated as M(d) to L(π *) charge transfer bands [86,87]. In the following sections, we will discuss the coordination of the dithione ligand and semi-1,2-dithione to a metal ion resulting in mono, bis and tris complexes.

From the discussion on the electronic structure of the dithione ligands, it is clear that dithione ligands can be viewed as electron-deficient and thus can serve as an acceptor moiety in a molecular architecture. This electron deficiency has been utilized in developing molecular donor–acceptor systems, also described as push-pull molecules (where an electron-rich moiety acts to push electron density to an electron-deficient moiety). Molecular donor–acceptor systems are of great interest in the chemical and materials science. Typically, such systems have been organic-based, where the charge transfer moves from a donor orbital to the acceptor orbital in an intramolecular charge transfer (ICT) along with a π conjugated system, such as benzene or stilbene [88–91]. Such systems have been utilized in classical molecular engineering designs and can be useful in the development of light-emitting diodes and sensors [92,93]. Coordination compounds incorporating organic ligands with π conjugated systems have gained interest due to their charge transfer capabilities. Donor-acceptor systems that generate charge-transfer transitions are of interest due to their potential applications such as artificial photosynthesis and nonlinear optics (NLO) [94–103]. Charge transfer transitions such as metal–ligand (MLCT) and ligand–metal (LMCT) charge transfers are common examples of charge transfer processes in coordination complexes [104]. When the ligand environment surrounding the metal center includes ligands that are in different oxidation states, it is possible to observe inter-ligand charge transfers (ILCT)

[105,106]. Dithione ligands have been utilized as electron receptors in developing such molecular architectures.

5.3. Comparison to 1,2-Dithiete coordination

As shown in Figs. 1 and 3, dithione ligands are in resonance with dithiete ligands, although dithiete ligands coordinate to metal centers in a much different manner. Unlike dithione ligands, dithiete ligands do not maintain their native oxidation state upon reaction with the metal center. Dithiete ligands initially act as an oxidizing agent and are reduced by 2 electrons to their ene-1,2-dithiolate(2−) state before coordinating to the metal. For example, a reaction between the zerovalent molybdenum compound $Mo(CO)_6$ with three equivalents of the neutral ligand bis-(trifluoromethyl)-dithiete (tfd) first results in a redox reaction. Here, Mo^0 is oxidized to Mo^{VI} and the three equivalents of tfd are reduced to their ene-1,2-dithiolate(2−) state in a 6 electron process. Only after the dithiete is reduced to its dianion state will the ligand be able to coordinate to the metal [107]. Metal(ene-1,2-dithiolate(2−)) complexes of Mo [108,109], Ni [110], Pd [111], Fe and Ru [112] have been synthesized using dithiete ligands to produce mono, bis, and tris metal dithiolene complexes.

The majority of dithiete ligands that have been used for metal coordination are acyclic ligands, which are in resonance with the R_2Dt α-dithione ligand. Bulky and strong electron-withdrawing substituents on the R_2Dt ligand favor the formation of the dithiete resonance. Heterocyclic ligands prefer the dithione resonance over the dithiete due to unfavorable conformational changes associated with the dithiete. Conversion to dithiete for heterocyclic dithione ligands is like the reduction of dithione to ene-1,2-dithiolate(2−). As described in Section 3.1, DFT calculations of the different oxidation states $^iPr_2Dt^0$ show an increase in HOMO/SOMO energy as the C2-C3 bond order increases. A similar increase in bond order must occur for the dithione to fully convert to the dithiete resonance structure. The conformational limitations imposed by the unsaturated cyclic ring pushes the equilibrium heavily towards the dithione resonance structure.

5.4. The structure and coordination of Semi-1,2-dithione

The term dithiolene is broad and includes a wide variety of bidentate sulfur ligands in various oxidation states. Of the possible oxidation states available to dithiolene ligands, the anionic radical (Dt^{1-}) is the least well characterized. The molecular structure of the semi-1,2-dithione **5** allows for the comparison of C–C and C-S bond lengths to Me_2Dt^0 and, the well-known ene-1,2-dithiolate ligand, maleonitriledithiolate (mnt^{2-}) (Table 2). The anionic radical **5** exhibits intermediate bond lengths between the extreme oxidation states, and the change in C–C and C-S bond lengths follow the same trend that was calculated for the $^iPr_2Dt^{0/1-/2-}$ ligand series. The EPR spectrum and DFT calculations of **5** (Scheme 2) agree that the SOMO is predominantly C-S π-antibonding and C–C π-bonding in character. This strongly agrees with the spin density plot of $^iPr_2$-Dt^{1-} and further supports that the unpaired electron is based primarily on the S-C–C-S unit.

There are few examples of compound **5** coordinating to metal centers and they are limited to Mg [114] and Ge [51] to produce mono- and bis-complexes. Compound **5** coordinates to a metal like a 1,2-dithiete, resulting in the reduction of the ligand during coordination.

This single electron reduction of **5** produces the corresponding ene-1,2-dithiolate(2−) ligand to produce the reduced dithiolene complex. There are no examples of **5** retaining its initial oxidation state or oxidizing during coordinating to a metal. However, **5** does maintain its radical nature in the synthesis of boron dithiolene radicals shown in Scheme 2 [115].

5.5. Mono(dithione) complexes

Several coordination complexes have been synthesized using a single dithione ligand in conjunction with other stabilizing ligands to produce a metal complex with a mixed ligand system. Such complexes include metal ions such as Ni^{2+}, Pd^{2+}, Pt^{2+}, Au^{2+} and Hg^{+} [53,116,117]. Initial reports of $M(X)_n(Dt^0)$ complexes include halide and carbonyl complexes: $M(R_2dto)X_2$, (M = Ni, Pd, Pt, R_2-dto = dithiooxamide family; X = halide) [118], $Re(CO)_3(R_2dto)X$ (R = Et, Bz; X = Br and Cl) [42], $Mo(CO)_{4-n}(PR_3)_ndto$ (n = 0, 1, 2) [119], and $[Fe(S_2C_2(SMe)_2)(CO)_2PPh_3]$[30]. Significant progress in the development of the coordination chemistry has been made with heterocyclic dithione ligand based on the piperazine framework. X-ray crystallographic analyses of complexes with heterocyclic dithione ligands (R_2Dt^0; R = Me, Bz), shows that the ligand remains oxidized while coordinated. This is supported by the measured C-S and C-N bond lengths of 1.66 Å and 1.326 Å, respectively, as observed in $Zn(Bn_2Dt^0)Cl_2$[117] and $[ReBr(CO)_3(Me_2Dt^0)]$ [42]. Depending on the R group, the dihedral angle between thioamide moieties can differ. For example, the ring system imposes a *cis*-conformation on the dithione ligand of $[ReBr(CO)_3(Me_2Dt^0)]$, which results in a dihedral angle of 35.4°. The electronic spectra of these complexes exhibit two intense ligand-based absorption bands, (ε) of ~4×10^3 $M^{-1}cm^{-1}$, with a low energy band of around 530 nm (Fig. 15) [42].

There is a positive solvatochromic effect, displaying a significant bathochromic shift when spectra were collected in acetonitrile instead of chloroform. The band at 530 nm has been designated a metal to ligand charge transfer (MLCT) character, as the dithione acts as a relatively strong electron-accepting ligand.

Complexes that contain both a dithione and ene-1,2-dithiolate (2−) show a redistribution of π-electrons towards the electron-rich ligand. In this case, the HOMO is predominantly the push ligand (ene-1,2-dithiolate(2−)) whereas the LUMO is mostly the pull ligand (dithione) with some metal character in both molecular orbitals. Inter-ligand charge transfer between HOMO-LUMO has been observed in such systems, and the presence of electron distribution on the metal centers in both molecular orbitals indicates that the metal actively facilitates charge transfer between ligands. Deplano and coworkers have taken advantage of this behavior and utilized mixed ligand complexes in the development of second order nonlinear optical materials [120–122]. This has led to the development of square planar $[M(Dt^{2-})(Dt^0)]$ complexes, mainly with the d^8 metal centers (Ni^{2+}, Pt^{2+}, and Pd^{2+}) [72]. The ligands of these square planar complexes can be tuned with electron-withdrawing and donating properties to aid in the redistribution of the π-electrons. Such tuning allows for the achievement of properties geared toward enhanced NLO applications [72]. Mono(dithiolene) complexes, consisting of a single dithione and other non-dithiolene ligands, have also been developed for material science applications [123,124].

Nemykin et al. have reported a mono(dithione) complex, Mo $(CO)_4(Me_2Dt^0)$ (Me_2Dt^0 = *N,N′*-dimethyl piperazinedithione) (Fig. 16), where spectroscopic studies and DFT calculations indicate that Mo is zero-valent [125]. ^{13}C NMR spectrum exhibits a peak at 184.4 ppm due to the presence of C=S moiety, which is shifted from 189 ppm C=S resonance of the free ligand. The ^{13}C NMR spectrum supports that the ligand is fully oxidized while coordinated. In solution, the complex exhibits a negative solvatochromic effect. The complex shows a low energy band at 650 nm that shifts to higher energy as the solvent becomes more polar. TDDFT-PCM calculations indicated the band at 650 nm was predominantly a d_{xz} to LUMO transition, while the d_{xy} and d_{yz} to LUMO transitions showed minor contributions. The low energy band was determined to be a MLCT band. Density functional theory (DFT) calculations demonstrated the energetically isolated lowest unoccupied molecular orbital (LUMO) is practically a pure **π*** orbital that is localized on the C(=S)-C(=S) fragment of the dithione ligand. This energetically isolated LUMO accepts electron density from orbitals comprised of the metal and carbonyl ligands. This transition giving rise to a solvent sensitive band at ~600 nm [125].

The dithione ligand coordinates to the metal center through the interaction of out-of-plane sulfur orbitals with metal orbitals. The HOMO of molybdenum complexes with a dxy ground state is the result of interactions between in-plane sulfur orbitals and the d_{xy} atomic orbital of the molybdenum. Calculations show that the HOMO of $Mo(CO)_4(Me_2Dt^0)$ is predominantly dxy atomic orbital in character, which shows Mo $d_{xy} \rightarrow$ CO**π*** back bonding interactions (Fig. 17). The HOMO-1 and HOMO-2 predominantly consist of molybdenum d_{xz} and d_{yz} atomic orbitals with significant contributions from carbonyl **σ**orbitals. These three nearly degenerate orbitals are energetically well-separated from the other doubly occupied orbitals. The HOMO and the two lower nearly degenerate orbitals are dominated by molybdenum atomic orbitals, which is consistent with a $4d^6$ electronic configuration of the metal ion.

Tetracarbonyl complexes of tungsten either with a dithiolene or a dithione have been reported [126]. Ligand oxidation state determines the geometry of the complex. For example, $W(CO)_4(Me_2Dt^0)$ exhibits an octahedral geometry while $W(CO)_4$(mdt) (mdt = 1,2-d imethyl-1,2-dithiolate) adopts a trigonal prismatic (TP) geometry. Structural data supports a zero-valent W^0 oxidation state for the dithione complex and a W^{2+} oxidation state for the ene-1,2-dithiolate(2−) complex. The bond lengths between Mo and W dithione complexes are similar (Table 3). The 0.006 Å shortening of the C–C bond and 0.012 Å increase in C-S bond length suggests that the dithione ligand of the W complex has slightly more electron density than that of the Mo dithione ligand. This could be due to the larger shell of W^0, making it a softer Lewis acid than Mo^0. Also, the similarities in bond distances between W^0 and Mo^0 complexes demonstrate that the addition of f-block electrons does not impact coordination of the dithione ligands and any lanthanide contraction effects are irrelevant.

The electrochemical study of $W(CO)_4Me_2Dt^0$ and $W(CO)_4$(mdt) produced two ligand-based redox couples from their respective dithiolene ligands [126]. In the context of their tungsten-tetracarbonyl complexes, the Me_2Dt^0 ligand showed couples at moderately more reducing potentials ($E_{1/2}$ = −1.30 V, −1.68 V) than the mdt ligand ($E_{1/2}$ = −1.14

V, −1.36 V). The reduction couples for the dithione ligand are more negative due to unfavorable ring conformation changes associated with reducing cyclic dithione ligands. Peak-to-peak separations for dithione couples (ΔE_p = 66 mV, 82 mV) also differ from the ene-1,2-dithiolate(2−) ligand (ΔE_p = 130 mV, 91 mV). The smaller ΔE_p values for $W(CO)_4(Me_2\text{-}Dt^0)$ suggest that no geometric change occurs as the complex is reduced. The dithione complex remains in its octahedral conformation throughout electrochemical perturbation while the ene-1,2-dithiolate(2−) complex changes from TP to octahedral, which is support by DFT calculations.

DFT studies of $W(CO)_4$(mdt),model the HOMO to be composed of metal–ligand **π**-bonding orbitals, while the LUMO is the antibonding counterpart. The ene-1,2-dithiolate(2−) complex, $W(CO)_4$(mdt), has a trigonal pyramidal geometry (TP) due to improved symmetry allowed mixing between W and dithiolene orbitals. Conversely, the dithione compound adopts an octahedral geometry. An octahedral geometry is preferred for the dithione compound due to greater ligand–metal orbital overlap and higher energy ligand **π**-orbitals generated by the conjugated N-C-S unit. Dichloromethane solutions of $W(CO)_4(Me_2Dt^0)$ exhibit a strong band at 669 nm while the corresponding Mo complex exhibits a band at a similar position 678 nm in the same solvent.

Several mono(dithione) complexes have been synthesized while developing sensors to chelate heavy metals for environmental remediation. Dihalogen and dithione ligands can be reacted together to produce dihalogen-dithione adducts that can dissolve precious or toxic metals quantitatively and in a short time under mild conditions (Fig. 18) [127].

The adducts react by the interaction of an **σ**-donor with a high energy HOMO and a dihalogen that acts as an acceptor through its low lying LUMO(**σ***). Dithione-iodine adducts (DI_2) of the type D-I-I and $D\text{-}I^+\text{-}I^-$ have been isolated and characterized by Raman spectroscopy [128]. Me_2Dt^0 is most suitable for dissolving Pd, Au, and Pt (Fig. 18). These adducts can be altered to chelate heavy toxic metals such as cadmium and mercury, potentially providing a remediation strategy for toxic metals in electronic devices [129–131]. The Deplano group have synthesized, isolated, and characterized dithione-dihalogen adducts of Hg and Cd mono(dithione) complexes $[CdI(Me_2Dt^0)_2]I_3$ and $[HgI_2(Me_2Dt^0)]$. These compounds were isolated by reacting elemental cadmium (powder) and mercury (liquid) with their respective dithione-dihalogen adducts [10]. Dithione ligands have also been used in dissolution of gold [132] and recovery of mercury under mild conditions [130]. IR spectroscopy of the recovered mercury compound, $[Hg(Me_2\text{-}dazDt^0)I_2]$, ($Me_2dazDt^0$ = *N,N'*-dimethylperhyrodiazepine-2,3-dithione) produced a ν(CN) = 1,532 cm^{1-} vibration for coordinated ligand and a ν(CN) = 1,493 cm^1 vibration for free ligand. The 40 cm^{1-} increase in vibration frequency is the result of greater CN double bond participation as sulfur atoms donate electron density to the metal.

Complexes that possess both a fully oxidized and fully reduced dithiolene ligand have also been presented, which result in electronically asymmetric complexes. Electronically asymmetric square planar complexes with a d^8 metal ion result in a ground state that is **π**-delocalized, and such a complex can act as a donor–acceptor system much like their electronically symmetric counterparts $[M(II)(Et_2dazDt^0)(mnt)]$ (where M = Ni, Pd,

or Pt; Et_2dazDt^0 = *N,N'*-diethylperhyrodiazepine-2,3-dithione) is an example of such an asymmetric system. All three complexes exhibit either one or two low energy, strong charge transitions in the UV–Vis region. From DFT and TDDFT calculations the low energy transitions were attributed to mixed metal–ligand-to-ligand charge transfer (MMLL'CT); such transitions have been indicated in NLO properties such as molecular hyperpolarizability [95,98,122].

In complexes where one fully oxidized dithione and one fully reduced dithiolene ligand coordinate to the metal ion, the C_2S_2 unit from the dithiolene serves as an electron-donor, while the C_2S_2 unit from the dithione acts as an electron-acceptor, resulting in LL'CT bands. Electron donating substituents on the dithione raises the energy of the LUMO and, to some extent, that of the HOMO [43]. In general, the π-acceptor nature of the dithione ligand favors the formation of low-valent complexes while the reduced form of the ligand stabilizes higher valent complexes. Despite this, higher valent Mo(IV) complexes have been stabilized by the fully oxidized dithione ligand [133–135]. An electronic asymmetry can also be induced with a single fully oxidized dithione ligand and two thiophenol ligands as observed in $Mo^{IV}O(SPh)_2(^iPr_2Dt^0)$ where SPh = thiophenol. This complex was synthesized from $[MoOCl(^iPr_2\text{-}Dt^0)_2][PF_6]$ through a ligand exchange reaction with SPh. The UV–Vis spectra of $Mo^{IV}O(SPh)_2(^iPr_2Dt^0)$ shown in Fig. 19. exhibited a low energy band at 540 nm, which is ~200 nm higher in energy than the ~750 nm band observed for the initial $[MoOCl(^iPr_2Dt^0)_2][PF_6]$ complex [135]. The molecular structure of this complex revealed a large folding of the dithione ligand, with a reported fold angle of ~70° along the S…S vector. Such a large fold angle is not typically observed in Mo(IV) dithiolene complexes [67,136,137]. A combination of electronic absorption and resonance Raman spectroscopies was used to probe the basic electronic structure responsible for the large fold-angle distortion. The intense charge transfer transition observed 540 nm (18,000 cm^{-1}) is assigned as a thiolate → dithione ligand-to-ligand charge transfer (LL'CT) transition, which also possesses Mo(IV) → dithione charge transfer character. DFT calculations showed a different electronic structure than what has been observed in complexes possessing ligands in the same oxidation state. In $Mo^{IV}O(SPh)_2(^iPr_2Dt^0)$ the HOMO is primarily SPh ligand character and the LUMO is $^iPr_2Dt^0$ in character [135].

Dithiolene ligand coordination to oxo metal or cyclopentadienyl metal centers results in a folding of the dithiolene moiety along the S…S vector. In bent metallocene dithiolate compounds, Cp_2M (dithiolate) (M = Ti, V, Mo, W, and Cp is η^5-cyclopentadienyl) with d^0, d^1, and d^2 electronic configurations, the dithiolene ligand folds to enable the sulfur π bond orbital to interaction with an empty in-plane metal d-orbital and increase stability. Fold angles from the crystal structures of Cp_2M(dithiolate) systems also indicated that more electron-deficient the metal centers resulted in greater fold angles [67]. In the last three decades, Enemark and others have conducted a series of spectroscopic studies demonstrating the dithiolene folding model in oxo-Mo(V) complexes. Several studies on the ligand fold of dithiolene complexes have been carried out using ene-1,2-dithiolate(2−) complexes. [137–142] A major consideration in these systems is the electron-deficient metal center that facilitates the ligand to metal charge transfer. For example, the complex $Mo^{IV}O(SPh)_2(^iPr_2Dt^0)$ has a d^2 metal electronic configuration that occupies the d-orbitals that are in the same plane as the dithione, so the metal cannot accept charge density. This

leaves the dithione ligand to act as the electron-accepting entity. From a state perspective, the dramatic ligand folding in $Mo^{IV}O(SPh)_2(^iPr_2Dt^0)$ is the result of a strong pseudo Jahn – Teller effect (pJT) effect with vibronic coupling between the A′ ground state and low-lying A' LL'CT excited states. Strong orbital mixing between occupied and virtual orbitals with Mo d^2_{xy} orbital character is derived from a strong pJT. The ligand folding distortion leads to an increase in the **π** acceptor ability of the dithione and the onset of new covalency. The pJT drives the large fold-angle distortion to yield a double-well potential in the electronic ground state, shown in Fig. 20 [135]. Thus, in this system, the thiolato ligands serve as the donor while the dithione serves as the acceptor entity resulting in the low-energy band. Such a Donor-Acceptor (D → A) haracter is typically observed in planar mixed-ligand metallodithiolene complexes [72,134,143], where the coplanar nature of the donor and acceptor ligands provide **π** orbital pathway for strong D → A charge transfer. The same concept can be extended to nonplanar systems when there exists a large acceptor ligand fold angle distortion that allows for in-plane orbitals of the donor to interact strongly with an out-of-plane orbital on the acceptor ligand. Recently, a set of mixed ligand Zn(II) dithione complexes, with either chloride or maleonitriledithiolate (mnt^{2-}) coligands, have been synthesized and characterized (Fig. 21) [144] .The molecular structures exhibit the expected tetrahedral geometry albeit the geometry is distorted. Zinc complexes **9** and **10** have mixed-valence dithiolene ligands and exhibit ligand-to-ligand charge transfer bands near 500 nm (Fig. 22), which is not observed in the corresponding chloro complexes. DFT calculations indicate that the HOMOs are heavily localized on the electron-rich (mnt^{2-}) ligand, and a LUMO comprised mostly of the electron-deficient dithione ligand. The molecular orbital diagram of Zn(mnt) ($^iPr_2Dt^0$), shown Fig. 23, [144] also supports the notion of the electron-deficient dithione ligand acting as the electron acceptor. Charge transfer is thus believed to proceed from the ene-1,2-dithiolate(2−) HOMO to dithione LUMO, showing ligand-to-ligand D → A property.

5.6. Bis(dithione) complexes

Bis(dithione) complexes have received attention in recent years due to their possible applications in the material science field [10,145–149]. Some of the first bis(dithione) complexes were $[Cu(R_2dto)_2][ClO_4]_2$ and $[Pd(R_2dto)_2]Cl_2$ (where R = *N,N'*-dibenzyldithio-oxamide and *N,N'*-dicyclodithiooxamide, respectively), which were structurally characterized with substituted derivatives of dithiooxamide (abbreviated R_2dto) [53]. Their bond lengths are shown in Table 4 as a representative summary.

The observed C=S bond lengths, 1.66–1.74 Å, are within the known range of structurally characterized dithione complexes, which suggests that the ligands are coordinated in their fully oxidized state [126,150,151]. S-M–S angles of nearly 90° suggest that complexes $[Pd(R_2dto)_2]Cl_2$ and $[Cu(R_2dto)_2][ClO^-_4]$ are square planar in geometry. The reported C–C bond length of 1.50 Å also supports that there is no electron delocalization across thioamide moieties in the ground state.

^{13}C NMR characterization of $[M(R_2dto)_2]X_2$ and $[M(R'_2dto)_2]X_2$ (where M = Pt, Pd or Ni; R_2dto = N,N'-diisobutyldithiooxamide (H_2-dibudto), or R'_2dto = N,N'-dimethyldithiooxamide (H_2dmdto) have been performed in both solution and solid states.

(Table 5). The C=S downfield chemical shift of δ 186–190 ppm is characteristic of dithiooxamide [53].

The electronic behavior of Cu(II) dithiooxamide complexes (Table 6) has been recorded at both room and liquid nitrogen temperatures with EPR spectroscopy. The reported ($g > g_e$ (2.0023) value supports a predominant d^2_{xy} ground state. Compound [Cu $(H_2dto)_2][ClO_4]_2$, exhibits a spectrum with $g_{\parallel} > g_{\perp} > g_e$, which implies a tetragonal molecular geometry. However, the possibility of a ClO^-_4 occupying a tetragonal position of a square planar molecule cannot be ruled out as the molecular structure was not discussed. The powdered sample did show a transition in the $\Delta M_s = 2$ region of the spectra, which indicates that all compounds were monomeric. Sulfur coordination to Cu(II) for these complexes is also thought to be strongly covalent, as indicated by the $g_{\parallel}$ values.

The synthesis of homoleptic bis(dithione) complexes is readily achieved and can be performed with metal salts and the desired dithione ligands. Several bis(dithione) complexes $[M(R_2Dt^0)_2]$ $[BF_4]_4$ (M = Pt, Ni, Pd and R = Me, ^{i}Pr) with a d^8 metal center electron configuration have been isolated and characterized. Homoleptic bis(dithione) complexes have mostly served as reactants in the synthesis of mixed ligand complexes as described earlier. For example, bis(dithione) complexes are used as starting material for the synthesis of $[M(R_2Dt^0)_2][M(mnt)_2]$ from $[M(Me_2Dt^0)_2]$ $[BF_4]_2$. Anionic bis(ene-1,2-dithiolate(2−)) complex of the same metal could also be used instead of the BF_4^- counter anion. Such bimetallic complexes show low energy bands between 450 and 700 nm (Fig. 24) [10]. Recently, a set of $Cu^{I/II}$ bis(dithione) salts of the formula $[Cu(R_2Dt^0)_2][PF_6]_X$ (R = Me, ^{i}Pr and X = 1,2) have been synthesized and characterized [152]. The D → A character for these complexes is dictated by their molecular geometries. The tetrahedral Cu^I complexes exhibit a strong MLCT at 530 nm that the square planar Cu^{II} complexes do not. The ability for Cu to participate as an electron donor in such D → A systems is determined by geometry-gated orbital mixing between Cu and S, which is limited in the case of square planar geometries.

The electrochemistry of dithiolene complexes demonstrates both ligand and metal redox chemistry, as the redox-active nature of dithiolene ligands also allows them to participate electron transfer activities. Cyclic voltammetry of bis(dithione) complexes show four quasi-reversible ligand-based redox couples (Fig. 25).

The $[Ni(Me_2Dt^0)_2]^{2+}$ complex for example, exhibits the ability to shuttle reversibly with the charge state 2+/+/0/−/2− as listed in Table 7 [147,153], which is characteristic of bis(dithione)M(II) complexes. The redox processes of these complex occur at essentially the same potential, which indicates that electron transfer is ligand-based and occurs independently of the metal center.

The properties of cationic $[Ni(R_2Dt^0)_2]^{2+}$ (R = Me and ^{i}Pr) have been investigated in solution, solid, and gas phases. The crystal structure of $[Ni(^iPr_2Dt^0)_2][BF_4]_2$ shows a square planar geometry of the nickel center, very similar to that observed for the Ni(ene-1,2-dithiolate(2−))$_2$ complex (Fig. 26). The C=S and C–C bond distances in $[Ni(^iPr_2Dt^0)_2]$ $[BF_4]_2$ are very similar to that of the ligand. The C=S and C–C bond distances are consistent with an oxidized form of the ligand coordinated to the metal. The observed C=S and C–C

distances are different than those for Ni(ene-1,2-dithiolate(2−)) complexes and reflect the change in ligand oxidation state [154]. For example, in $[NEt_4][Ni(mnt)_2]$ complex, the C-S and the C–C distances are ~1.725 Å and ~1.375 Å, respectively [155], which are consistent with the trend in the calculated and experimental bond distances listed in Table 2.

The complex, $[Ni(^iPr_2Dt^0)_2][BF_4]_2$, has also been examined in the gas phase by IRMPD spectroscopy and predicted vibrational frequencies were calculated with DFT level of theory [156]. A prominent peak at 1506 cm^{-1}, expected for imine –C=N- stretching, was assigned to the symmetric stretching (for the given dithione ligand) of the ring C=N bond. A minor absorption corresponding to the asymmetric –C=N- stretching mode was predicted to appear at 1520 cm^{-1}. This peak is not resolved in the IRMPD spectrum but may contribute to the shoulder to the high-frequency side of the absorption centered at 1506 cm^{-1}. The presence of C=N stretching suggests that in the gas phase the ligand exists, at least partially, in the dithiolato tautomeric form which is similar to the dizwitterionic character observed in the case of oxo-molybdenum complexes (*vide infra*) [134].

In solution, ^{13}C NMR spectra show a resonance δ ~180 ppm due to C=S moiety indicative of an oxidized ligand [156], which is shifted significantly from the C=S resonance, δ ~150 ppm, of ene-1,2-dithiolate(2−) complexes [157]. In acetonitrile, the electronic spectra exhibits two charge-transfer bands at 604 nm (ε, 5,690 $M^{-1}cm^{-1}$) and 540 (ε, 4,830 $M^{-1}cm^{-1}$) (Fig. 27). This is in contrast to the Ni(II) complexes containing fully reduced dithiolene ligands, where such bands are observed at higher energies. For example, the absorption spectrum of acetonitrile solutions of $[Bu_4\text{-}N]_2[Ni(S_2C_2(CN)_2)_2]$ exhibits bands at 468 nm (ε, 4,474 $M^{-1}cm^{-1}$) and 514 nm (ε, 1,736 $M^{-1}cm^{-1}$). Room temperature cyclic voltammetry of $[Ni(^iPr_2Dt^0)_2][BF_4]_2$ and $[Ni(Me_2Dt^0)_2][BF_4]_2$ in acetonitrile revealed four one-electron reduction couples in the negative region and no reversible couple in the positive region, which have been attributed to ligand-based couples. Each ligand being reduced one-electron at a time, as opposed one ligand being reduced by two electrons before an electron is being added to the second ligand (Scheme 3). This also suggests that two complexes with differing redox states can be generated under cyclic voltammetric conditions.

From these ligand-based processes, comproportionation constants (K_c) for the first and the second mixed-ligands were calculated to be 0.7–2.8 × 10^5. A mixed ligand complex, generated *in situ* spectroelectrochemically by reducing the system by one-electron, shows a band near 732 nm that is shifted to lower energy (Fig. 27). [156] This trend is consistent with the electronic spectra of Ni(I) and Ni(II) bis(ene-1,2-dithiolate(2−)) complexes. The charge transfer band for $[Bu_4N][Ni(mnt)_2]$ shifts to a lower energy (863 nm, ε, 9700 $M^{-1}cm^{-1}$) when compared to its oxidized counterpart $[Bu_4N]_2[Ni(mnt)_2]$. In addition, spectroelectrochemistry also revealed a weak broad band at a lower energy (at ~1940 nm). This band was assigned as the intervalence charge transfer (IVCT) band. Analysis of this IVCT band suggests class II/III character in the mixed-valence $[Ni(^iPr_2Dt^0)(^iPr_2Dt^{1-})]^-$ with H_{AB} to be ~350 cm^{-1} (Fig. 28).

5.7. Electronic structure of bis(dithione) complexes

The electronic structure of bis(dithione) complexes has been modeled with DFT and is shown in Fig. 29 [156]. Similar to what was observed for mono(dithione) complexes, the

LUMO of bis (dithione) complexes are mainly ligand-based. DFT calculations are also consistent with the assignment of the four ligand-based reduction couples. The electronic structure of $[Ni(^{i}Pr_2Dt^0)_2][BF_4]_2$ resembles a classic case of a d^8 Ni^{2+} ion in a square planar environment. The molecular orbital composition diagram clearly shows four doubly occupied predominantly nickel-centered MOs in the HOMO region. The first three nickel-centered MOs are closely spaced in HOMO- HOMO-2 region and dominantly contain nickel d_{xz}, d_{yz}, and d^2_z character with the last two being nearly degenerate [156].

Similar to $[Ni(^{i}Pr_2Dt^0)_2][BF_4]_2$, bis(dithione) complexes utilizing molybdenum as the metal center with $^{i}Pr_2Dt^0$ and Me_2Dt^0 ligands have been synthesized. The dithione ligand in $[MoO(^{i}Pr_2Dt^0)_2Cl][PF_6]$, was probed using resonance Raman spectroscopy. The spectrum supported the presence of dizwitterionic character of the enolate form(Fig. 30).

Electron delocalization is focused on the thioamide ($N_2C_2S_2$), which is also observed in uncoordinated ligand. The electronic structure predictions HOMO and HOMO-1 orbitals that are mostly metal in character, and redox-active virtual orbitals that are largely ligand in character. $[MoO(^{i}Pr_2Dt^0)_2Cl][PF_6]$ exhibits a low energy transition, which has been assigned to the MLCT transition from detailed DFT calculations. Low energy bands 1 (HOMO to LUMO) and 2 (HOMO to LUMO + 1) were assigned as MLCT (Fig. 31). The electron density difference map (EDDM) shows the electron accepting orbital is delocalized across the thioamide unit of both dithione ligands [134].

Fully oxidized dithione ligands can also stabilize a very unique low coordinate Mo-cluster; $[(^{i}Pr_2Dt^0)Mo]_4[BF_4]$ shown Fig. 32 [133]. The cluster is formed from $[MoO(BF_4)(^{i}Pr_2Dt^0)_2][BF_4]$ and $[MoOCl(^{i}Pr_2Dt^0)_2][MoOCl_4]$, which were the first examples of oxo-Mo(IV) complexes possessing two dithione ligands [133]. $[MoOCl(^{i}Pr_2Dt^0)_2][MoOCl_4]$ was reacted with silver tetrafluoroborate forming $[MoO(BF_4)(^{i}Pr_2Dt^0)_2][BF_4]$, which formed the cluster $[(^{i}Pr_2Dt^0)Mo]_4[BF_4]$ while solvated in pyridine. Both $[MoOCl(^{i}Pr_2\text{-}Dt^0)_2][MoOCl_4]$ and $[MoO(BF_4)(^{i}Pr_2Dt^0)_2][BF_4]$ exhibit a low energy d-d transition between 718 and 741 nm. Typically, such a transition is not observed in monooxo-Mo(IV) complexes possessing two fully reduced dithiolene ligands. DFT calculations of $[MoOCl(^{i}\text{-}Pr_2Dt^0)_2]^+$ showed that the LUMO and LUMO + 1 are dithione ligand-based. TDDFT indicates that the low energy transition is MLCT in character. Electron density maps of the transition demonstrated that the metal does not donate electron density exclusively to one of the ligand, and that ligands, indeed, act as the electron accepting moiety [133].

Kisch's groups has extensively investigated the charge transfer property of cation–anion pair type complexes [158]. The application of charge transfer reactions involving dioxygen was explored using redox-active and light-sensitive ion-pair complexes of $[A]^{2+}$ $[ML_2]^{2-}$ (where A^{2+} = organic acceptor, $[ML_2]^{2-}$ = planar dithiolene metalate) dioxygen [158–161]. Similarly, other cation–anion pair complexes have been synthesized using bis(dithione) complexes as the cation and bis(ene-1,2-dithiolate(2−)) as the anion. These were used to form complexes like $[M(R_2Dt^0)_2][M(mnt)_2]$ (M = Pd and Pt; R_2Dt^0 = *N,N'*-dialkylpiperazine-2,3-dithione, R = Me or Et). Similar features have been found between these complexes and the $[A^{2+}][ML_2]^{2-}$ complexes [10]. Charge transfer transition of these complexes has been assigned to $\pi \rightarrow \pi^*$. Another similarity is seen in the behavior of the

cation/dianion (dithione/alkene-1,2-dithiolate) charge transfer. The LUMO of the dithione complex is composed of π * ligands and the HOMO is dominated by the dianion [162]. The charge transfer in this systems are also π → π * transitions involving [M(ene-1,2-dithiolate (2−))]$^{2+}$ → [M(dithione)]$^{2+}$. Electroconducting properties of charge transfer salts, such as [Pt(R_2Dt^0)$_2$][Pt(dtcr)$_2$] (R = Me, Et; dtcr = 4, 5-disulfanylcyclopent-4-ene-1,2,3-trionate, known as dithiocroconate) have been explored. These complexes show strong near IR charge transfer features that lead to their semiconducting and photoconducting properties [145]. The molecular structure of Pd (II) and Pt(II) [M(Me_2Dt^0)$_2$][M(mnt)$_2$] complexes show that both [Pt(Me_2Dt^0)$_2$]$^{2+}$ and [Pt(mnt)$_2$]$^{2-}$ are isomorphous to one another. These complexes form an infinite anion-cation one-dimensional stack with a Pt…Pt distance of 3.392 Å and a <Pt-Pt-Pt angle of 180° [151]. Inspecting the Hirsh surfaces of both cation and anion allowed for the determining the environment surrounding each complex [151].

As mentioned previously, most of the bis(dithione) complexes have seen more use as precursors for other mixed ligand complexes. The asymmetric electronic framework of mixed ligand dithiolene allows for potent charge-transfer capabilities. Mixed dithiolene ligand systems are being actively explored for various applications that include nonlinear optics (NLO) [72,79,97,98,120,121]. Such molecules have been reviewed in detail elsewhere [72].

5.8. Tris(dithione) complexes

There are very few tris(dithiolene) complexes, and even fewer tris(dithione) complexes have been reported [163–168]. Recent work by Wieghardt has revisited the idea of redox-active non-innocent ligands in tris(dithiolene) complexes. This work included analysis of bonding in the electronic and molecular structure of $Re(Dt^{2-})_3^{1+/0/1-}$ and $V(Dt^{2-})_3^{1+/0/1-/2-/3-/4-}$ complexes. [63,169] Tri (ene-1,2-dithiolate(2−) complexes of Cr, Mo, and W central atoms were assigned as d^0 configurations. The molecular geometry of these complexes preferred the stability offered by TP over octahedral geometry. The increased stability of the TP geometry was thought to be a result of partial oxidation of the dithiolene ligands. However, more characterization of tris(dithiolene) complexes is needed to better understand their chemistry.

In addition to the remarkable ability of forming complexes with localized π-electrons, giving rise to exciting optical properties, complexes with dithione ligands exhibit remarkable molecular features e.g., formation of a [Ni($^iPr_2Dt^0$)$_3$][PF_6]$_3$ which is the only reported structure of an octahedral nickel(II) complex possessing three fully oxidized dithione ligands. The molecular structure of [Ni($^iPr_2Dt^0$)$_3$][PF_6]$_3$ demonstrated that the dithione ligands remained fully oxidized during synthesis and crystallization. When compared to the molecular structure of [Ni($^iPr_2Dt^0$)$_2$][BF_4]$_2$, the tris (dithione) complex, [Ni($^iPr_2Dt^0$)$_3$][PF_6]$_3$, exhibited shorter Ni-S bonds (~0.2 Å) due to a steric crowding of the nickel center. The electronic spectra of [Ni($^iPr_2Dt^0$)$_3$][PF_6]$_3$ and [Ni($^iPr_2Dt^0$)$_2$][BF_4]$_2$ exhibit different charge transfer transitions in the UV–Vis region and no NIR transitions were observed for either complex. [Ni($^iPr_2$-Dt^0)$_2$][BF_4]$_2$ exhibits two intense low energy transitions (604 nm, 5690 $M^{-1}cm^{-1}$ and 540 nm, 4830 $M^{-1}cm^{-1}$). DFT calculations for [Ni($^iPr_2Dt^0$)$_3$][PF_6]$_3$ follow a similar trend to what was calculated for [Ni($^iPr_2Dt^0$)$_2$][BF_4]$_2$. Molecular orbitals

show that the HOMO, HOMO-1, and HOMO-2 are mainly is nickel in character whereas the LUMO is primarily dithione ligand-based. The LUMO + 1 and LUMO + 2 exhibit more nickel $d^2_x -^2_y$ character as the metal center helps to facilitate charge transfer. This would result in a MLCT band in the UV–Vis spectrum in the low energy region, and intra-ligand and nickel d-d transitions at higher energies. These results are further supported by TDDFT calculations. As mentioned earlier, d^8 metal complexes possessing fully oxidized dithione ligands exhibit similar electronic properties to those of complexes possessing fully reduced dithiolene ligands. $[Ni(^iPr_2Dt^0)_3][PF_6]_3$, on the other hand, exhibits an intense transition at 413 nm (4674 $M^{-1}cm^{-1}$) and a weak band at 750 nm (337 $M^{-1}cm^{-1}$). DFT calculations supported a paramagnetic Ni^{2+} electronic state. The SOMO and SOMO-1 of the α-set are mostly nickel in character, whereas the LUMO is predominantly dithione ligand. Assignment of these molecular orbitals suggests low energy bands d-d transitions and a higher energy bands to be MLCT transition [156]. Bigoli et al. have presented a similar nickel dithione complex, $[Ni(Me_2Dt^0)_2][BF_4]_2$, that exhibits similar UV–Vis transitions to that of $[Ni(^iPr_2Dt^0)_2][BF_4]_2$, showing two strong transitions at 540 nm (4000 $M^{-1}cm^{-1}$) and 605 nm (4000 $M^{-1}cm^{-1}$). DFT calculations showed that, much like $[Ni(^iPr_2\text{-}Dt^0)_2][BF_4]_2$, the HOMO and HOMO-1 molecular orbitals are composed of metal frontier orbitals and the LUMO is virtually purely dithione ligand-based resulting in MLCT transitions [10].

6. Dithiolene vs catechol ligands

A discussion on the non-innocent nature of dithiolene ligands is not complete without a comparison with the related catechol ligand. Similar to dithiolene, catechol are bidentate ligands with two oxygen atoms that can provide metal chelation (Fig. 33) [170,171]. The catechol system is very similar to that of the aromatic dithiolene. The fundamental backbone of catechol ligands includes an RC(-O) = C(-O)R unit that can exist in the 2−/1−/0 oxidation states. Differences in anionic and neutral catechol metal chelation can be distinguished by their structural properties when coordinated. However, identifying the anionic radical cannot be done by bond lengths alone [172,173]. Computational studies of phenoxyl and thiyl radicals show that structural change is not observed with thiyl radicals. This is thought to be due to the difference in spin density of the thiyl radical [174]. The coordination of a radical anionic ligand can be probed by a variety of structural and spectroscopic studies [175].

Challenges remain in the determination of the electronic structure of dithiolene complexes. A complex like $[Ni(S_2C_2R_2)_2]^{2-}$ has been well characterized and is known to oxidize in two one-electron reversible oxidation step to $[Ni(S_2C_2R_2)_2]$ [176–179]. In its oxidized state, the complex is thought to be in a resonance hybrid, in which the metal center be either 2 + or 4 + with ligands that range dianionic to neutral (Fig. 34). Although the electronic properties of the reduced ligand are consistent with the M^{II} state, there are multiple possible formulations. As observed with dithione and ene-1,2-dithionlate(2−), different metal oxidation states can be favored by different ligands. Therefore, a combination of spectroscopic, structural, and computational studies needs to be used in tandem to determine the oxidation state of each component in metal(dithiolene) complexes.

7. Summary

The concept of non-innocent ligands remains an exciting area of research in chemistry. Of many non-innocent ligands, dithiolene ligands remain as a cornerstone as new chemistry continues to emerge. The dithiolene ligands can exist in different redox states and can form metal complexes in each redox state. The fully oxidized dithiolene ligand, i.e., the dithione has received less attention but equally, offer exciting chemistry. The frontier orbitals in these ligands are dominated by the sulfur atomic orbitals that foster efficient interaction with metal orbitals. Exploration of dithione ligand as an electron-deficient moiety has led to the development of charge transfer salts, donor–acceptor molecular complexes, and materials of metal recovery processes. It is expected that dithione chemistry will continue to flourish.

Acknowledgments

Our research was supported by the National Institutes of Health. Over the years we were fortunate to have insightful discussion with former and current students and collaborators. We thank Dr. Sara A. Dille for discussions and careful reading of this manuscript.

References

[1]. Kaim W, Schwederski B, Coord. Chem. Rev 254 (2010) 1580–1588.

[2]. Kaim W, Eur. J. Inorg. Chem 2012 (2012) 343–348.

[3]. Kaim W, Inorg. Chem 50 (2011) 9752–9765. [PubMed: 21744793]

[4]. Joergensen CK, Coord. Chem. Rev 1 (1966) 164–178.

[5]. Chirik PJ, Inorg. Chem 50 (2011) 9737–9740. [PubMed: 21894966]

[6]. Ward MD, McCleverty JA, Dalton Trans. (2002) 275–288.

[7]. Camerel F, Jeannin O, Yzambart G, Fabre B, Lorcy D, Fourmigue M, New J. Chem 37 (2013) 992–1001.

[8]. Su-Kyung L, Kyong-Soon S, Dong-Youn N, Olivier J, Frederic B, Jean-Francois B, Marc F, Chem. Asian J 5 (2010) 169–176. [PubMed: 20013993]

[9]. Tenderholt AL, Szilagyi RK, Holm RH, Hodgson KO, Hedman B, Solomon EI, J. Inorg. Biochem 101 (2007) 1594–1600. [PubMed: 17720249]

[10]. Bigoli F, Deplano P, Mercuri ML, Pellinghelli MA, Pilia L, Pintus G, Serpe A, Trogu EF, Inorg. Chem 41 (2002) 5241–5248. [PubMed: 12354058]

[11]. McCleverty JA, Locke J, Wharton EJ, Winscom CJ, Chem. Commun (1966) 677–678.

[12]. Hille R, Hall J, Basu P, Chem. Rev 114 (2014) 3963–4038. [PubMed: 24467397]

[13]. Hille R, Chem. Rev 96 (1996) 2757–2816. [PubMed: 11848841]

[14]. Basu P, Burgmayer SJN, JBIC J Biol. Inorg. Chem 20 (2015) 373–383.

[15]. Basu P, Burgmayer SJN, Coord. Chem. Rev 255 (2011) 1016–1038. [PubMed: 21607119]

[16]. Johnson JL, Hainline BE, Rajagopalan KV, Arison BH, J. Biol. Chem 259 (1984) 5414–5422. [PubMed: 6546929]

[17]. Hine FJ, Taylor AJ, Garner CD, Coord. Chem. Rev 254 (2010) 1570–1579.

[18]. Enemark JH, Cooney JJA, Wang J-J, Holm RH, Chem. Rev. (Washington, DC, U. S.), 104 (2004) 1175–1200.

[19]. Holm RH, Solomon EI, Majumdar A, Tenderholt A, Coord. Chem. Rev 255 (2011)993–1015.

[20]. Pimkov IV, Serli-Mitasev B, Peterson AA, Ratvasky SC, Hammann B, Basu P, Chem. – Eur. J 21 (2015) 17057–17072. [PubMed: 26541355]

[21]. Pimkov IV, Peterson AA, Vaccarello DN, Basu P, RSC Adv. 4 (2014) 19072–19076. [PubMed: 24921040]

[22]. Williams BR, Fu Y, Yap GPA, Burgmayer SJN, J. Am. Chem. Soc 134 (2012) 19584–19587. [PubMed: 23157708]

[23]. Bradshaw B, Dinsmore A, Ajana W, Collison D, Garner CD, Joule JA, J. Chem. Soc., Perkin Trans 1 (2001) 3239–3244.

[24]. Burgmayer SJN, Williams BR, Basu P, Pterin-Inspired Model Compounds of Molybdenum Enzymes, in: Hille R, Schulzke C, Kirk ML (Eds.), Molybdenum and Tungsten Enzymes, Royal Society of Chemistry, Cambridge, 2017, pp. 8–67.

[25]. Stiefel EI, Dithiolene Chemistry: Synthesis, Properties, and Applications. [In: Progress in Inorganic Chemistry, Volume 52], John Wiley & Sons, Inc., 2003.

[26]. Eisenberg R, Gray HB, Inorg. Chem 50 (2011) 9741–9751. [PubMed: 21913669]

[27]. Eisenberg R, Coord. Chem. Rev 255 (2011) 825–836.

[28]. Sproules S, Prog. Inorg. Chem 58 (2014) 1–144.

[29]. Mueller-Westerhoff UT, Vance B, Yoon DI, Tetrahedron 47 (1991) 909–932.

[30]. Touchard D, Fillaut J, Khasnis DV, Dixneuf PH, Organometallics 7 (1988) 67–75.

[31]. Yu Y, Lin Y, Liu B, Acta Crystallographica Section E 65 (2009) 511.

[32]. Miller JG, Chenoweth B, Brody MT, J. Pharm. Exp Ther 121 (1957) 32–42.

[33]. Hurd RH, De La Mater G, Mcelheny GC, Turner RJ, Wallingford VH, J. Org. Chem 26 (1961) 3980–3987.

[34]. Perec M, Acta. Cryst, C51 (1995) 2182–2184.

[35]. Tom DH, Form M, Angew. Chem 87 (1975) 245–246.

[36]. Tom DH, Form M, Anorg Z, Allg. Chem 515 (1984) 19–35.

[37]. Green RM, Jubran N, Bursten BE, Busch DH, Inorg Chem 26 (1987) 2326–2332.

[38]. Draganjac M, Minick D, Cordes AW, J. Cryst. Spectr. Res 23 (1993) 265–271.

[39]. Al-Maydama H, El-Shekeil A, Khalid MA, Al-Karbouly A, Ecletica Quimica 31 (2006) 45–52.

[40]. Woodburn H, Platek W, Graminski E, J. Org. Chem 23 (1958) 319–320.

[41]. Chen C, Liao S, Lin K, Lai L, Adv. Mater 3 (1998) 334–338.

[42]. Servaas PC, Stukens DJ, Oskam A, Vernooijs P, Baerends EJ, De Ridder DJA, Stam CH, Inorg. Chem 28 (1989) 4104–4113.

[43]. Geary EAM, Yellowlees LJ, Parsons S, Pilia L, Serpe A, Mercuri ML, Deplano P, Clark SJ, Robertson N, Dalton Trans. (2007) 5453–5459. [PubMed: 18026595]

[44]. Piotrkowska B, Małgorzata M, Gdaniec M, Herman A, Połonski T, J. Org. Chem 73 (2008) 2852–2861. [PubMed: 18335961]

[45]. Küsters W, de Mayo P, J. Am. Chem. Soc 95 (1973) 2383–2384.

[46]. Russell GA, Zaleta M, J. Am. Chem. Soc 104 (1982) 2318.

[47]. Russell GA, Law WC, Zaleta M, J. Am. Chem. Soc 107 (1985) 4175–4182.

[48]. Buddensiek D, Koepke B,Voss J, Chem. Ber 120 (1987) 575–581.

[49]. Roth B, Bock H, Gotthardt H, Phosphorus Sulfur 22 (1985) 109–119.

[50]. Wang Y, Xie Y, Abraham MY, Wei P, Schaefer HF III, Schleyer P.v.R., Robinson GH, J. Am. Chem. Soc 132 (2010) 14370–14372. [PubMed: 20863065]

[51]. Wang Y, Hickox HP, Xie Y, Wei P, Blair SA, Johnson MK, Schaefer HF, Robinson GH, J. Am. Chem. Soc 139 (2017) 6859–6862. [PubMed: 28482154]

[52]. Wang Y, Xie Y, Wei P, Schaefer HF, Robinson GH, Dalton Trans. 48 (2019) 3543–3546. [PubMed: 30747182]

[53]. Antolini L, Fabretti AC, Franchini G, Menabue L, Pellacani GC, Desseyn HO, Dommisse R, Hofmans HC, J. Chem. Soc., Dalton Trans (1987) 1921–1928.

[54]. Sengar RS, Nemykin VN, Basu P, New J. Chem 27 (2003) 1115–1123.

[55]. Interrante LV, in, Gen. Electr. Corp. Res. Dev, 1982, pp. 27.

[56]. Crews P, Rodriquez J, Jaspars M, Organic Structure Analysis, Oxford University Press, 2010.

[57]. Vidal MCF, Lens I, Castiñeiras A, Matilla Hernández A,Tercero Moreno JM, Niclós-Gutiérrez J, Polyhedron 18 (1999) 3313–3319.

[58]. Jean YC, Acta Cryst., C 50 (1994) 1163–1165.

[59]. Shimanouch H, Sasada Y, Acta Cryst., B 35 (1979) 1928–1930.

[60]. Mattes R, Altmeppen D, Johann G, Schulte-Coerne M, Weber H, Monatsh Chem 113 (1982) 191–196.

[61]. Brown MG, Trans. Faraday Soc 55 (1959) 694–701.

[62]. Alvarez S, Vicente R, Hoffmann R, J. Am. Chem. Soc 107 (1985) 6253–16211.

[63]. Sproules S, Banerjee P, Weyherm€uller T, Yan Y, Donahue JP, Wieghardt K, Inorg. Chem 50 (2011) 7106–7122. [PubMed: 21699192]

[64]. Neese F, Petrenko T, Ganyushin D, Olbrich G, Coord. Chem. Rev 251 (2007) 288–327.

[65]. Kirk ML, McNaughton RL, Helton ME, Prog. Inorg. Chem 52 (2003) 111–212.

[66]. Szilagyi RK, Lim BS, Glaser B, Holm RH, Hodgson KO, Solomon EI, J. Am. Chem. Soc 125 (2003) 9158–9168. [PubMed: 15369373]

[67]. Lauher JW, Hoffmann R, J. Am. Chem. Soc 98 (1976) 1729–1742.

[68]. Sunil K, Vinod K, Singh SP, Pericyclic reactions : a mechanistic and problem solving approach, Academic Press, 2006.

[69]. Shimizu T, Murakami H, Kamigata N, J. Org. Chem 64 (1999) 8489–8494.

[70]. Hartke K, Quante J, Kämpchen J, Liebigs Annalen der Chemie (1980) 1482–1488.

[71]. Mills WH, Clark RED, J. Chem. Soc. A (1936) 175–181.

[72]. Deplano P, Pilia L, Espa D, Mercuri ML, Serpe A, Coord. Chem. Rev 254 (2010) 1434–1447.

[73]. Bruno G, Almeida M, Artizzu F, Dias JC, Mercuri ML, Pilia L, Rovira C, Ribas X, Serpe A, Deplano P, Dalton Trans. 39 (2010) 4566–4574. [PubMed: 20383385]

[74]. Cerrada E, Garcia JF, Laguna M, Terroba R, Villacampa MD, J. Chem. Soc., Dalton Trans (1998) 3511–3516.

[75]. Wang K, Stiefel EI, Science 291 (2001) 106–109. [PubMed: 11141557]

[76]. CCDC, in, Cambridge Crystallographic Data Centre, April 17, 2019.

[77]. Yan-Hong C, Wei QT, Feng J, Li W, Liu Z, J. Mol. Struct.: Theochem 897 (2009) 61–65.

[78]. Ray K, George SD, Solomon EI, Wieghardt K, Nees F, Chem. Eur. J 13 (2007) 2783–2797. [PubMed: 17290468]

[79]. Curreli S, Deplano P, Faulmann C, Ienco A, Mealli C, Mercuri ML, Pilia L, Pintus G, Serpe A, Trogu EF, Inorg. Chem 43 (2004) 5069–5079. [PubMed: 15285683]

[80]. Widlicka DW, Wong EH, Weisman GR, Sommer RD, Incarvito CD, Rheingold AL, Inorg. Chim. Acta 341 (2002) 45–53.

[81]. Nagao Y, Ikeda R, Iijima K, Kubo T, Nakasuji K, Kitagawa H, Synth. Met 135–136 (2003) 283–284.

[82]. Kanaizuka K, Haruki R, Sakata O, Yoshimoto M, Akita Y, Kitagawa H, J. Am. Chem. Soc 130 (2008) 15778–15779. [PubMed: 18983147]

[83]. Veit R, Girerd JJ, Kahn O, Robert F, Jeannin Y, Murri NE, Inorg Chem 23 (1984) 4448–4454.

[84]. Piotrkowska B, Wasilewska A, Gdaniec M, Polonski T, CrystEngComm. 10 (2008) 1421–1428.

[85]. Singh B, Lakshmi U, Agarwala, Inorg. Chem 8 (1969) 2341–2346.

[86]. Schrauzer GN, Mayweg VP, J. Am. Chem. Soc 87 (1965) 1483–1489.

[87]. Shupack SI, Billig E, Clark RJH, Williams R, Gray HB, Journal of the American Chemical Society 86 (1964) 4594–4602.

[88]. Meyers F, Marder SR, Pierce BM, Bredas JL, J. Am. Chem. Soc 116 (1994) 10703–10714.

[89]. Albert IDL, Marks TJ, Ratner MA, J. Am. Chem. Soc 119 (1997) 6575–6582.

[90]. Suguna S, Anbuselvi D, Jayaraman D, Nagaraja KS, Jeyaraj B, Spectrochim. Acta, Part A 132 (2014) 330–338.

[91]. Raja R, Seshadri S, Gnanasambandan T, Saravanan RR, Spectrochim. Acta, Part A 138 (2015) 13–20.

[92]. Miyasaka H, Acc. Chem. Res 46 (2013) 248–257. [PubMed: 23128042]

[93]. Gnaim S, Shabat D, Acc. Chem. Res 47 (2014) 2970–2984. [PubMed: 25181456]

[94]. Di Bella S, Fragala I, Ledoux I, Marks TJ, J. Am. Chem. Soc 117 (1995) 9481–9485.

[95]. Cummings SD, Cheng L-T, Eisenberg R, Chem. Mater 9 (1997) 440–450.

[96]. Base K, Tierney MT, Fort A, Muller J, Grinstaff MW, Inorg. Chem 38 (1999) 287–289.

[97]. Espa D, Pilia L, Marchio L, Mercuri ML, Serpe A, Barsella A, Fort A, Dalgleish SJ, Robertson N, Deplano P, Inorg. Chem 50 (2011) 2058–2060. [PubMed: 21288030]

[98]. Pilia L, Espa D, Barsella A, Fort A, Makedonas C, Marchio L, Mercuri ML, Serpe A, Mitsopoulou CA, Deplano P, Inorg. Chem 50 (2011) 10015–10027. [PubMed: 21939192]

[99]. Vogler A, Adamson AW, J. Amer. Chem. Soc 90 (1968) 5943–5945.

[100]. Adamson AW, Chiang A, Zinato E, J. Amer. Chem. Soc 91 (1969) 5467–5475.

[101]. Demas JN, Adamson AW, J. Amer. Chem. Soc 95 (1973) 5159–5168.

[102]. Bock CR, Meyer TJ, Whitten DG, J. Amer. Chem. Soc 96 (1974) 4710–4712.

[103]. Young RC, Meyer TJ, Whitten DG, J. Am. Chem. Soc 98 (1976) 286–287.

[104]. Kivala M, Diederich F, Acc. Chem. Res 42 (2009) 235–248. [PubMed: 19061332]

[105]. Vogler A, Kunkely H, Comments Inorg. Chem 9 (1990) 201–220.

[106]. Vogler A, Kunkely H, Top. Curr. Chem 158 (1990) 1–30.

[107]. King RB, Inorg. Chem 2 (1963) 641–642.

[108]. Donahue JP, Goldsmith CR, Nadiminti U, Holm RH, J. Am. Chem. Soc 120 (1998) 12869–12881.

[109]. Harrison DJ, Lough AJ, Nguyen N, Fekl U, Angew. Chem., Int. Ed 46 (2007) 7644–7647.

[110]. Harrison DJ, Nguyen N, Lough AJ, Fekl U, J. Am. Chem. Soc 128 (2006) 11026–11027. [PubMed: 16925411]

[111]. Martyanov KA, Cherkasov VK, Abakumov GA, Baranov EV, Shavyrin AS, Kuropatov VA, Dalton Trans. 46 (2017) 16783–16786. [PubMed: 29165468]

[112]. Balch AL, Miller J, Inorg. Chem 10 (1971) 1410–1415.

[113]. Draeger M, Gattow G, Anorg Z, Allg. Chem 387 (1972) 300–316.

[114]. Wang Y, Maxi NA, Xie Y, Wei P, Schaefer HF, Robinson GH, Chem. Commun (Cambridge, U. K.), 55 (2019) 8087–8089.

[115]. Wang Y, Xie Y, Wei P, Blair SA, Cui D, Johnson MK, Schaefer HF III, Robinson GH, Angew. Chem., Int. Ed 57 (2018) 7865–7868.

[116]. Hatfield WE, Elliot CM, Ensling J, Kozo A, Inorg. Chem 26 (1987) 1930–1933.

[117]. Luciano A, Antonio FC, Giancarlo F, Pellacani LMCG, Herman DO, Roger D, Hofmans HC, J. Chem. Soc., Dalton trans (1987) 1921–1928.

[118]. Hurd H, Delamater G, Chem. Rev 61 (1961) 45–86.

[119]. Tom DHF, Michael Z Anorg. Allg. Chem 515 (1984) 19–35.

[120]. Espa D, Pilia L, Marchio L, Artizzu F, Serpe A, Mercuri ML, Simao D, Almeida M, Pizzotti M, Tessore F, Deplano P, Dalton Trans. 41 (2012) 3485–3493. [PubMed: 22327944]

[121]. Espa D, Pilia L, Marchio L, Pizzotti M, Robertson N, Tessore F, Mercuri ML, Serpe A, Deplano P, Dalton Trans. 41 (2012) 12106–12113. [PubMed: 22914884]

[122]. Espa D, Pilia L, Makedonas C, Marchio L, Mercuri ML, Serpe A, Barsella A, Fort A, Mitsopoulou CA, Deplano P, Inorg. Chem 53 (2014) 1170–1183. [PubMed: 24405208]

[123]. Espa D, Pilia L, Attar S, Serpe A, Deplano P, Inorg. Chim. Acta 470 (2018) 295–302.

[124]. Attar SS, Artizzu F, Marchio L, Espa D, Pilia L, Casula MF, Serpe A, Pizzotti M, Orbelli-Biroli A, Deplano P, Chem.-Eur. J 24 (2018) 10503–10512. [PubMed: 29767426]

[125]. Nemykin VN, Olsen JG, Perera E, Basu P, Inorg. Chem 45 (2006) 3557–3568. [PubMed: 16634586]

[126]. Yan Y, Chandrasekaran P, Mague JT, DeBeer S, Sproules S, Donahue JP, Inorg. Chem 51 (2012) 346–361. [PubMed: 22145751]

[127]. Skabara PJ, Pozo-Gonzalo C, Lardies MN, Laguna M, Cerrada E, Luquin A, Gonzalez B, Coles SJ, Hursthouse MB, Harrington RW, Clegg W, Dalton Trans. (2008) 3070–3079. [PubMed: 18521449]

[128]. Mancini A, Aragoni MC, Bingham AL, Castellano C, Coles SL, Demartin F, Hursthouse MB, Isaia F, Lippolis V, Maninchedda G, Pintus A, Arca M, Chem.-Asian J 8 (2013) 3071–3078. [PubMed: 24027238]

[129]. Mercuria ML, Serpe A, Marchiò L, Artizzu F, Espa D, Deplano P, Inorg. Chem. Comm 39 (2014) 47–50.

[130]. Bigoli F, Cabras MC, Deplano P, Mercuri ML, Marchio L, Serpe A, Trogu EF, Eur. J. Inorg. Chem (2004) 960–963.

[131]. Bigoli F, Pellinghelli MA, Deplano P, Trogu EF, Inorg. Chim. Acta 170 (1990) 245–249.

[132]. Cau L, Deplano P, Marchio L, Mercuri ML, Pilia L, Serpe A, Trogu EF, Dalton Trans. (2003) 1969–1974.

[133]. Perera E, Basu P, Dalton Trans. (2009) 5023–5028. [PubMed: 19662295]

[134]. Mtei RP, Perera E, Mogesa B, Stein B, Basu P, Kirk ML, Eur. J. Inorg. Chem 2011 (2011)5467–5470. [PubMed: 23956683]

[135]. Yang J, Mogesa B, Basu P, Kirk ML, Inorg. Chem 55 (2016) 785–793. [PubMed: 26692422]

[136]. Joshi HK, Cooney JJA, Inscore FE, Gruhn NE, Lichtenberger DL, Enemark JH, Proc. Natl. Acad. Sci. U. S. A 100 (2003) 3719–3724. [PubMed: 12655066]

[137]. Wiebelhaus NJ, Cranswick MA, Klein EL, Lockett LT, Lichtenberger DL, Enemark JH, Inorg. Chem 50 (2011) 11021–11031. [PubMed: 21988484]

[138]. Drew SC, Hanson GR, Inorg. Chem 48 (2009) 2224–2232. [PubMed: 19235982]

[139]. van Stipdonk MJ, Basu P, Dille SA, Gibson JK, Berden G, Oomens J, J. Phys. Chem. A 118 (2014) 5407–5418. [PubMed: 24988369]

[140]. Micera G, Garribba E, Eur. J. Inorg. Chem (2011) 3768–3780.

[141]. Chandrasekaran KAP, Upul Jayarathne P, Perez Lisa M., Mague Joel T., Donahue James P., Inorg. Chem 48 (2009) 2103–2113. [PubMed: 19235970]

[142]. Wiebelhaus NJ, Cranswick MA, Gruhn N, Lichtenberger DL, Enemark JH, in, 2008, pp. 570.

[143]. Yang J, Kersi DK, Giles LJ, Stein BW, Feng C, Tichnell CR, Shultz DA, Kirk ML, Inorg. Chem 53 (2014) 4791–4793. [PubMed: 24773363]

[144]. Ratvasky SC, Mogesa B, van Stipdonk MJ, Basu P, Polyhedron 114 (2016) 370–377. [PubMed: 27667891]

[145]. Paola Deplano MLM, Marchiò Luciano, Pilia Luca, Salidu Marco, Serpe Angela, Congiu Francesco, Sanna Samuele, Eur. J. Inorg. Chem (2005) 1829–1835.

[146]. Francesco Bigoli C-TC, Wei-Ching Wu, Deplano Paola, Mercuri Maria Laura, Pellinghelli Maria Angela, Luca Pilia GP, Emanuele Angela Serpecand, Trogu F, Chem. Commun (2001) 2246–2247.

[147]. Bigoli F, Deplano P, Mercuri ML, Pellinghelli MA, Pintus G, Serpe A, Trogu EF, J. Am. Chem. Soc 123 (2001) 1788–1789. [PubMed: 11456792]

[148]. Serpe A, Artizzu F, Marchi L, Mercuri ML, Pilia L, Deplano P, Cryst. Growth Des 11 (2011) 1278–1286.

[149]. Emiko Fujiwara KY, Shimamura Mina, Zhou Biao, Kobayashi Akiko, Takahashi Kazuyuki, Okano Yoshinori, Cui Hengbo, Kobayashi H, Chem. Mater 19 (2007) 553–558.

[150]. Espa D, Pilia L, Makedonas C, Marchiò L, Mercuri ML, Serpe A, Barsella A, Fort A, Mitsopoulou CA, Deplano P, Inorg. Chem 53 (2014) 1170–1183. [PubMed: 24405208]

[151]. Espa D, Pilia L, Luciano M, Laura MM, Serpe A.n., Sessini E, Deplano P, Dalton Trans. 42 (2013) 12429–12439. [PubMed: 23863989]

[152]. Colston KJ, Dille SA, Mogesa B, Astashkin AV, Brant JA, Zeller M, Basu P, Eur. J. Inorg. Chem 2019 (2019) 4939–4948.

[153]. Bigoli F, Chen C-T, Wu W-C, Deplano P, Mercuri ML, Pellinghelli MA, Pilia L, Pintus G, Serpe A, Trogu EF, Chem. Commun (2001) 2246–2247.

[154]. Schlaepfer CW, Nakamoto K, Inorg. Chem 14 (1975) 1338–1344.

[155]. Basu P, Nigam A, Mogesa B, Denti S, Nemykin VN, Inorg. Chim. Acta 363 (2010) 2857–2864.

[156]. Mogesa B, Perera E, Rhoda HM, Gibson JK, Oomens J, Berden G, van Stipdonk MJ, Nemykin VN, Basu P, Inorg. Chem 54 (2015) 7703–7716. [PubMed: 26244772]

[157]. Elvers BJ, Schulzke C, Fischer C, Eur. J. Inorg. Chem 2019 (2019) 2796–2805.

[158]. Kisch H, Coord. Chem. Rev 159 (1997) 385–396.

[159]. Lemke M, Knoch F, Kisch H,Salbeck J, Chem. Ber 128 (1995) 131–136.

[160]. Schmauch G, Knoch F, Kisch H, Chem. Ber 128 (1995) 303–307.

[161]. Kisch H, Comments Inorg. Chem 16 (1994) 113–132.

[162]. Waters T, Woo H-K, Wang X-B, Wang L-S, J. Am. Soc 128 (2006) 4282–4291.

[163]. Stiefel YEI, Bennett LE, Dori Z, Crawford TH, Simo C, Gray HB, Inorg Chem 9 (1970).

[164]. Martin JL, Takats J, Inorg. Chem 14 (1975) 73–78.

[165]. Best PS, Robin J, Clark H, Roderick CS, McQueen S, Walton JR, Inorg. Chem 27 (1988) 884–890.

[166]. Hevert WB, Pearson WH, Polyhedron 15 (1996) 2199–2210.

[167]. Scott C, Harris S, Inorg. Chem 35 (1996) 3285–3288. [PubMed: 11666530]

[168]. Pilia L, Espa D, Concas G, Congiu F, Marchio L, Laura Mercuri M, Serpe A, Deplano P, New J. Chem, 39 (2015) 4716–4725.

[169]. Sproules S, Wieghardt K, Coord. Chem. Rev 255 (2011) 837–860.

[170]. Patra S, Sarkar B, Mobin SM, Kaim W, Lahin GK, Inorg. Chem 42 (2003) 6469. [PubMed: 14514323]

[171]. Pierpont CG, Lange CW, The Chemistry of Transition Metal Complexes Containing Catechol and Semiquinone Ligands, 1994.

[172]. Sellmann D, Geck M, Knoch F, Ritter G, Dengler J, Journal of the American Chemical Society 113 (1991) 3819–3828.

[173]. Alves H, Simao D, Novais IC, Polyhedron 22 (2003) 2481–2486.

[174]. Ray K, Weyhermuller T, Neese F, Wieghardt K, Inorg. Chem 44 (2005) 5345–5360. [PubMed: 16022533]

[175]. Ray K, Weyhermueller T, Goossens A, Craje MWJ, Wieghardt K, Inorg. Chem 42 (2003) 4082–4087. [PubMed: 12817965]

[176]. Gray HB, Williams R, Bernal I, Billig E, J. Am. Chem. Soc 84 (1962) 3596–3597.

[177]. Davison A, Edelstein E, Holm RH, Maki AH, J. Am. Chem. Soc 85 (1963) 2029–2030.

[178]. Baker-Hawkes MJ, Billig IE, Gray HB, J. Am. Chem. Soc 88 (1966) 4870–4876.

[179]. Fomitchev DV, Lim BS, Holm RH, Inorg. Chem 40 (2001) 645–654. [PubMed: 11225106]

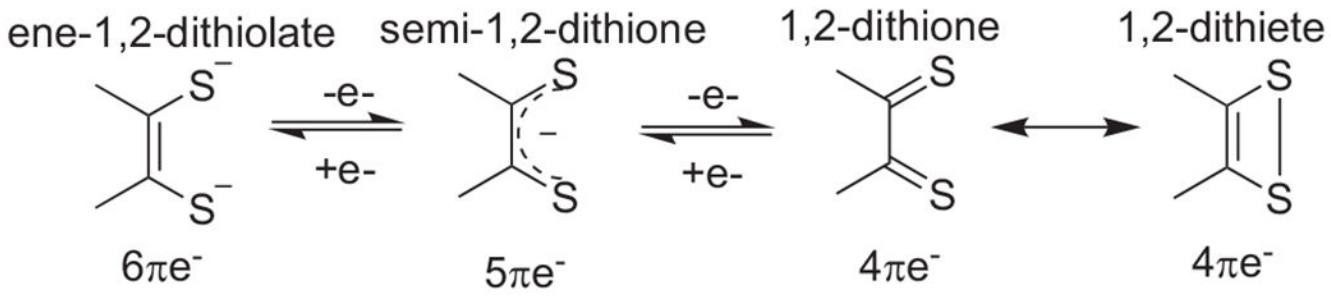

Fig. 1.
Representation of dithiolene ligands showing different oxidation states.

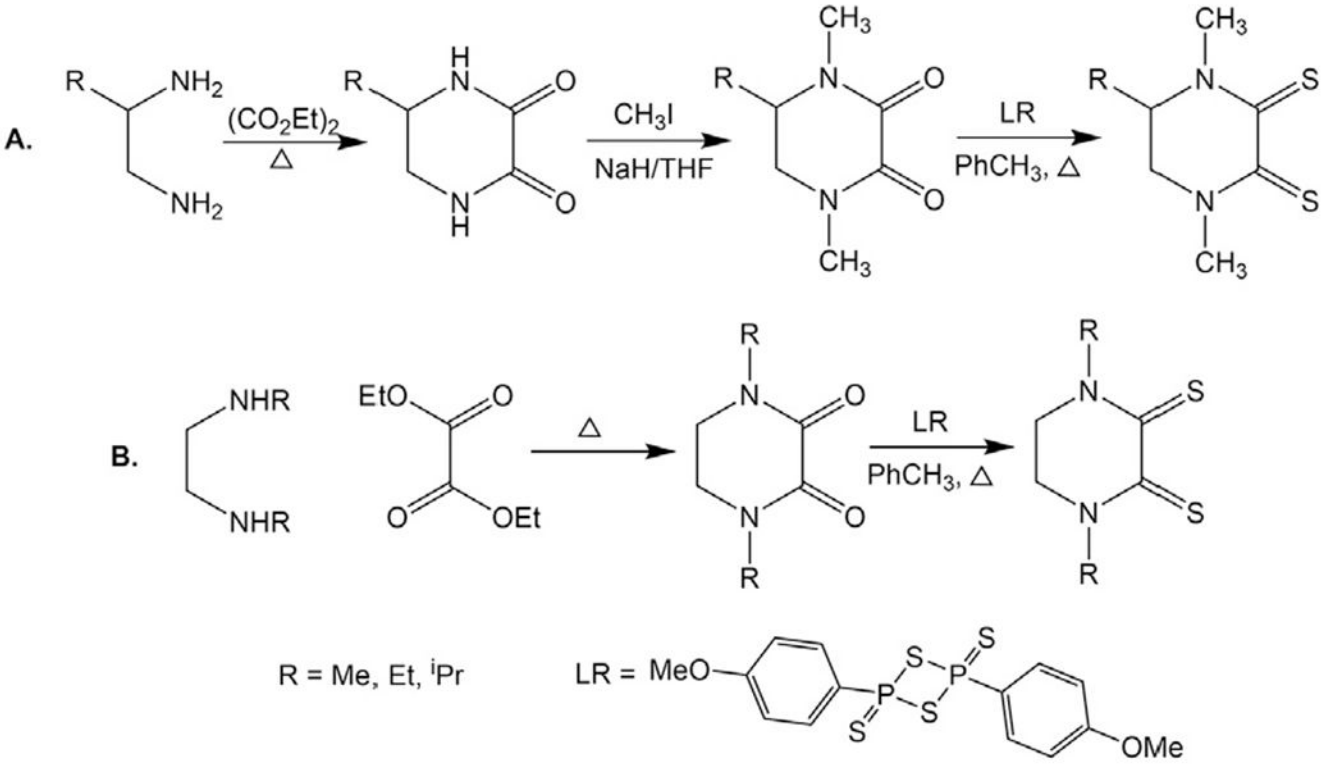

Fig. 2.
Synthesis of pyrazine based dithione ligands.

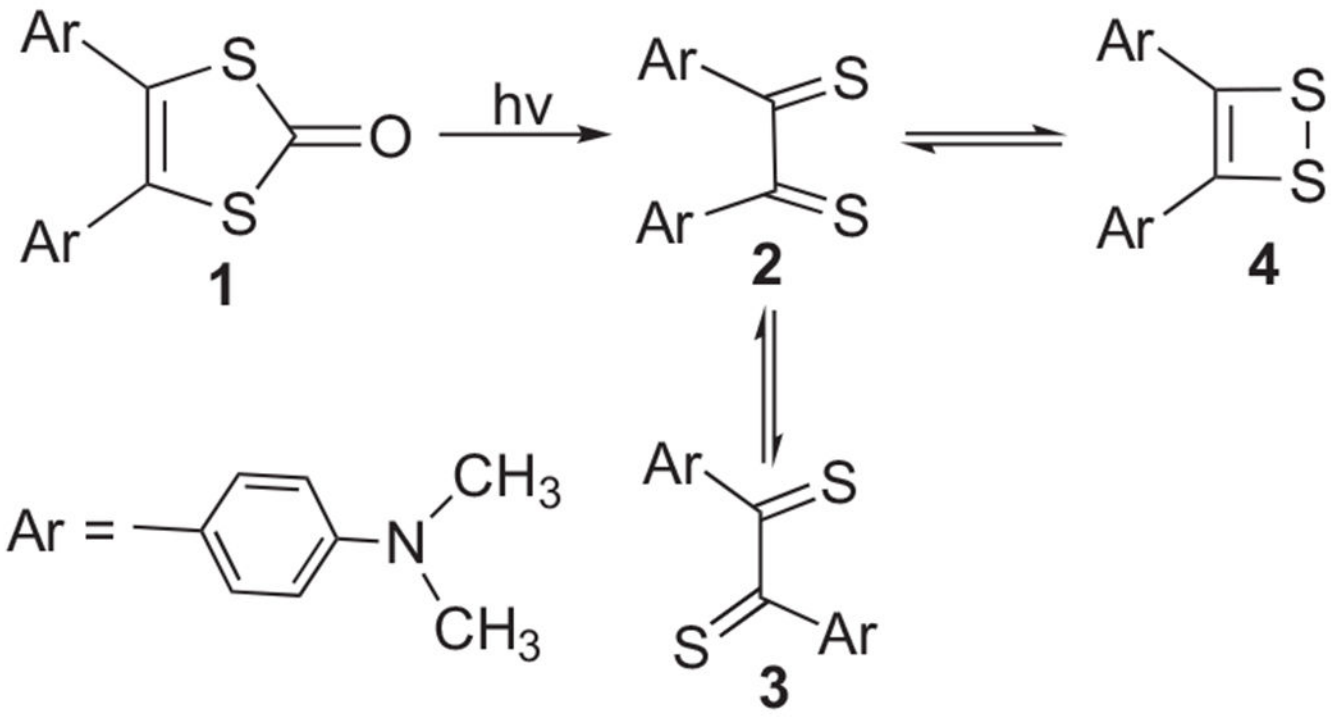

Fig. 3.
Photosynthesis of α-dithiones.

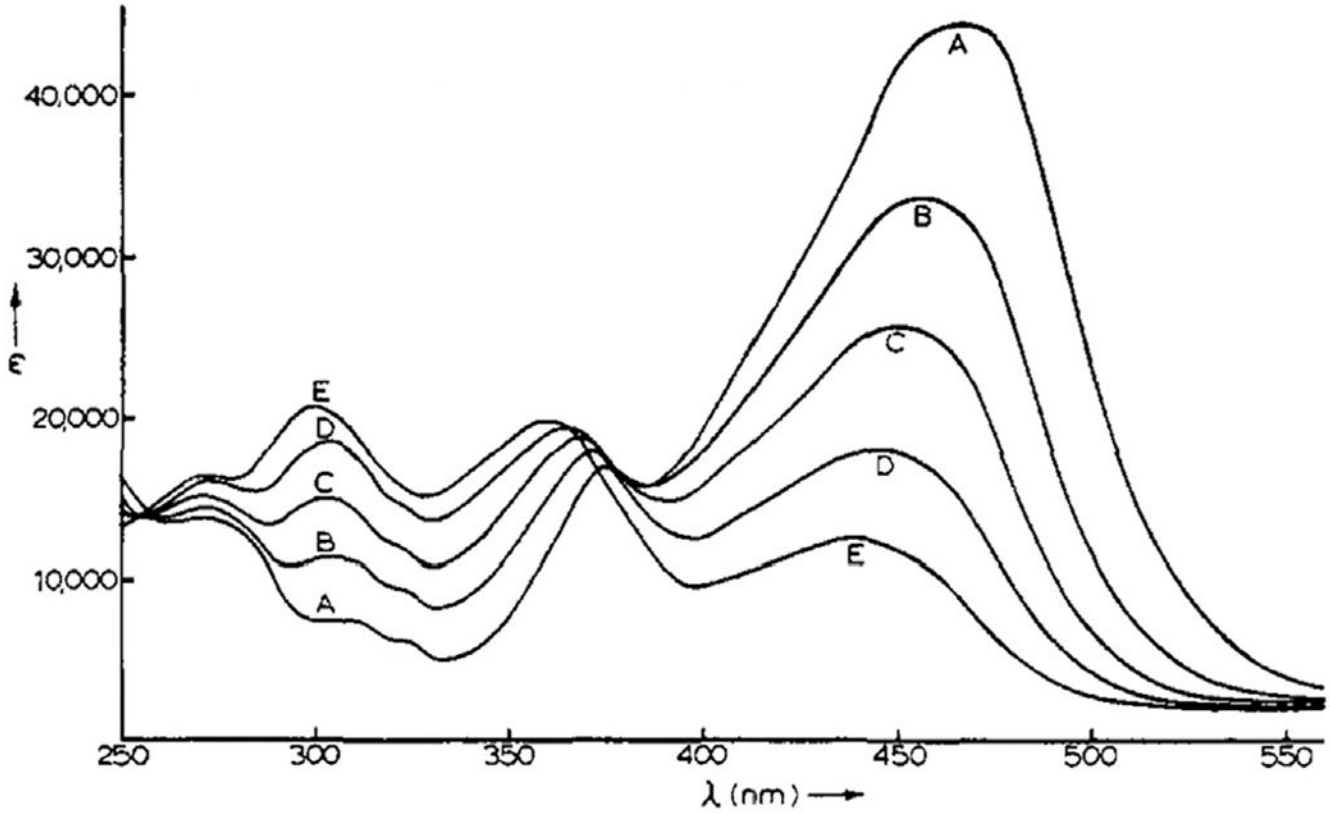

Fig. 4.

Absorption spectra of equimolar solutions of **3** and **2** in solvent mixtures of CH_2C1_2-C_6H_{14} at room temperature. Volume % C_6H_{14} in CH_2Cl_2: A, 0; B, 52; C, 72; D, 84; E, 92. Reprinted with permission from ref. [45]. Copyright 1973. American Chemical Society.

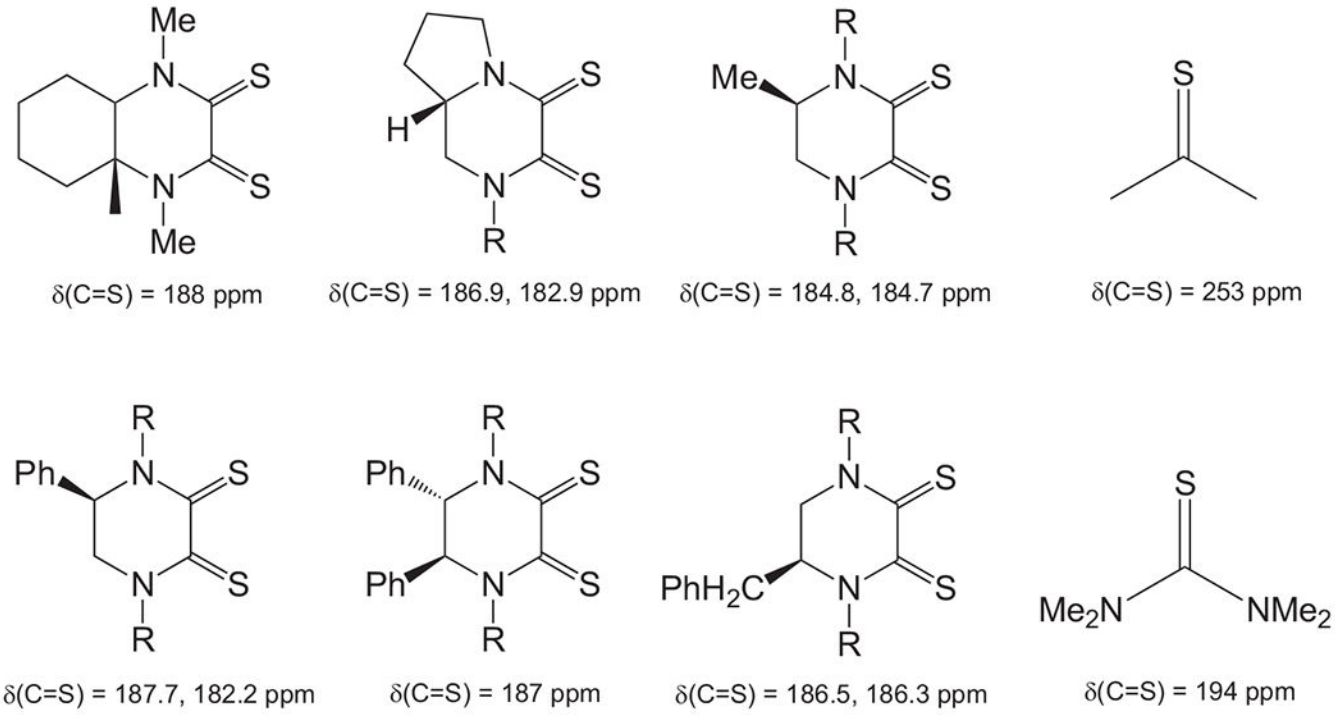

Fig. 5.
^{13}C NMR resonance of C=S in select dithione [55] and thioketone molecules [56].

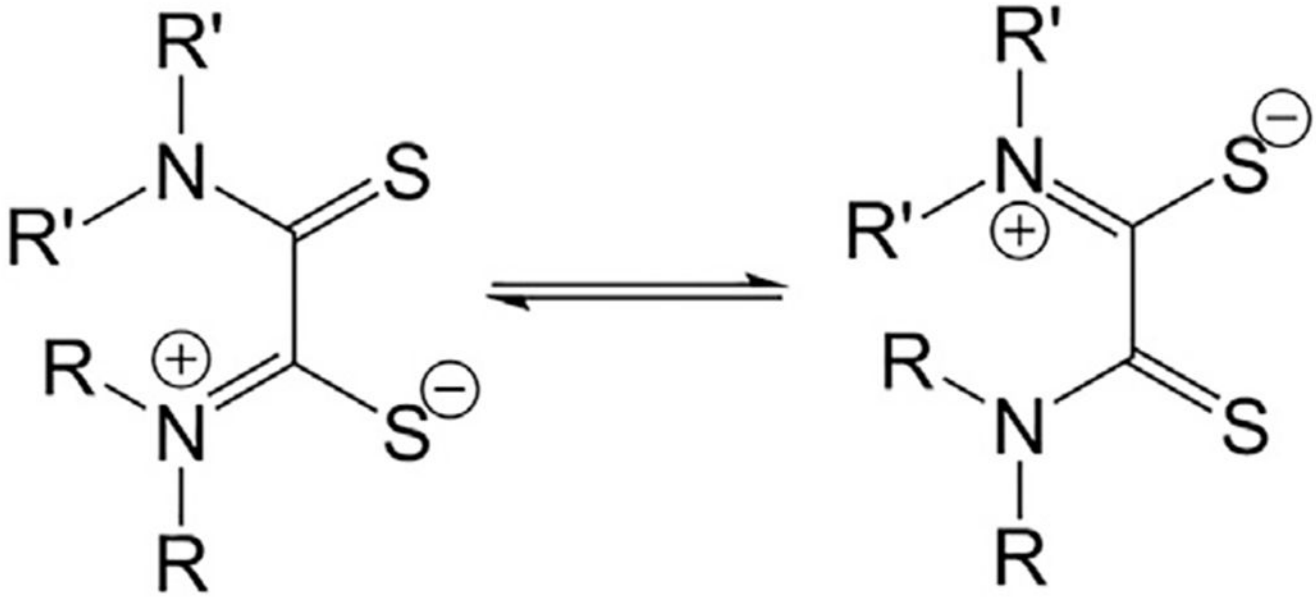

Fig. 6.
Thioamide enolate resonances of dithiooxamide.

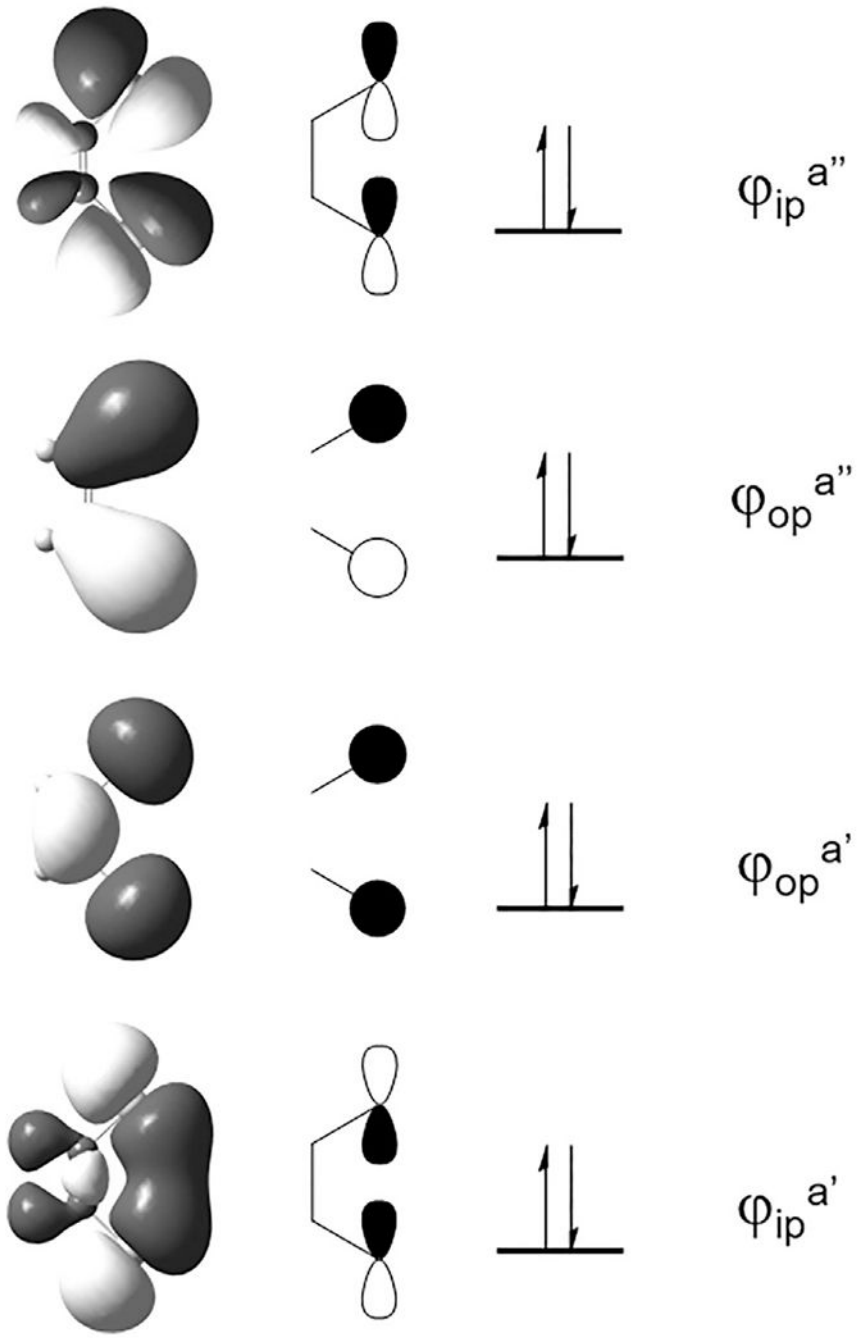

Fig. 7.

The four highest occupied MOs of the ethene-1,2-dithiolate (edt^{2-}) ligand as obtained from computational studies utilizing B3LYP/6–311 + G** level of theory.

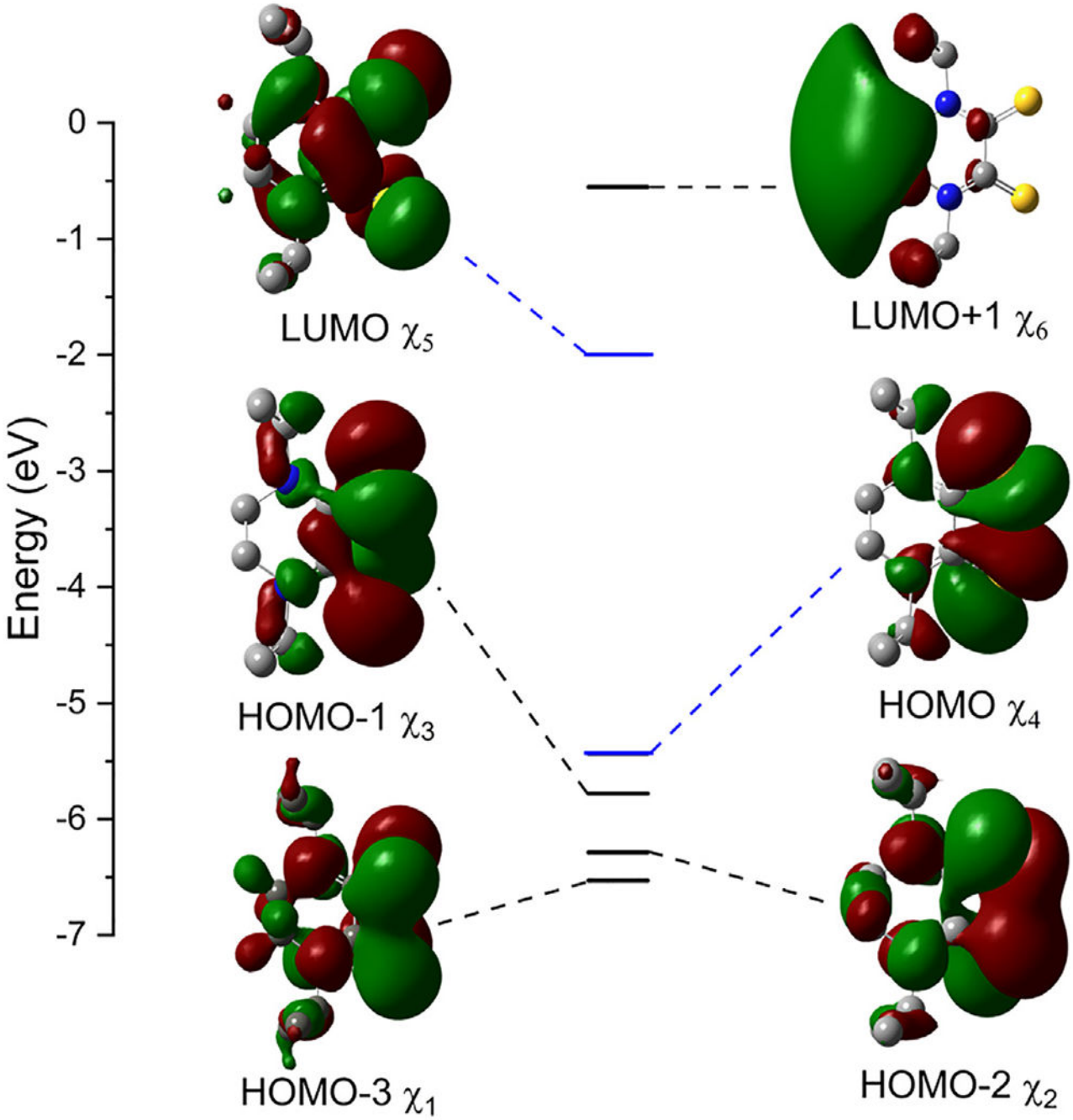

Fig. 8.

Frontier orbitals of $^{i}Pr_2Dt^0$ obtained from DFT calculatoins at B3LYP/6-311G+(d,p) level of theory.

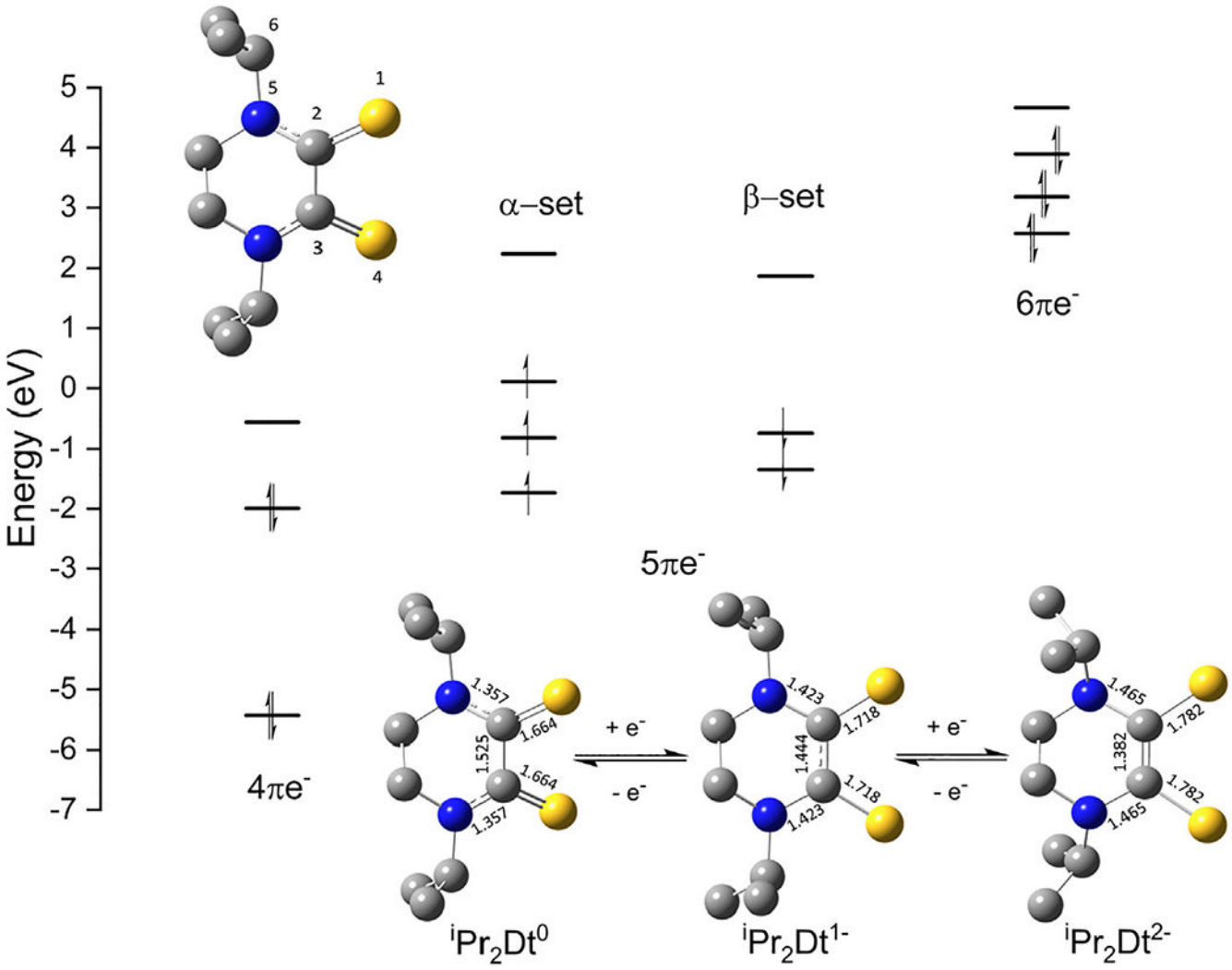

Fig. 9.

Orbital energy diagram of the π electrons of $^{i}Pr_2Dt^0$ and its semi-1,2-dithione and ene-1,2-dithiolate(2−) forms calculated as described in Fig. 8. Energies are relative and select bond lengths (Å) are shown in the bottom right. Select atoms used to determine dihedral angles are labeled in the upper left.

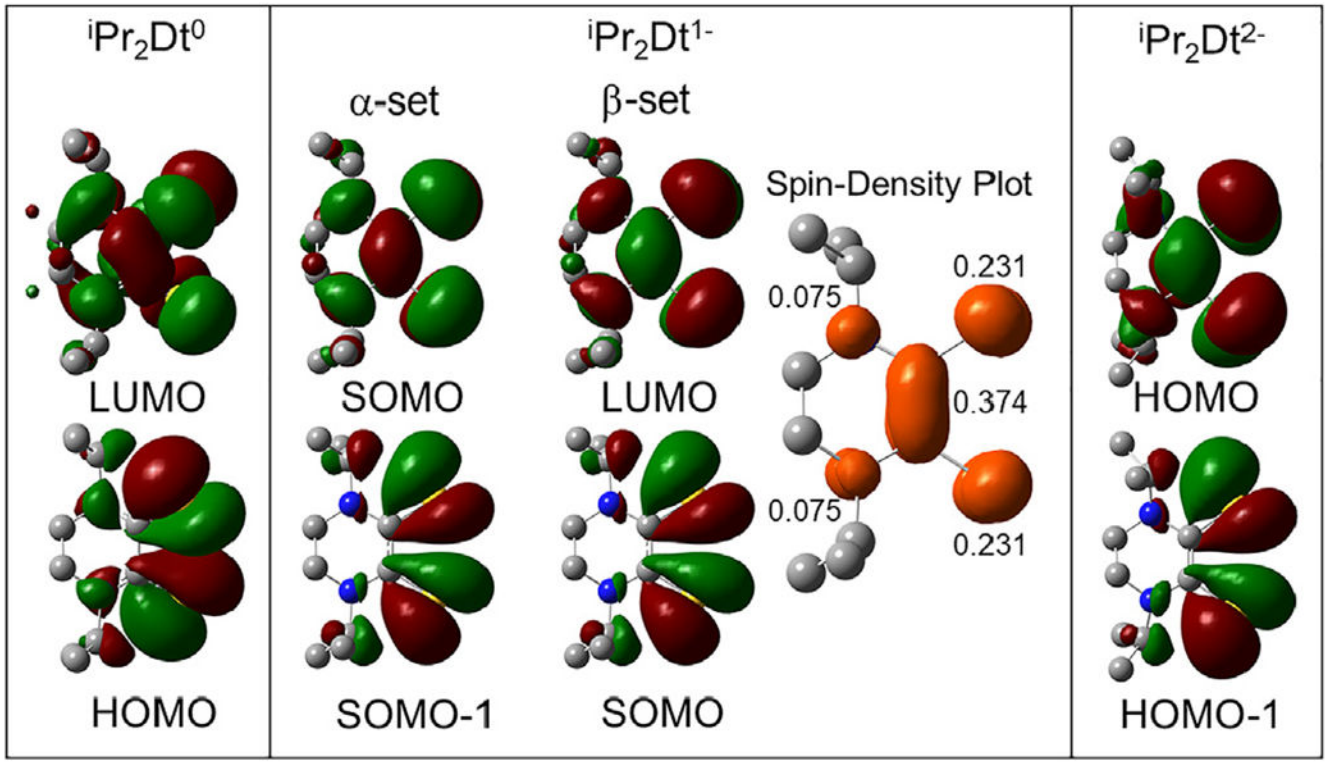

Fig. 10.

Comparison of the redox active orbitals for $^{i}Pr_2Dt^0$ and its semi-1,2-dithione and ene-1,2-dithiolate(2−) forms (isovalue = 0.02). The spin-density plot for $^{i}Pr_2Dt^{1-}$ as determined by Mulliken population analysis (isovalue = 0.0035).

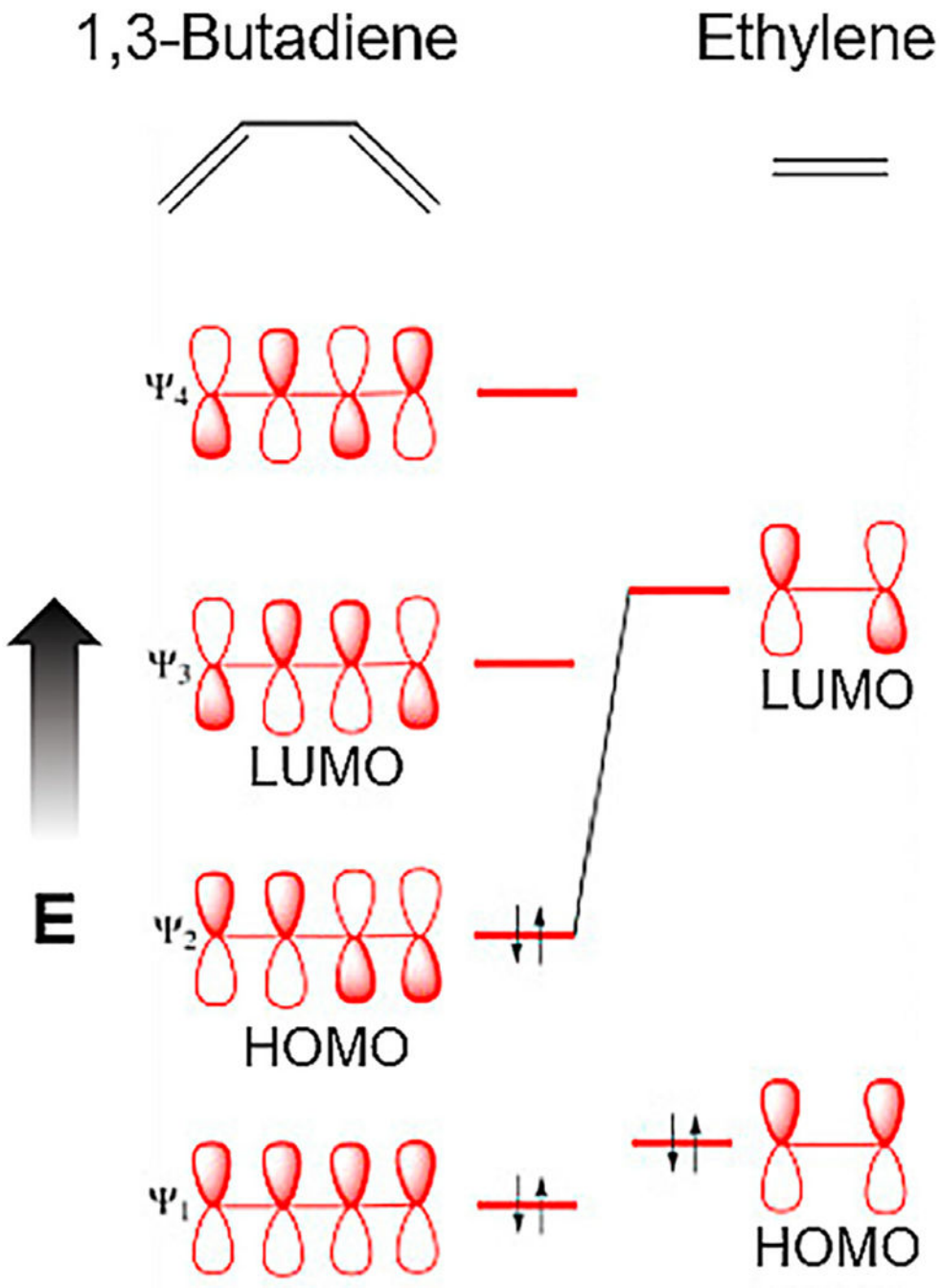

Fig. 11.

Frontier (π-orbitals) of 1,3-butadiene (left) and dienophile (right). Adapted from ref. [68]. Copyright 1973. Academic Press.

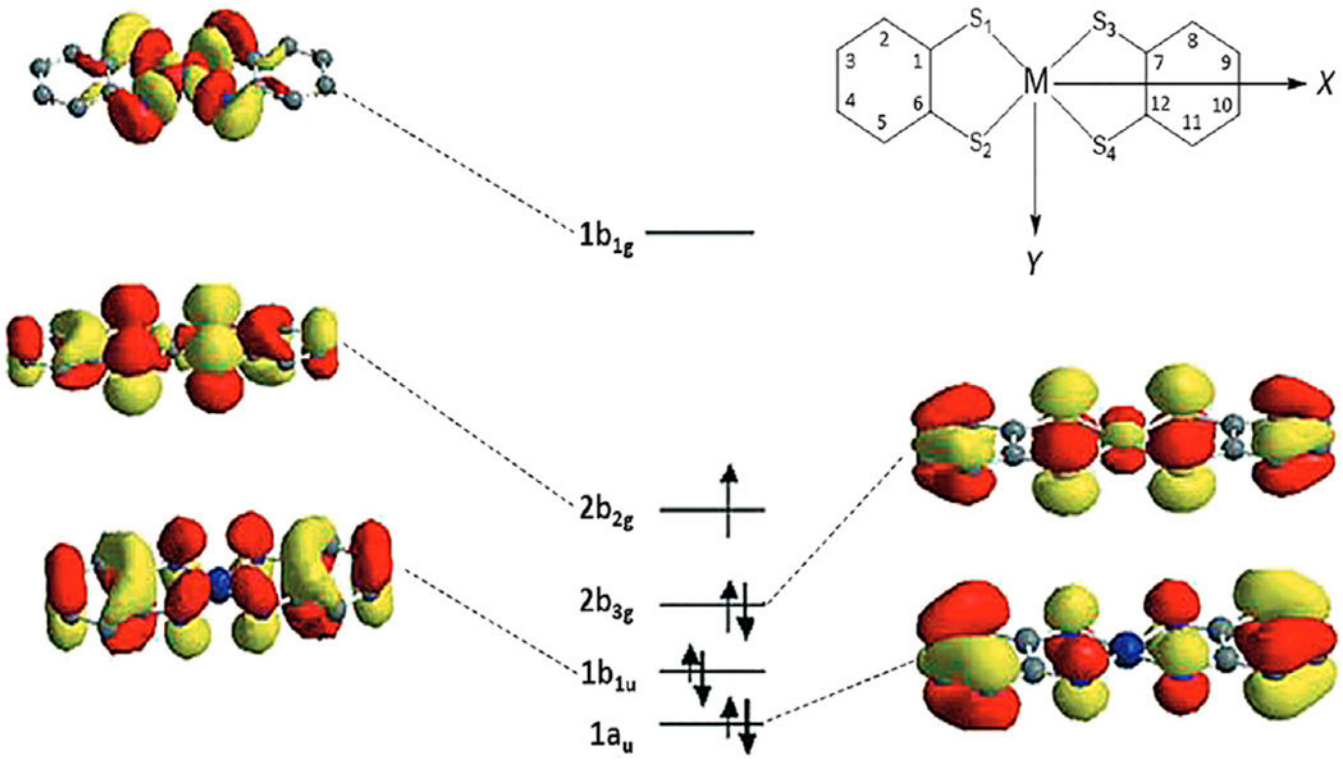

Fig. 12.

MO diagram of the $[M^{II}(Dt^{2-})(Dt^{1-})]^{1-}$(M = Ni, Pd and $[Au^{III}(Dt^{2-})(Dt^{1-})]$ complexes having a spin doublet ground state. Reprinted with permission from ref. [78]. Copyright 2007. Wiley-VCH.

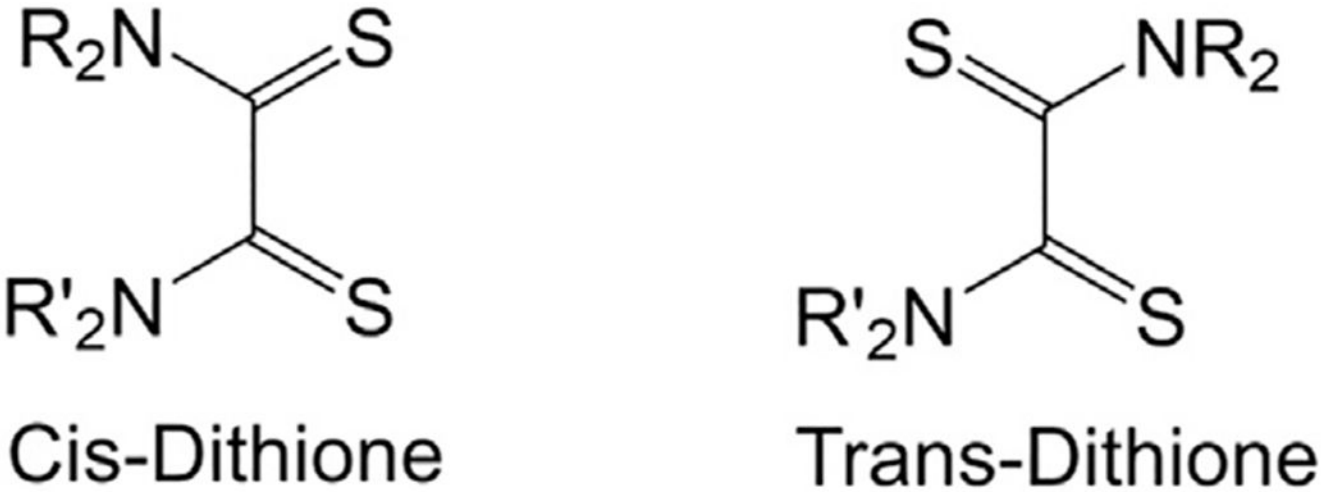

Fig. 13.
Two geometric isomers of an acyclic dithione ligand.

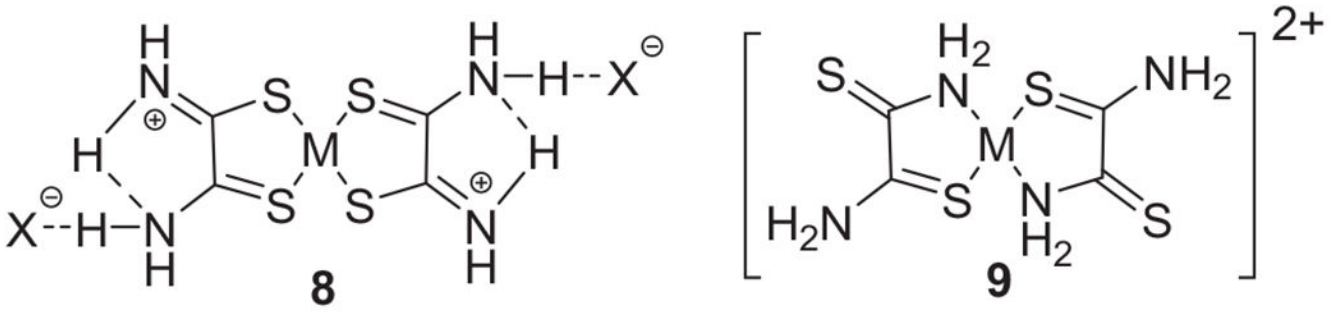

Fig. 14.
Coordination modes of a dithiooxamide ligand.

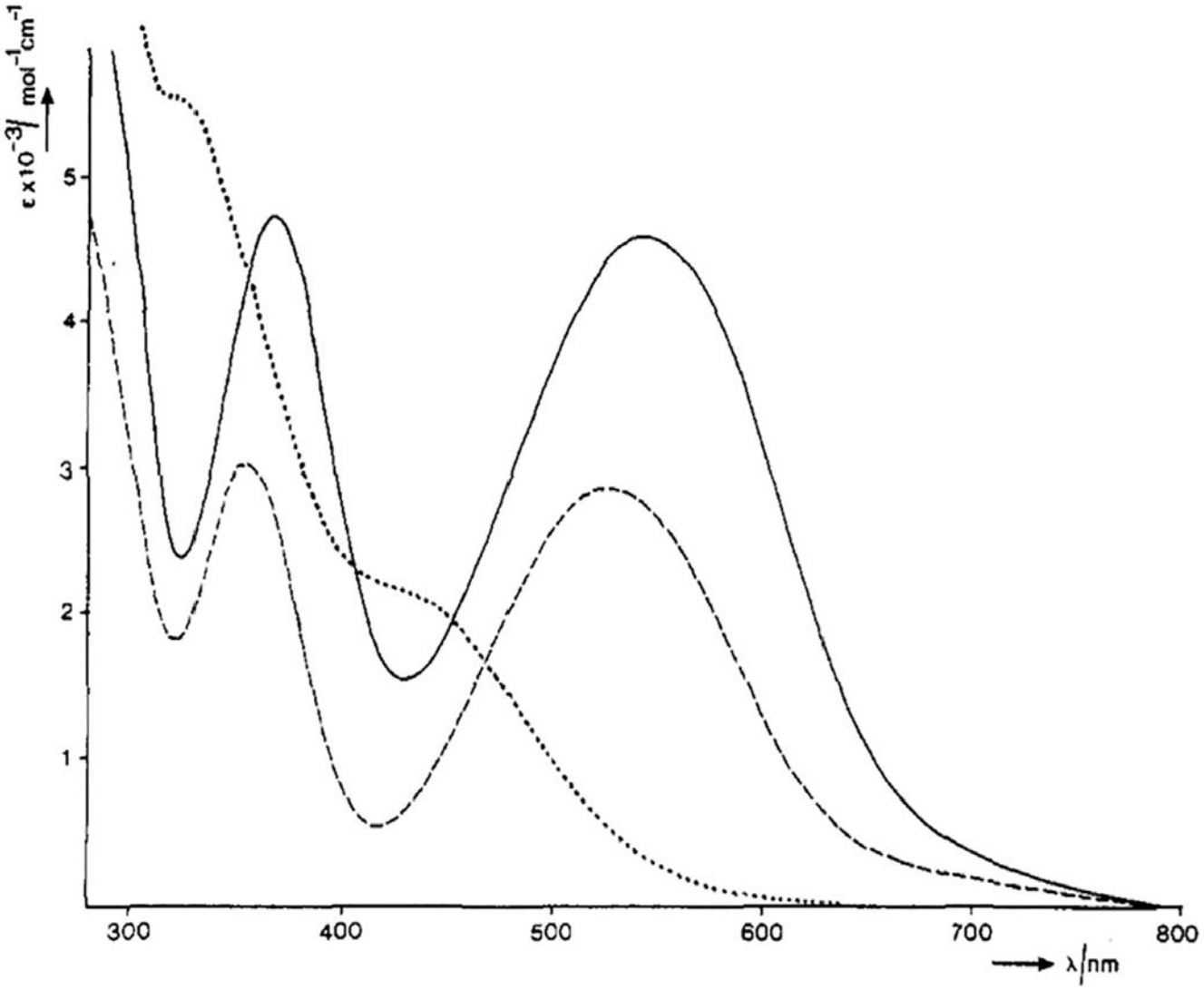

Fig. 15.

Electronic absorption spectra at 293 K in chloroform of $ReBr(CO)_3$(Cycdto) (−), $ReBr(CO)_3$(Bz1 $_2$dto) (– – –), and $ReBr(CO)_3$(Et_4dto) (…). Reprinted with permission from ref. [42]. Copyright 1989. American Chemical Society.

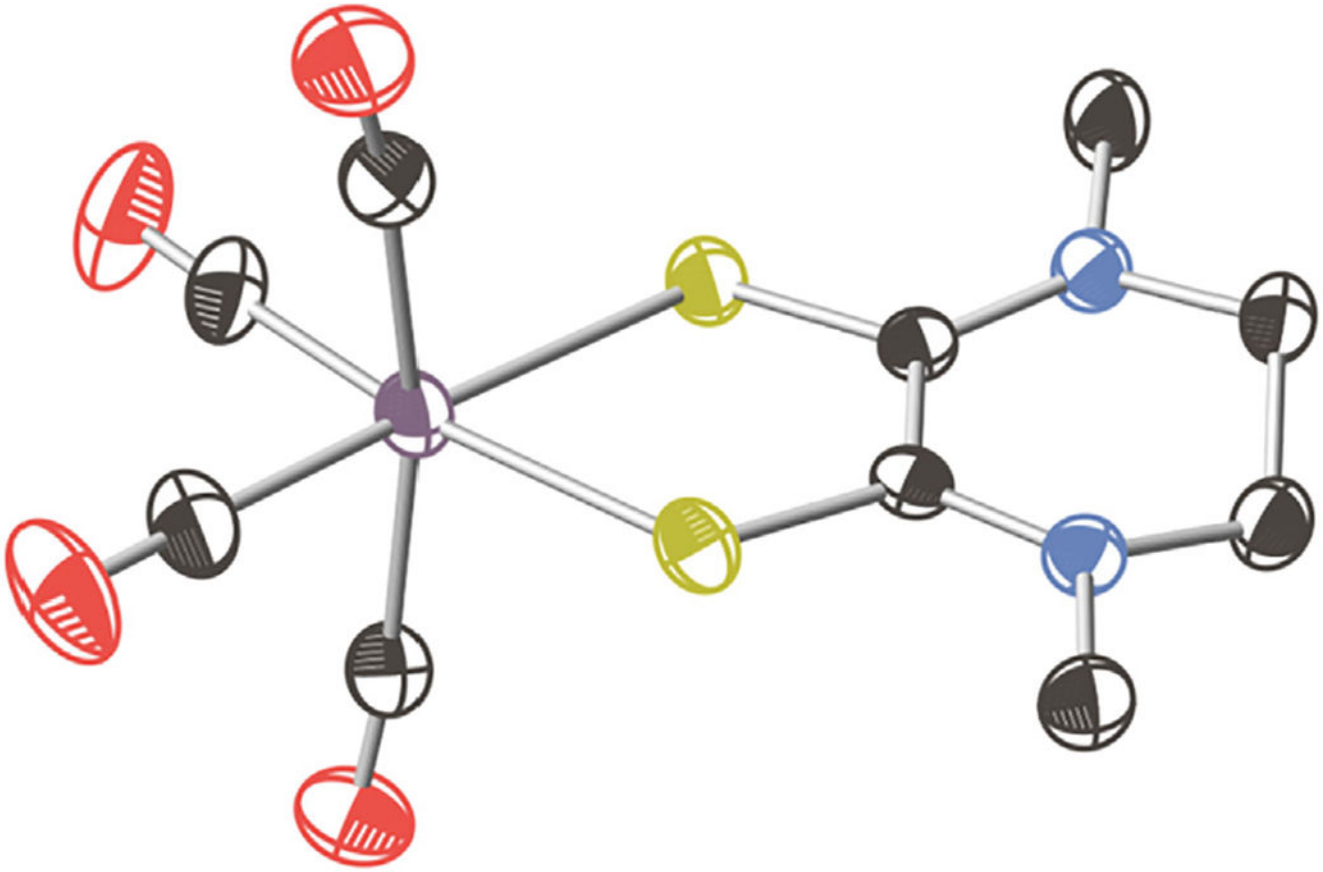

Fig. 16.

ORTEP of $Mo(CO)_4(Me_2Dt^0)$ (30%) with hydrogens omitted for clarity. Reprinted with permission from ref. [122]. Copyright 2006. American Chemical Society.

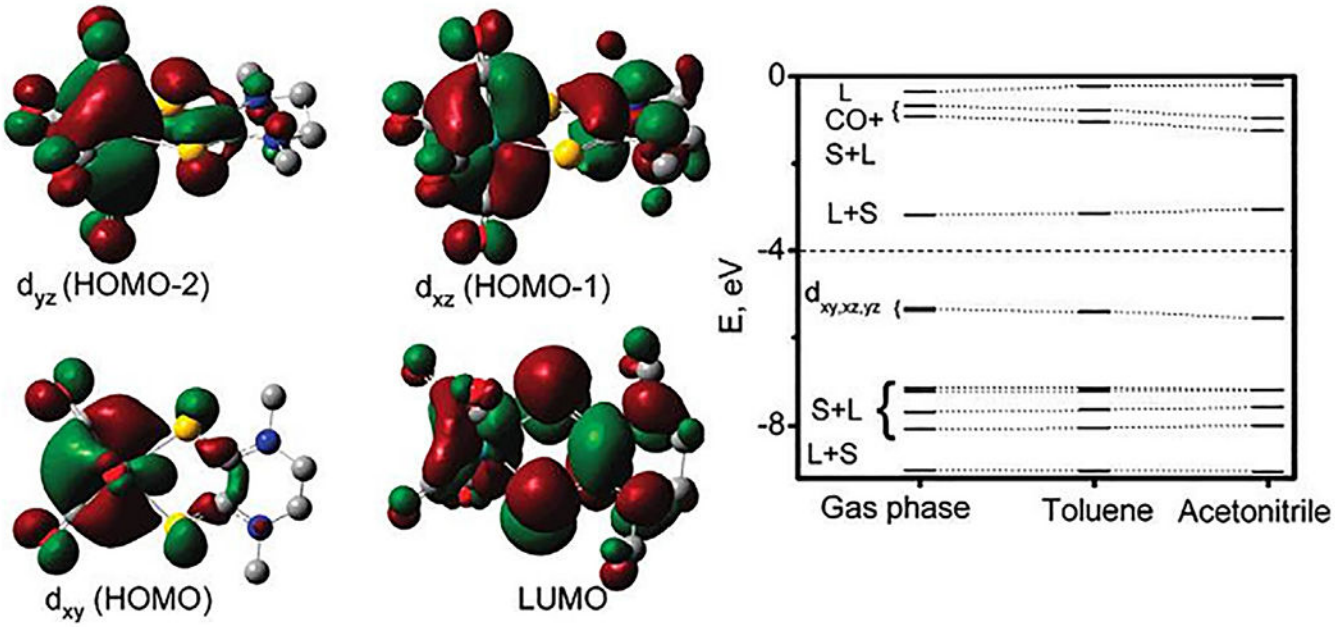

Fig. 17.

Selected MOs and energy diagram of $Mo(CO)_4(Me_2Dt^0)$. Reprinted with permission from ref. [122]. Copyright 2006. American Chemical Society.

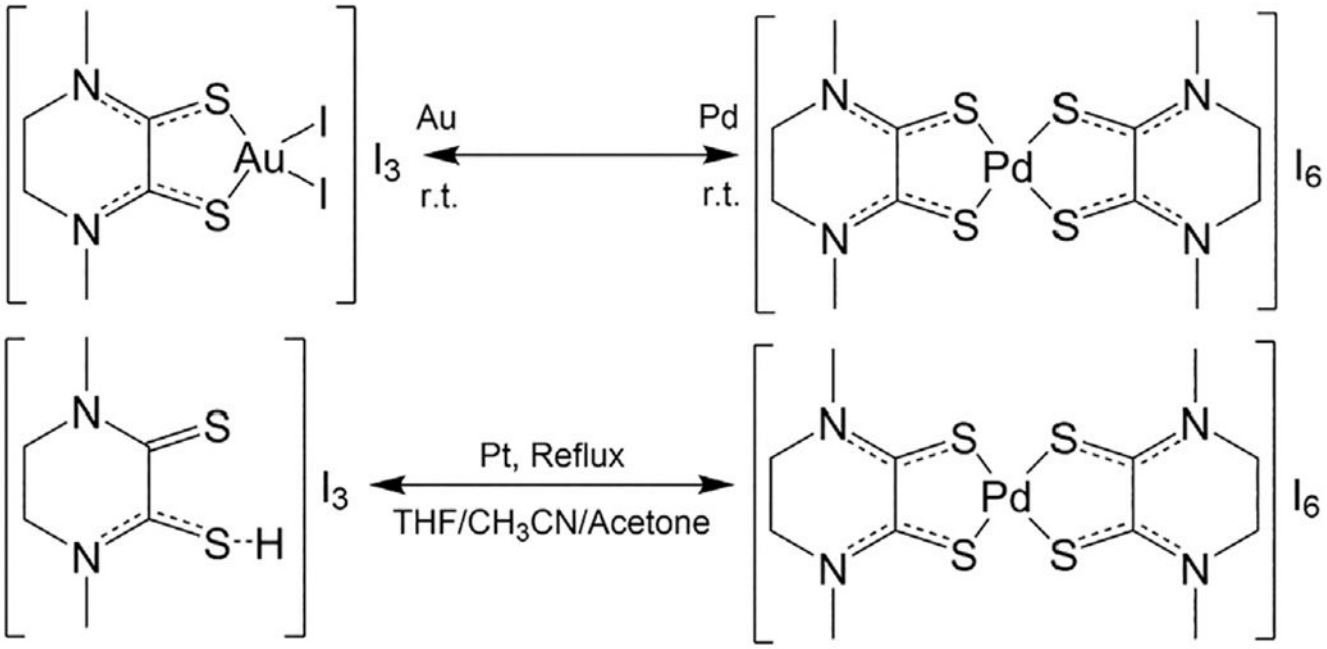

Fig. 18.
Reactivity of dithione-halogen complexes with metals.

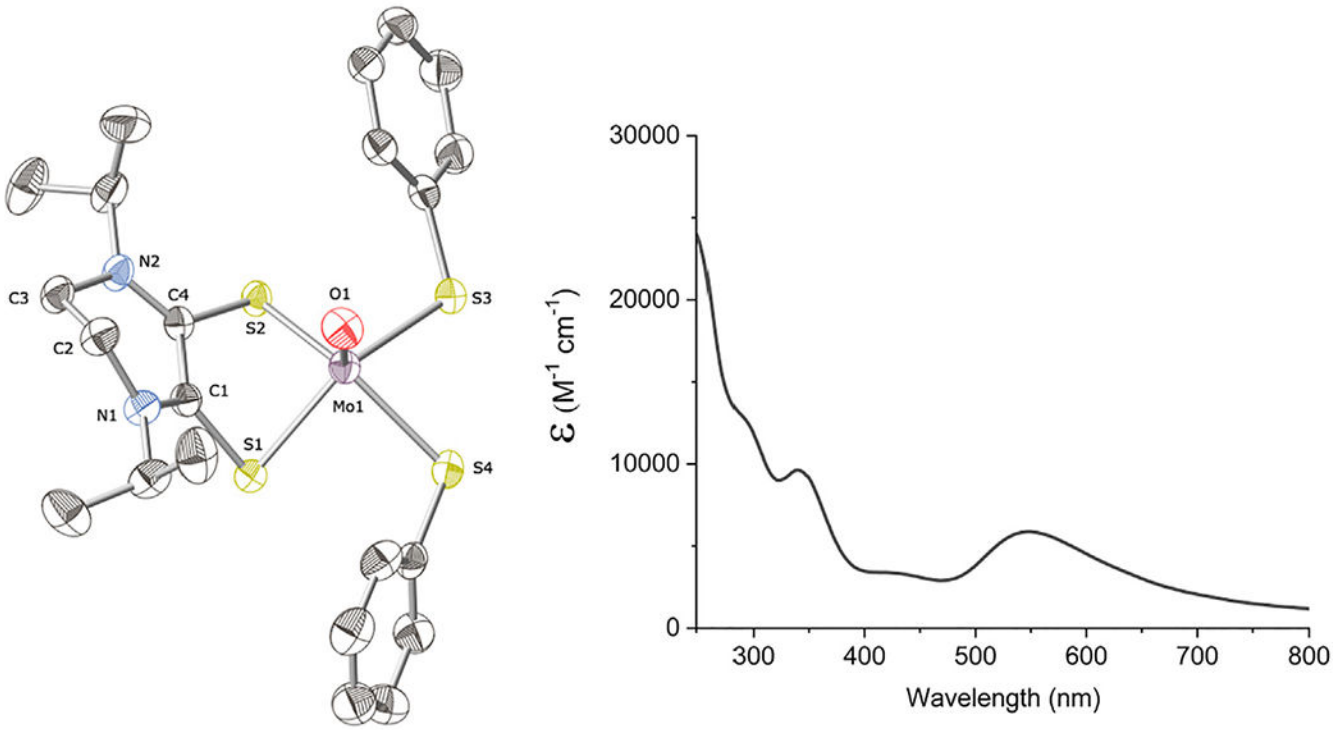

Fig. 19.

(Left) Thermal ellipsoid (40%) plot of $MoO(SPh)_2$ ($^iPr_2Dt^0$). Hydrogen atoms are omitted for clarity. The absorbance spectrum recorded in CH_3CN is shown on the right. Reprinted with permission from ref. [132]. Copyright 2016. American Chemical Society.

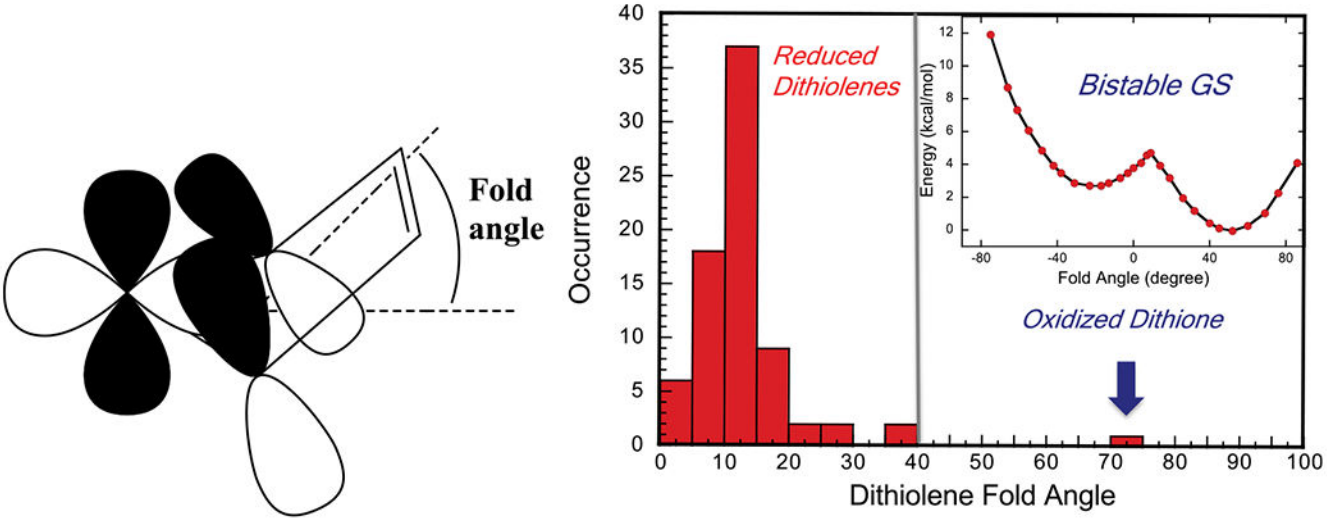

Fig. 20.

Left, the dithiolene fold angle, showing the stabilizing interaction of symmetric metal in-plane d-orbitals and sulfur p-orbital. Right, a histogram of the oxomolybdenum dithiolene fold angles determined by X-ray crystallography. The most common dithiolene fold angle is 12.5°, and the largest is ~37°. Note that the 70° dithione fold angle in $MoO(SPh)_2(^iPr_2Dt^0)$ represents an extreme deviation from the observed fold angles for reduced dithiolene ligands. Reprinted with permission ref. [122]. Copyright 2016. American Chemical Society.

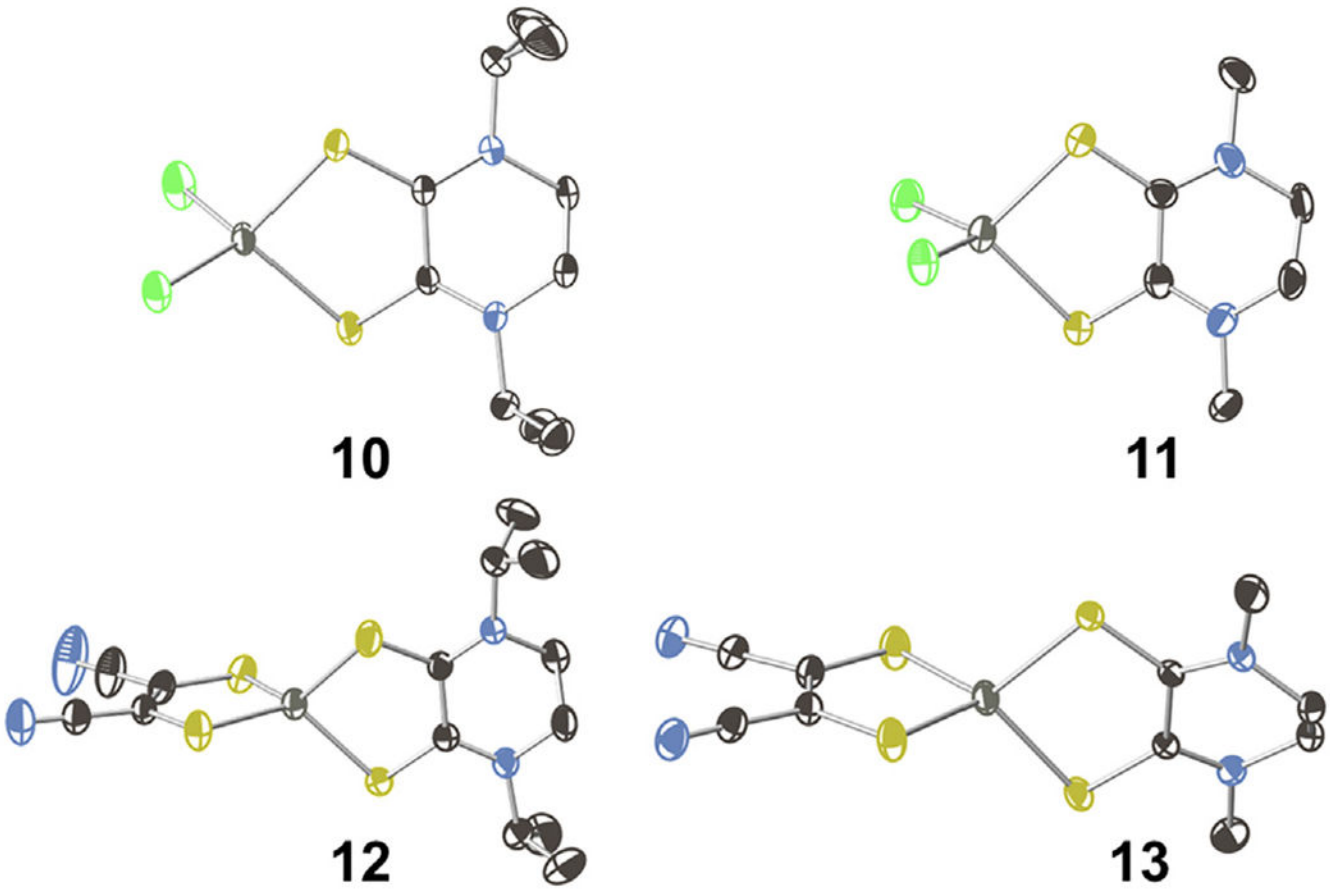

Fig. 21.

Molecular structures of $Zn(Cl)_2(^iPr_2Dt^0)$ (**7**), $Zn(Cl)_2(Me_2Dt^0)$ (**8**), Zn(mnt) ($^iPr_2Dt^0$) (**9**), $Zn(mnt)(Me_2Dt^0)$ (**10**) shown with 30% probability thermal ellipsoids. Hydrogens are removed for clarity. Reprinted with permission from ref. [141]. Copyright 2016. Elsevier.

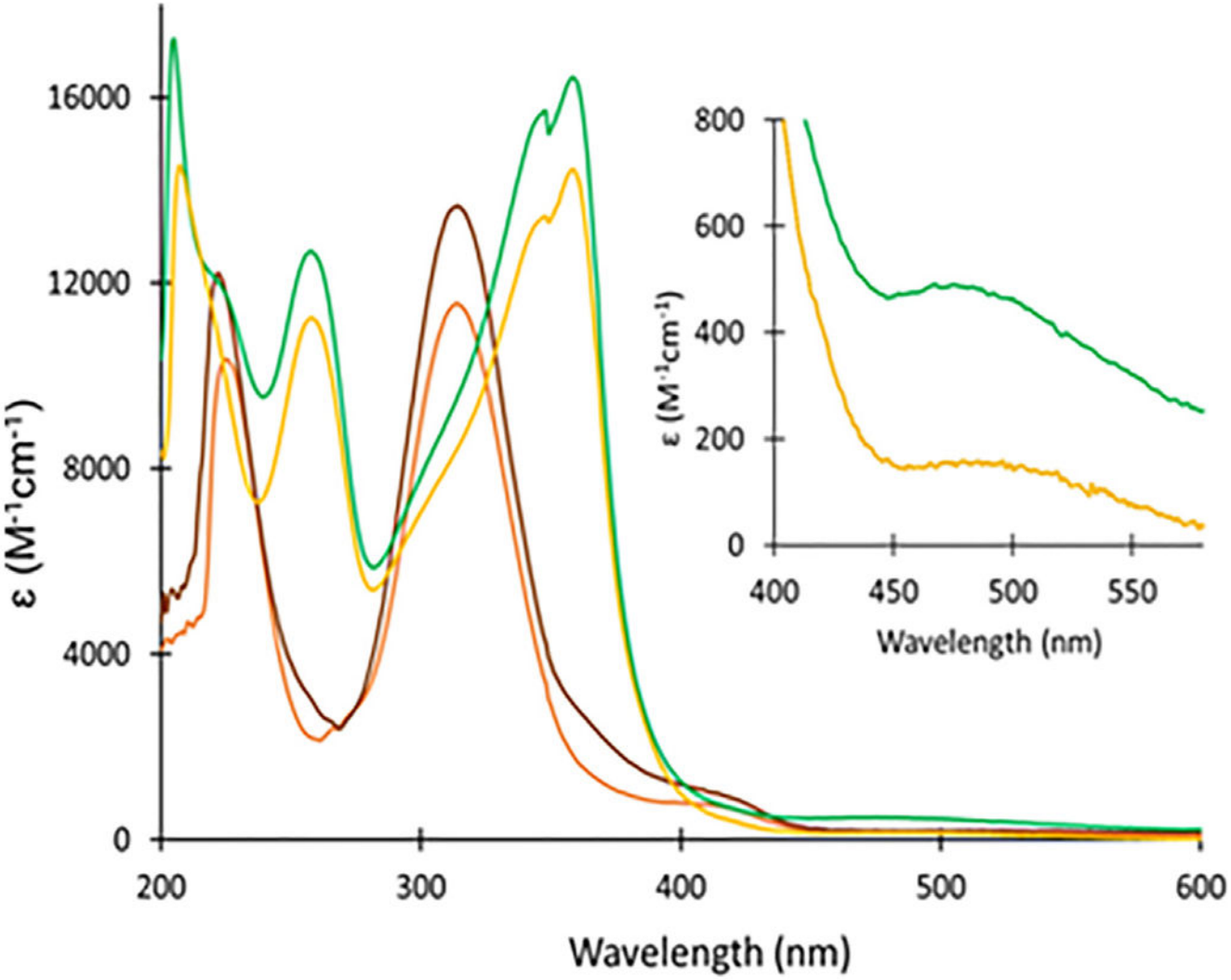

Fig. 22.

Electronic absorption spectra of Zn(II) dithione complexes in acetonitrile **7** (orange) **8** (brown) **9** (green) **10** (yellow). Low energy ligand-to-ligand charge transfer bands are shown in the inset. Reprinted with permission from ref. [141]. Copyright 2016. Elsevier.

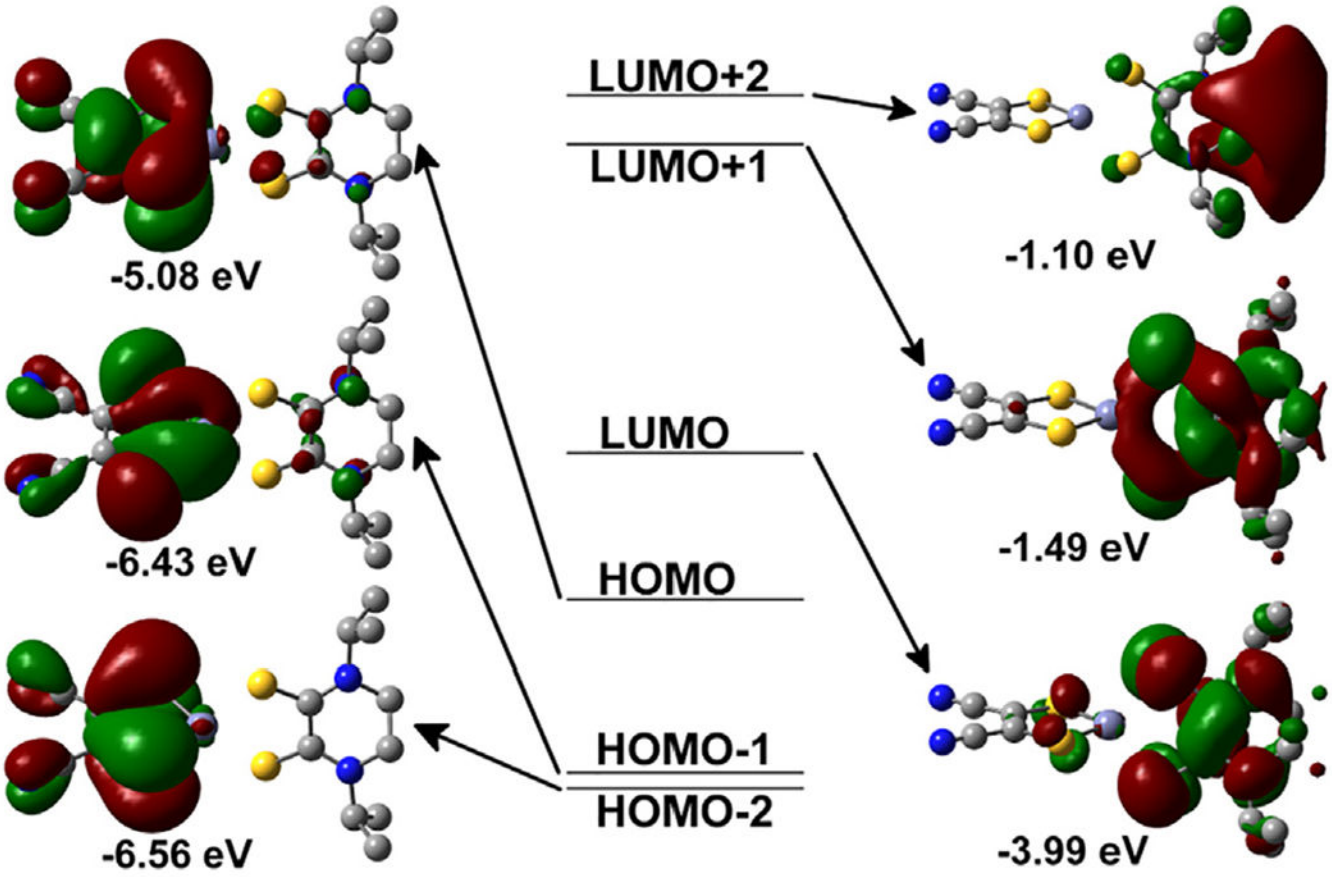

Fig. 23.

Frontier orbital diagram of Zn(mnt)($^{i}Pr_2Dt^0$) displayed with calculated energies. Reprinted with permission from ref. [141]. Copyright 2016. Elsevier.

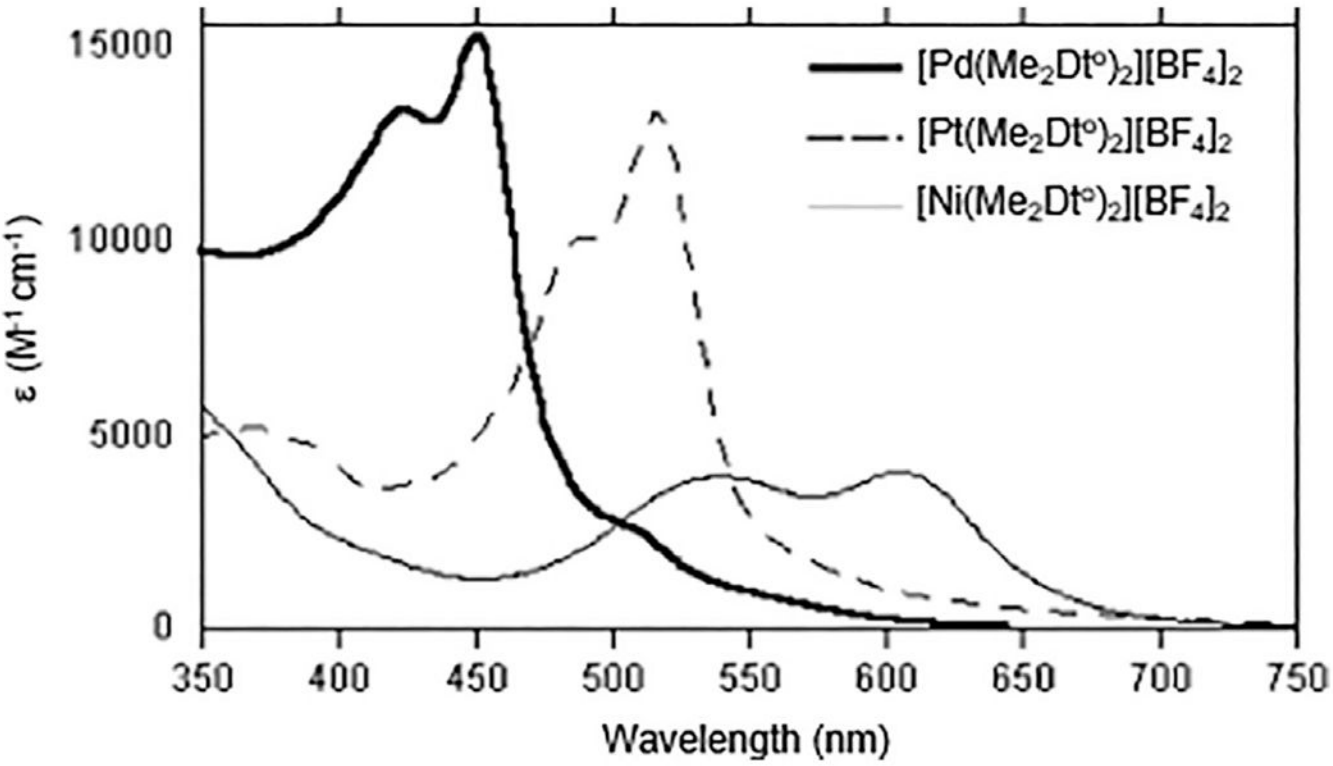

Fig. 24.

The electronic spectra of $[M(Me_2Dt^0)_2][BF_4]_2$ in MeCN solution. Reprinted with permission from ref. [10]. Copyright 2002. American Chemical Society.

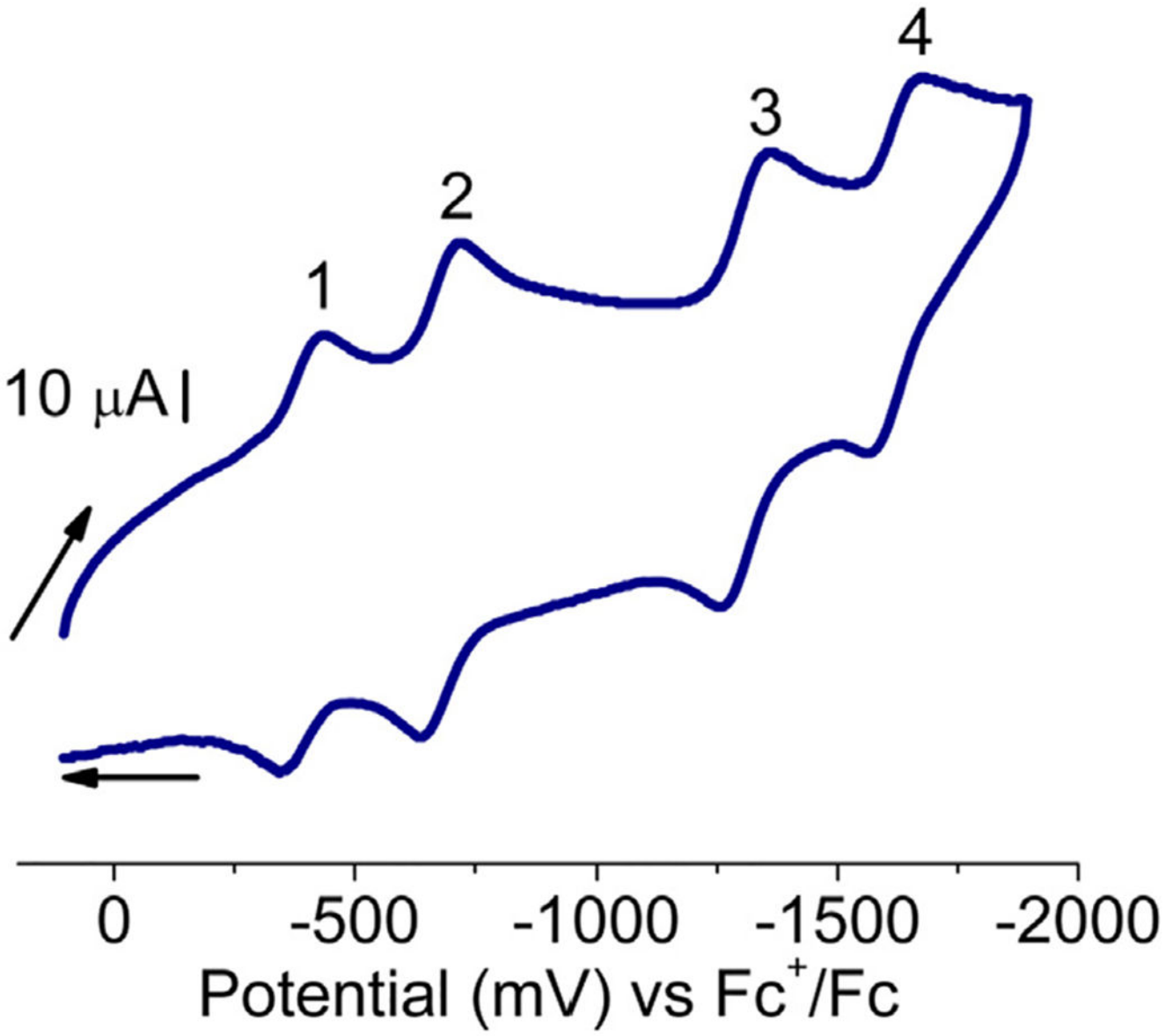

Fig. 25.

Cyclic voltammogram of $[Ni(^iPr_2Dt^0)_2][BF_4]_2$. Scan rate, 100 mVs^{-1}; temperature, 25 °C; in acetonitrile, carbon disk working electrode. Ag^+/Ag reference electrode, and a Pt-wire auxiliary electrode, supporting electrolyte, Et_4NBF_4. Potentials referenced internally with respect to Fc^+/Fc couple. Reprinted with permission form ref. [152]. Copyright 2015. American Chemical Society.

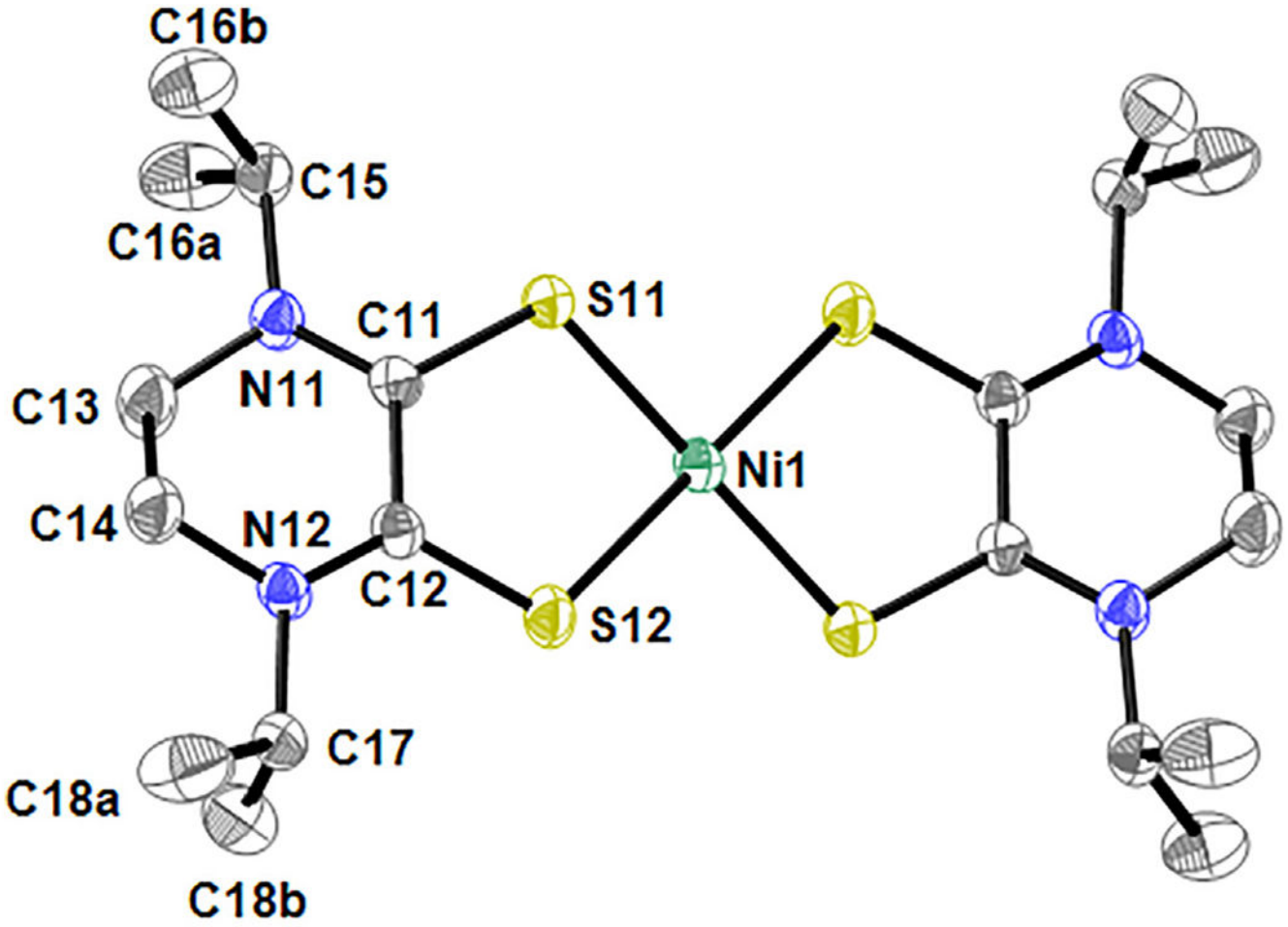

Fig. 26.

Molecular structure of $[Ni(^{i}Pr_2Dt^0)_2][BF_4]_2$ shown with 30% thermal ellipsoids, and hydrogen atoms and the anions are omitted for clarity. Reprinted with permission form ref. [152]. Copyright 2015. American Chemical Society.

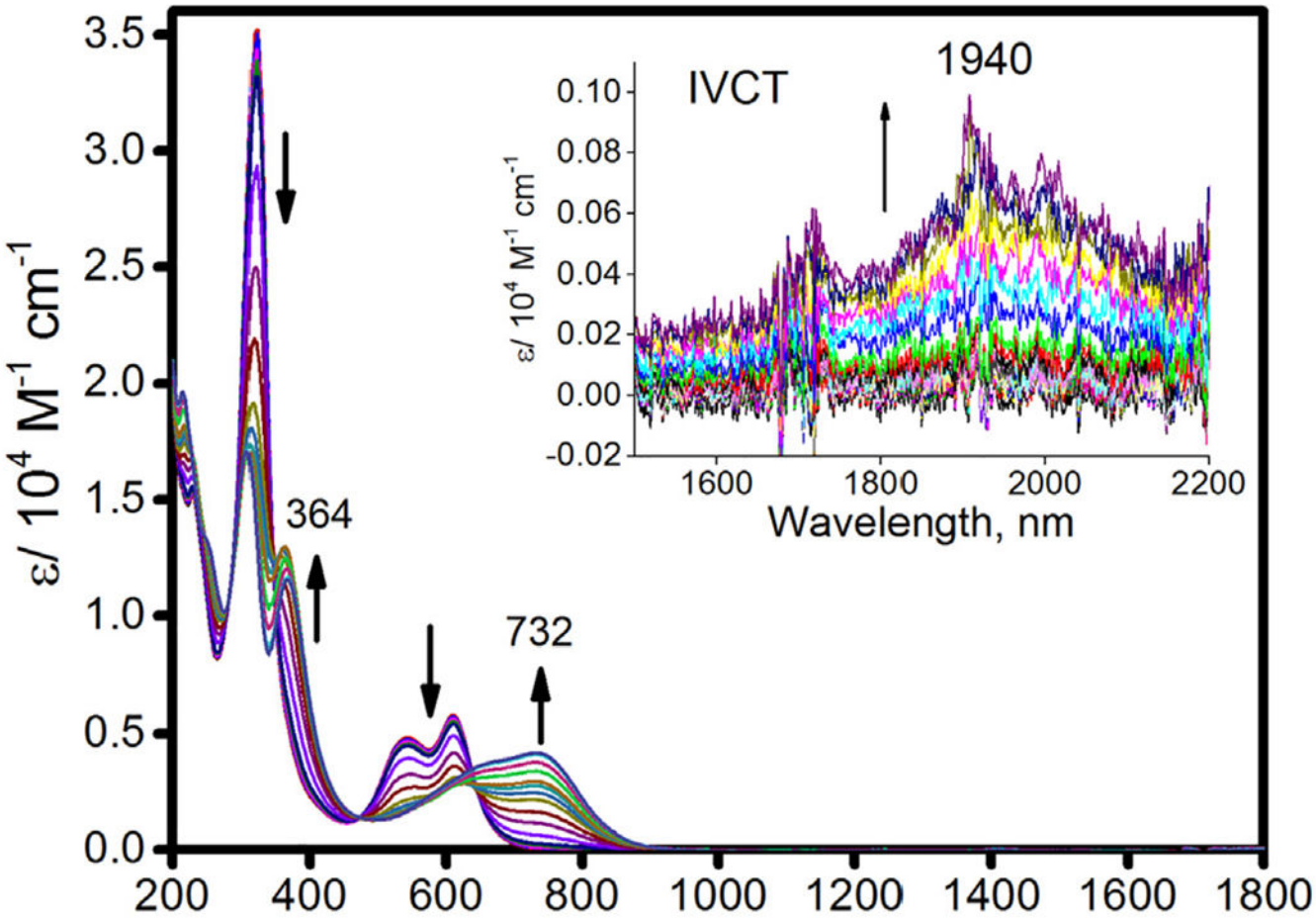

Fig. 27.

UV–visible spectra of $[Ni(^{i}Pr_2Dt^0)_2][BF_4]_2$ produced using spectroelectrochemistry (reduced in CD_3CN). Reprinted with permission form ref. [152]. Copyright 2015. American Chemical Society.

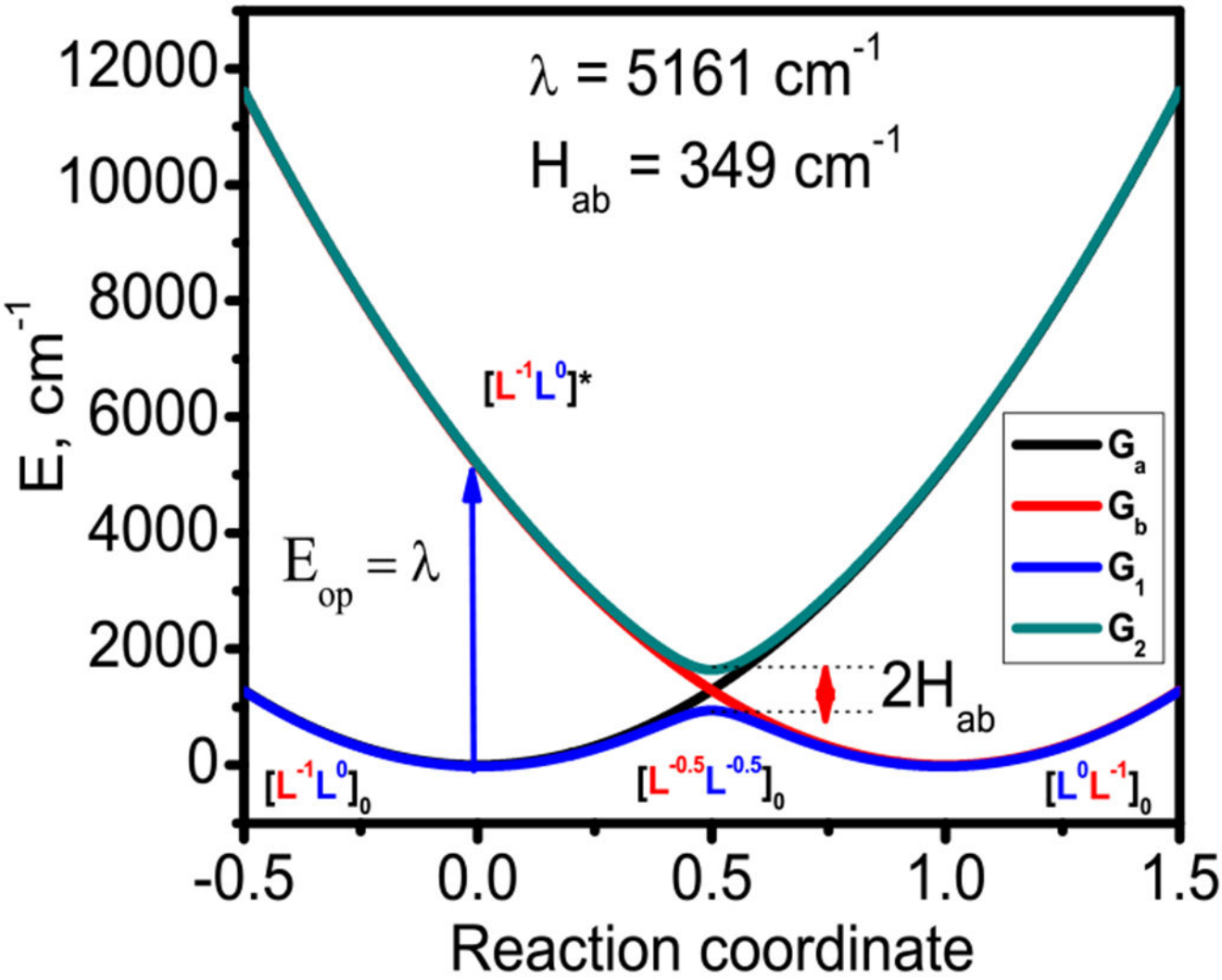

Fig. 28.

Diabatic (G_a and G_b) and adiabatic (G_1 and G_2) potential energy surfaces are calculated to determine their coupling (H_{ab}) for an intervalence electron transfer of $[Ni(^iPr_2Dt^0)_2][BF_4]_2$. Reprinted with permission form ref. [152]. Copyright 2015. American Chemical Society.

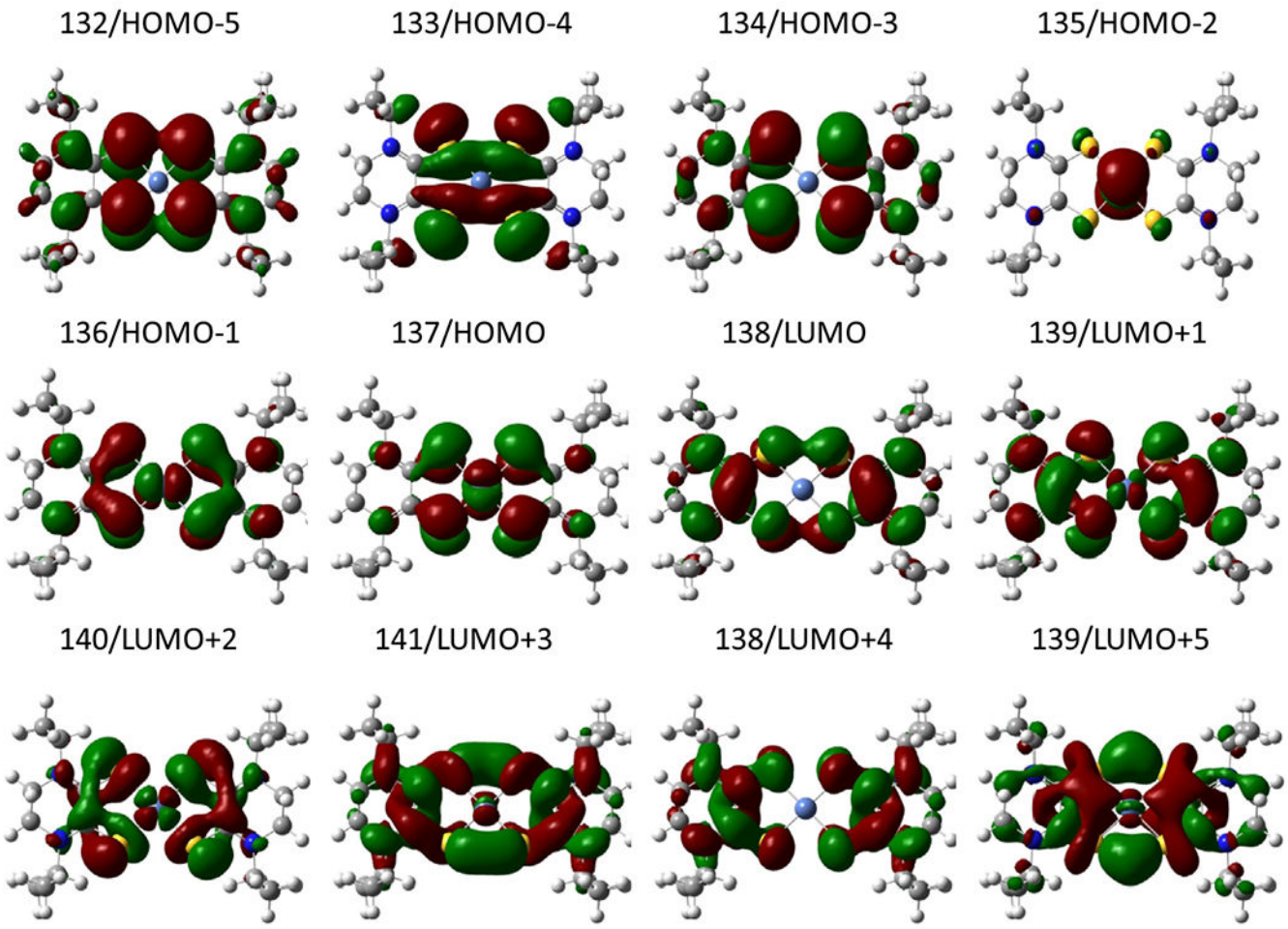

Fig. 29.

Predicted frontier molecular orbitals of $[Ni(^{i}Pr_2Dt^{0})_2]^{2+}$. Reprinted with permission form ref. [152]. Copyright 2015. American Chemical Society.

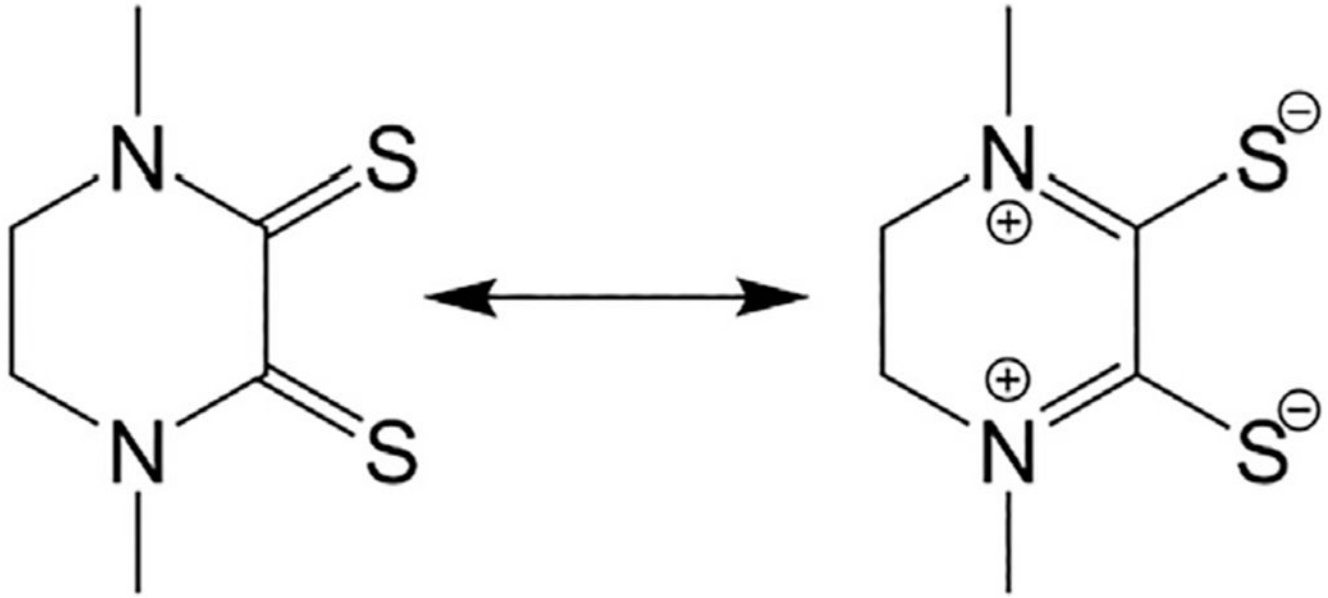

Fig. 30.

The contributing resonance structures for the R_2Dt^0 $N_2C_2C_2$ π-delocalization: dithione(right), dizwitterionic dithiol (left).

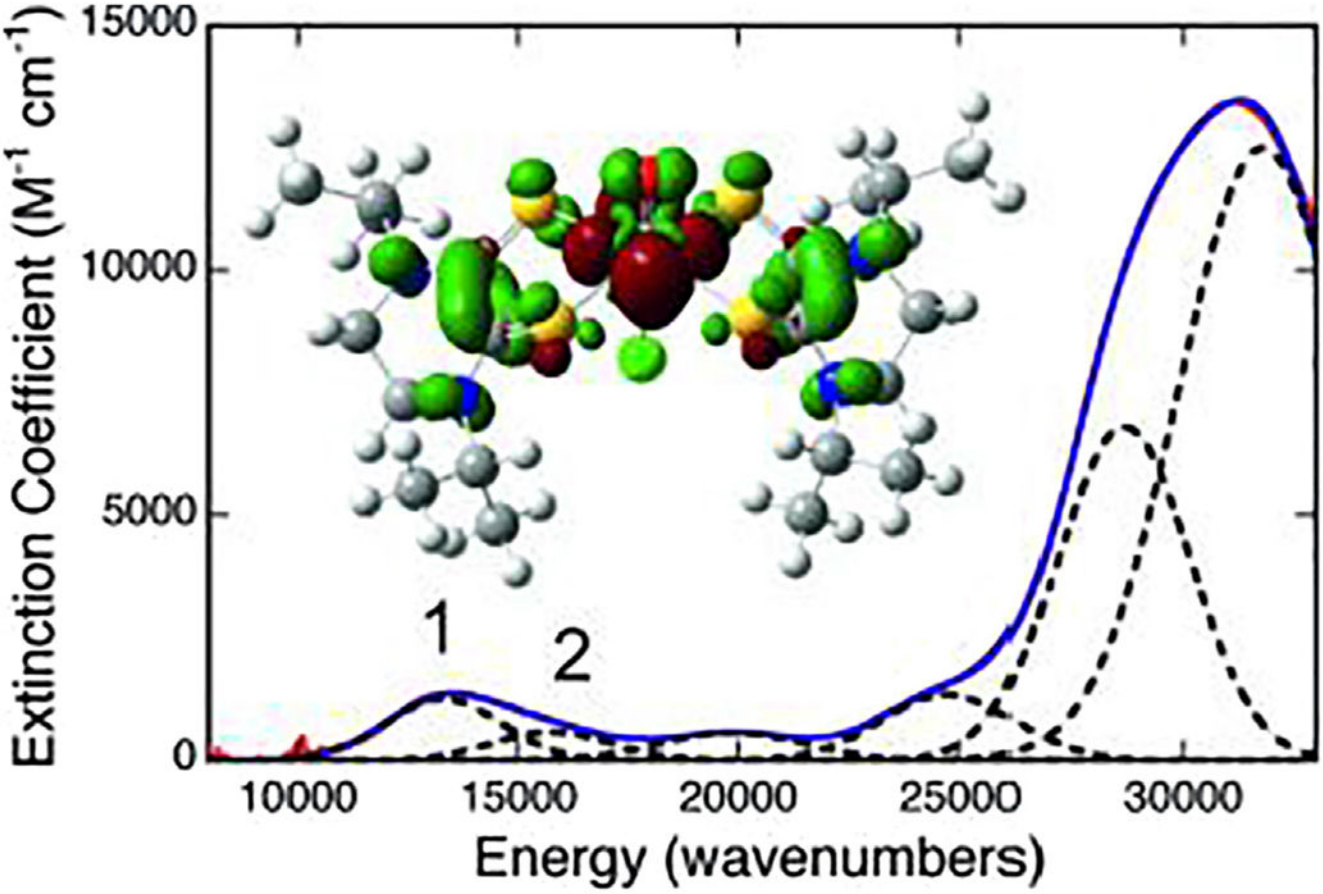

Fig. 31.

Gaussian resolved electronic absorption spectrum of $[MoOCl(^{i}Pr_2Dt^0)_2][PF_6]$ in MeCN. Inset: Electron density difference map (EDDM) that shows in detail the nature of the low-energy MLCT transition (band 1) in 1 (red: electron-density loss in transition; green: electron-density gain in transition). Reprinted with permission from ref. [131]. Copyright 2011. Wiley-VCH.

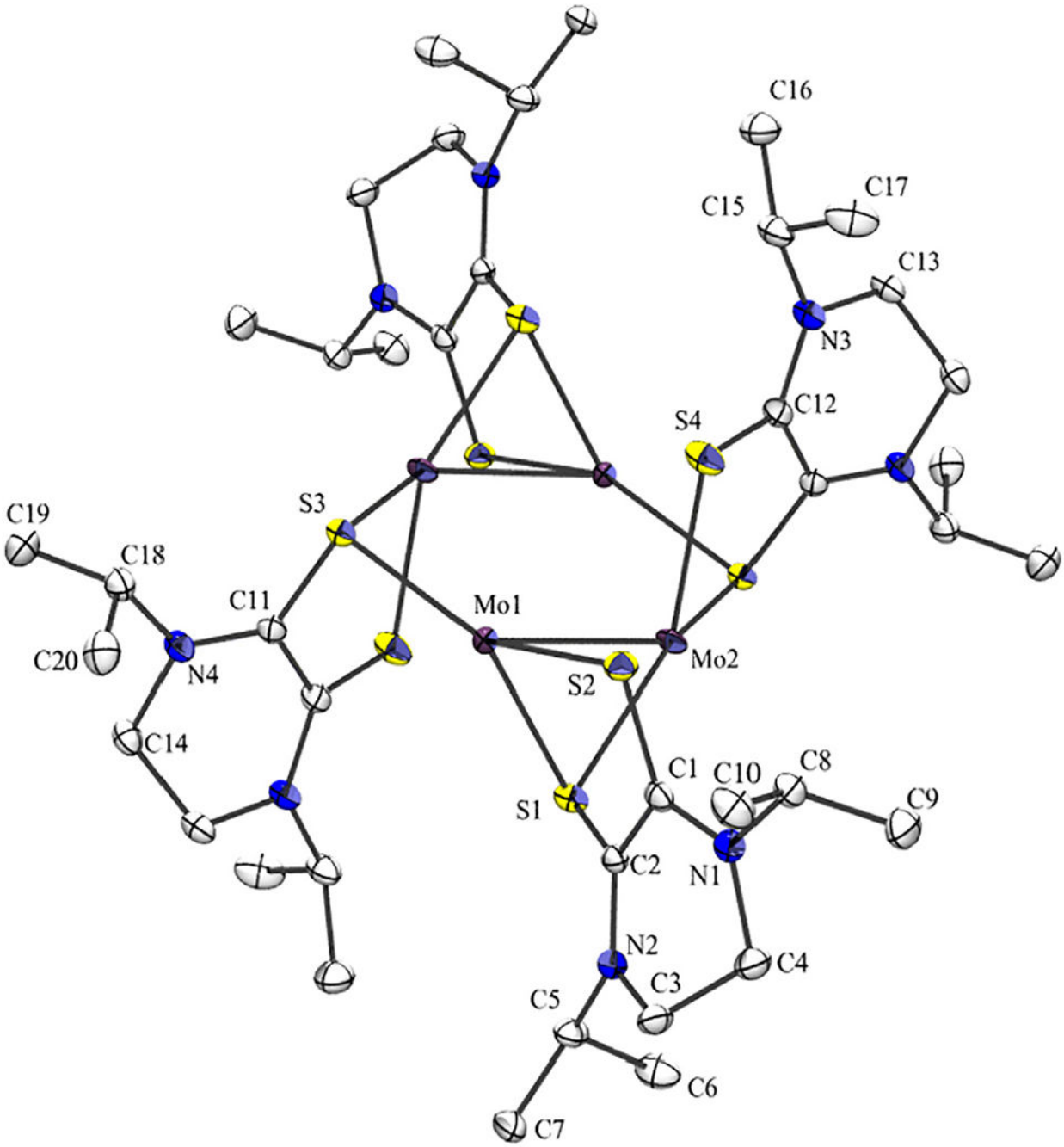

Fig. 32.

Thermal ellipsoid (30%) plot of [($^{i}Pr_2Dt^0Mo]_4BF_4$], counter anions are omitted for clarity. Adapted from ref. [130]. Copyright 2009. Royal Society of Chemistry.

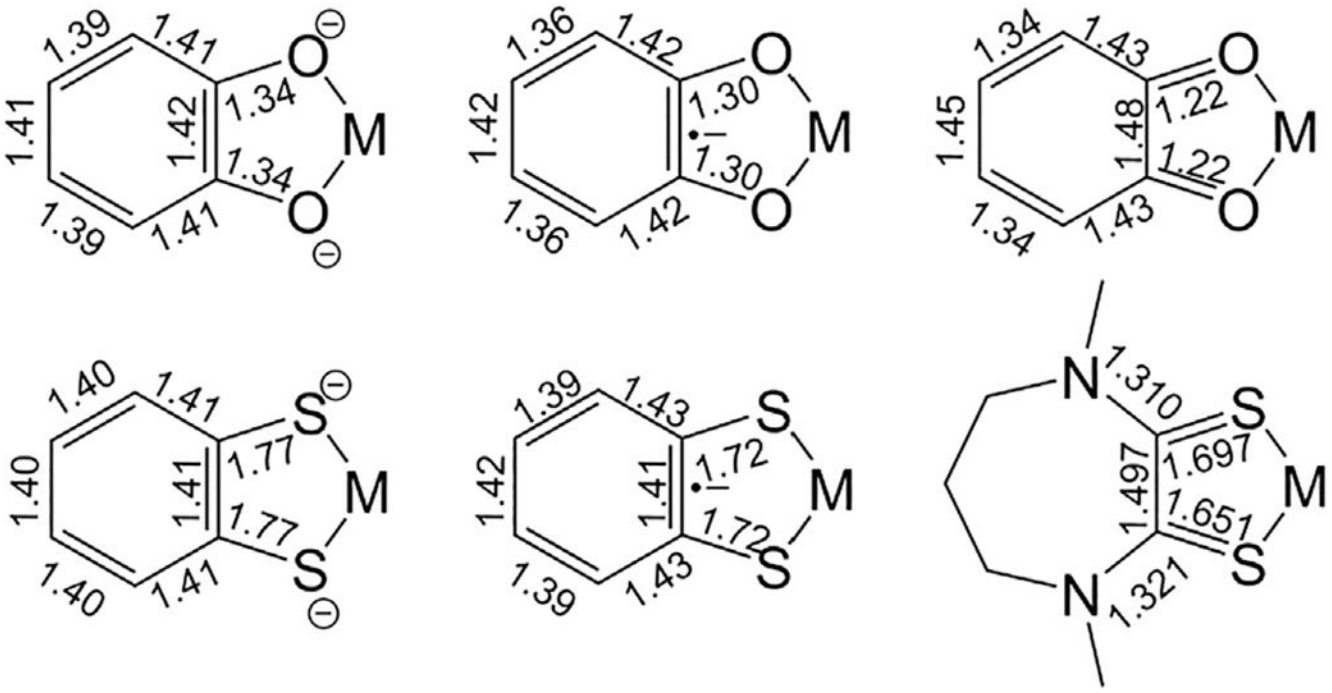

Fig. 33.

Bond lengths of dianionic, anionic radical, and neutral catechol and dithiolene ligands. Adapted from ref. [68]. Copyright 1994. Elsevier.

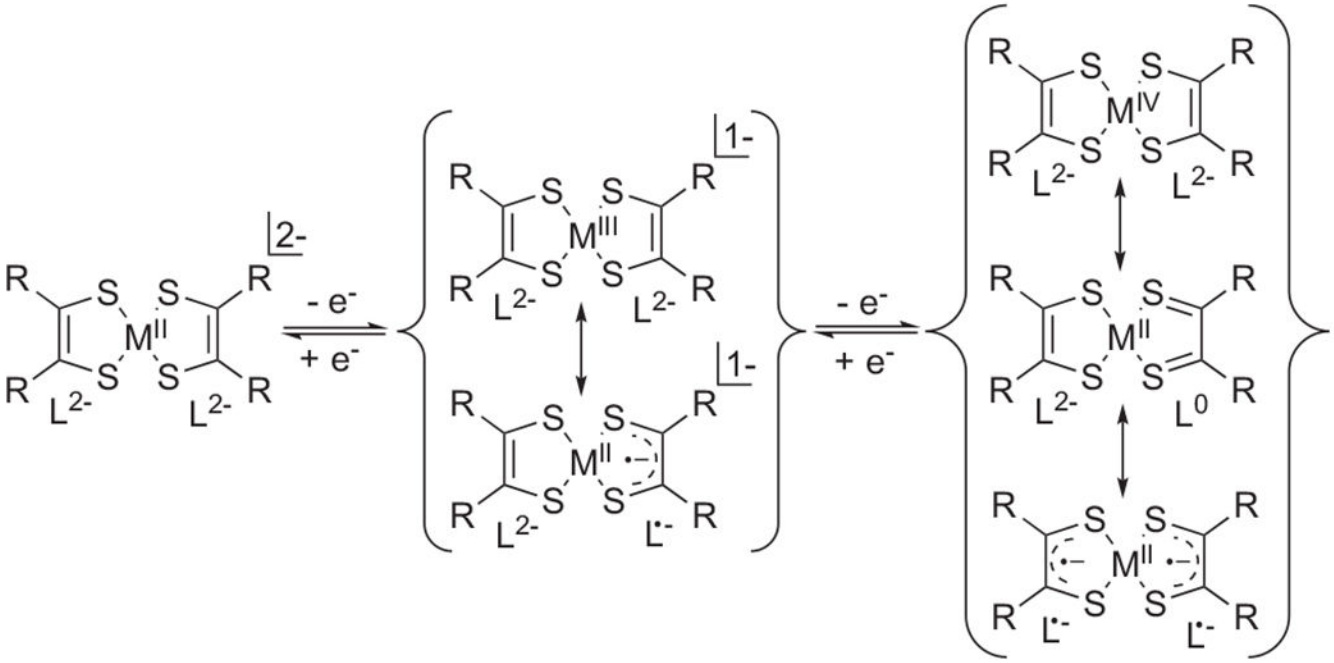

Fig. 34.

Possible resonance hybrid of the $[M(S_2C_2R_2)_2]^{0,1-,2-}$ series of complexes. Reprinted with permission form ref. [149]. Copyright 2015. American Chemical Society.

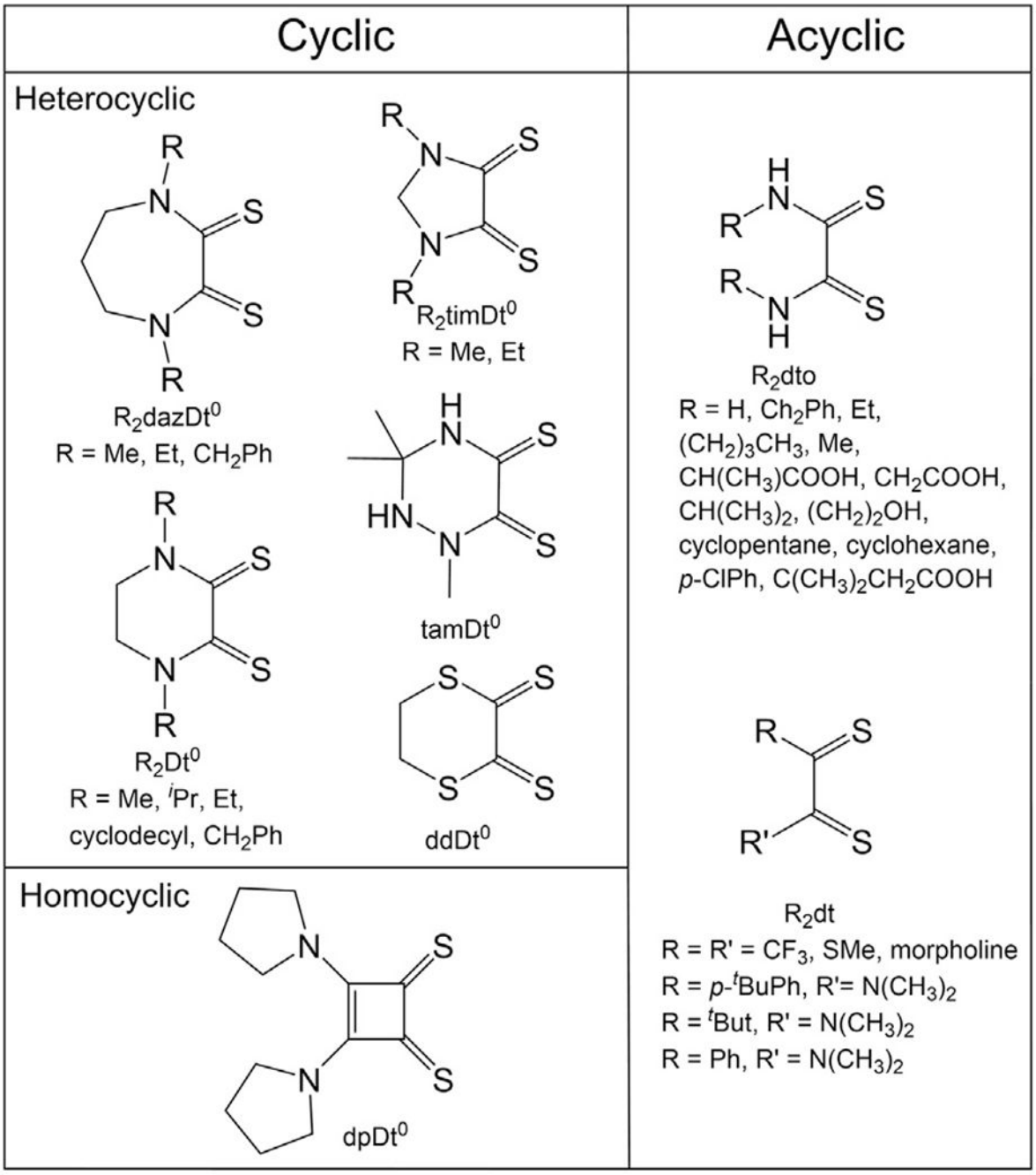

Chart 1.
Categorization of Dithione ligands.

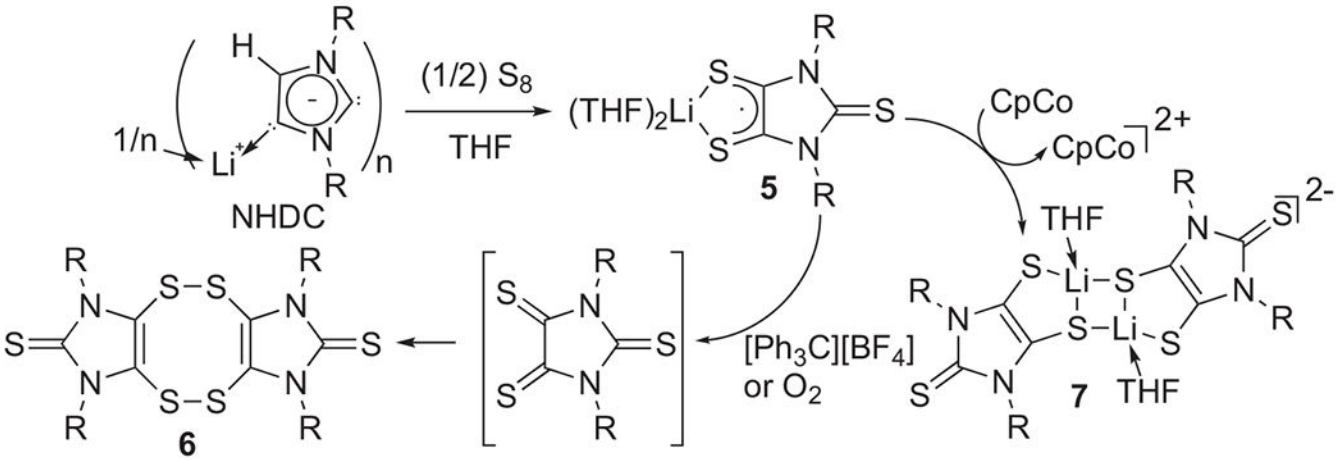

Scheme 1.

Synthesis of the first anionic radical dithiolene (**5**) and its redox chemistry.

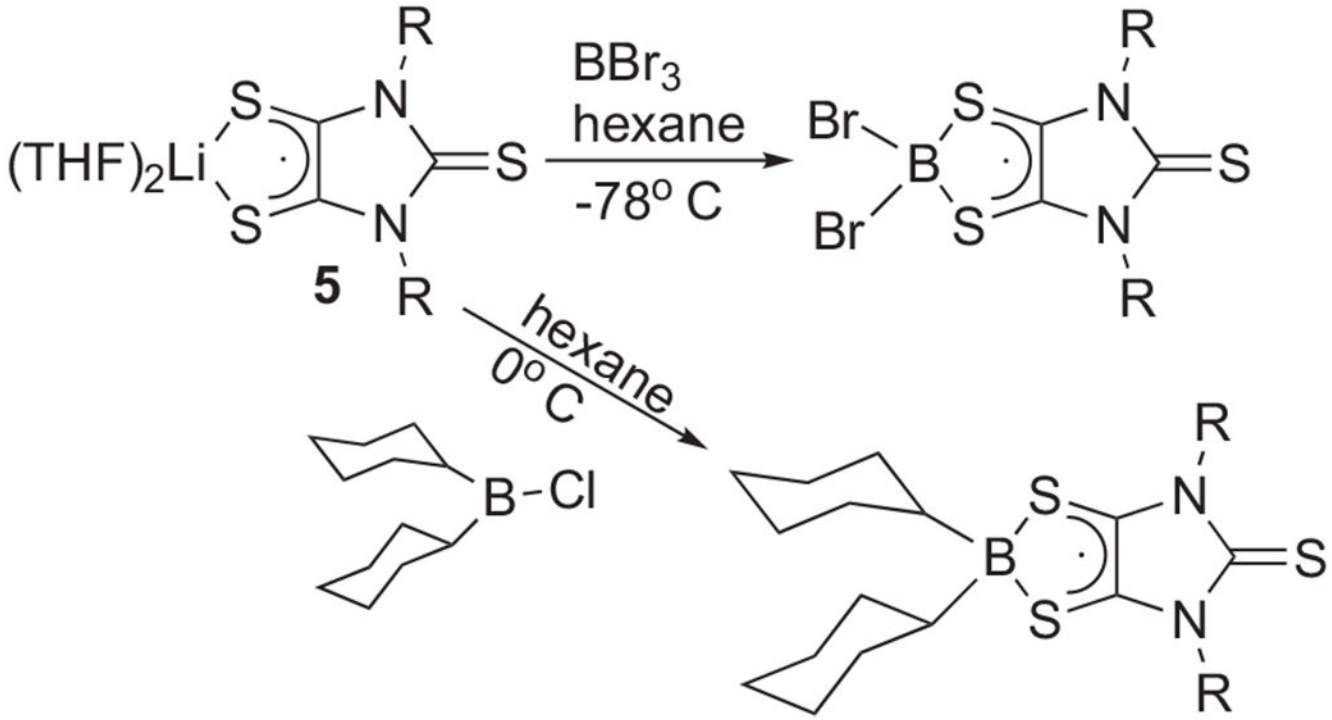

Scheme 2.
Synthesis of radical boron dithiolene compounds.

$$[Ni(Dt^0)_2]^{2+} \underset{-e^-}{\overset{+e^-}{\rightleftharpoons}} [Ni(Dt^0)(Dt^-)]^{+} \underset{-e^-}{\overset{+e^-}{\rightleftharpoons}} Ni(Dt^-)_2 \underset{-e^-}{\overset{+e^-}{\rightleftharpoons}} [Ni(Dt^-)(Dt^{2-})]^{-} \underset{-e^-}{\overset{+e^-}{\rightleftharpoons}} [Ni(Dt^{2-})_2]^{2-}$$

Scheme 3.

Electron transfer series in nickel dithione complex.

Table 1

Selected bond lengths of representative dithione ligands (Å).

Ligand	R-group	d(C–C)	d(C-N)	d(C=S)	Reference
R_2dto	−CH(CH_3)COOH	1.527(3)	1.322(3)	1.650(3)	[57]
	−CH_2COOH	1.528(4)	1.316(3)	1.655(2)	[57]
	−CH_2CH(OH)CH_3	1.522(4)	1.312(3)	1.654(3)	[58]
	−*p*-ClPh	1.537(10)	1.321(7)	1659(5)	[59]
dpDt^0		1.453(10)	–	1.645(7)	[60]
R_2Dt^0	Me	1.532(5)	1.323(5)	1.660(4)	[42]
	Cyclodecyl	1.523(2)	1.340(3)	1.661(10)	[41]

Table 2

Selected experimental and calculated bond lengths (Å) of dithiolene ligands in their 2−, 1−, and 0 oxidation states.

Ligand	d(C–C)	d(C-S)	d(C-N)	Reference
Me_2Dt^0	1.532(5)	1.660(4)	1.323(5)	[42]
5	1.417(3)	1.677(3)	1.389(3)	[51]
mnt^{2-}	1.334	1.756	–	[113]
$^iPr_2Dt^0$ *	1.525	1.664	1.357	This work
$^iPr_2Dt^{1-}$ *	1.444	1.718	1.423	This work
$^iPr_2Dt^{2-}$ *	1.382	1.782	1.465	This work

*Calculated value from Fig. 9.

Author Manuscript

Author Manuscript

Author Manuscript

Table 3

Select bond lengths (Å) of $M(CO)_4(Dt^0)$ (M = Mo and W) complexes.

Complex	M–C	M–S	C-S	C–C
$Mo(CO)_4Me_2Dt^0$	1.999	2.523	1.678	1.495
$W(CO)_4(Me_2Dt^0)$	2.002	2.511	1.690	1.489
$W(CO)_4$(mdt)	2.039	2.361	1.744	1.351

Table 4

Selected bond length (Å) and bite angle (°) of bis(dithiooxamide) complexes.

Complex	M–S	C=S	C–C	C-N	S-M–S
$[Pd(R_2dto)_2]Cl_2$	2.300	1.738(4)	1.497(6)	1.318(6)	90.00(5)
	2.291	1.683(4)			
$[Cu(R_2dto)_2][ClO_4^-]$	2.281(4)	1.67(1)	1.50(2)	1.32(1)	91.2(1)
	2.297(3)	1.66(1)	1.50(2)		

Table 5

^{13}C NMR chemical shift of $[M(R_2dto)_2]X_2$ complexes in solution and solid state with $CDCl_3$ [53].

Chemical shift in ppm				
	CH_3	**CH_2**	**CH**	**C=S**
In $CDCl_3$:				
$[Pd(R_2dto)_2]Cl_2$	20.69	56.97	26.63	186.98
$[Pt(R_2dto)_2]Cl_2$	20.75	56.64	26.57	186.74
$[Ni(R_2dto)_2]Cl_2$	20.69	57.76	26.88	187.77
In solid state:				
$[Pd(R_2dto)_2]Cl_2$	21.11	58.3	26.6	189.6
	23.0			186.9
$[Pd\ (R'_2dto)_2]Cl_2$	36.9			190.7
	35.0			187.2

R = N,N'-di-isobutyl (H_2dibu), R' = N,N'-dimethyl(H_2dmdto).

Table 6

Representative EPR data for *N,N'*-disubstituted dithio-oxamide Cu^{II} complexes [53].

Compound	g_1	$g_{\parallel}$	g_2	g_{-}	g_3	g_{iso}
$[Cu(H_2dto)Cl_2]$	–	–	–	–	–	2.080
$[Cu(H_2dto)Br_2]$	–	–	–	–	–	2.058
$[Cu(H_2dto)_2][ClO_4]_2$	–	2.094	–	2.027	–	–
$[Cu(R_2dto)_2[ClO_4]_2$	–	–	–	–	–	2.030
$[Cu(R_2dto)Cl_2]$	2.102	–	2.075	–	2.032	–
$[Cu(R_2dto)Br_2]$	2.100	–	2.070	–	2.030	–

R = *N, N'*-dibenzyl(H_2dbz); H_2dto = dithiooxamide

Table 7

Formal electrode potentials (V vs Ag/AgCl) for the redox processes exhibited by complexes $[M(Me_2Dt^0)_2]^{2+}$ in MeCN solution.

M	$E^{01}_{2+/+}$	$E^{01}_{+/0}$	$E^{01}_{0/-}$	$E^{01}_{-/2-}$
Ni	−0.16	−0.41	−0.96	−1.26
Pd	−0.18	−0.42	−0.87	−1.13
Pt	−0.15	−0.41	−0.92	−1.21